Addis Ababa University

(Since 1950)

Addis Ababa University
School of Graduate Studies
Department of Earth Sciences

INVESTIGATIONS OF LANDSLIDE PROBLEM USING GEOPHYSICAL TECHNIQUES AROUND DEBRESINA–ARMANIA MAIN ROAD IN TARMABER WOREDA, NORTHERN SHEWA ZONE, ETHIOPIA

BY: GEBRESELASSIE GEBREANENIA

A THESIS SUBMITTED TO THE SCHOOL OF GRADUATE STUDIES OF ADDIS ABABA UNIVERSITY IN PARTIAL FULFILLMENT OF THE REQUIREMENTS FOR THE DEGREE OF MASTER OF SCIENCE (MSc.) IN GEOPHYSICS.

JUNE, 2013

Addis Ababa University
School of Graduate Studies
Department of Earth Sciences

INVESTIGATIONS OF LANDSLIDE PROBLEM USING GEOPHYSICAL TECHNIQUES AROUND DEBRESINA–ARMANIA MAIN ROAD IN TARMABER WOREDA, NORTHERN SHEWA ZONE, ETHIOPIA

By: Gebreselassie Gebreanenia

Faculty of Science

Department of Earth Science

Approved by board of examiners:-

Dr. Seifu Kebede — Signature _____

Chairman, Department of Earth Science

Dr. Tigstu Haile — Signature Tigstu Haile

Advisor

Dr. Tilahun Mammo — Signature T. Lahun Dam

Advisor

Dr. — Signature _____

Internal Examiner

Dr. — Signature _____

External Examiner

ABSTRACT

Geophysical and geological investigations have been conducted for landslide problem characterization of the existing main road of the study area. The site is located in between Debresina and Armaniya towns, Tarmaber Wereda, northern Shewa Zone of Amhara Regional State. The main objective of the study was to image subsurface of the problematic main asphalt road, identify triggering mechanisms of landslide problem, and recommend possible mitigation measures based on the geo-electrical resistivity stratification of the site and magnetic anomalies obtained over the survey area. Geophysical investigations using 2D electrical imaging and magnetic methods have been conducted for the landslide problem of the road located at kebele Dokakit near Sar Amba Kidanemhiret locality between Debre Sina and Armania towns.

From the results of the survey, it has been possible to map the sliding subsurface of the geologic layers, their vertical and lateral extents. It has also been possible to map areas of weakness in the subsurface that could be causing and damaging to the life of the road. According to the interpretation of the geophysical results, the near surface geology of the study area includes fragmented and disturbed layers together with expansive clay soils which have also considerably cause of sliding problem over the area. In profile three the clay soils are much thicker than the other two profiles. In profile three low resistivity deposits are dominant particularly in the northeastern side of the survey area. These deposits are may be huge deposits of the fragmental basalt and expansive clay soils that are moved down the slope and accumulated in location of profile three which is just down the road.

Based on the joint interpretation of the results, the surveyed area has possible slide zone which is characterized by fragmented and structurally disturbed portion which starts from almost half of the surveyed line towards northeast direction. This is interpreted to be the response of the water saturated, weathered and fractured basalt rock. There is also landslide affected subsurface that exhibits intermediate apparent resistivity values comprises of the southwest end of the surveyed profiles. This zone consists of surface of weakness and some displaced rock units.

As conclusion from the work, the asphalt road parallel to the survey profiles has active sliding problem and cracks especially at the two ends of the profiles. The different weak zones, deeply weathering conditions, action of rain fall, springs and slope nature of the study area were the causing factors for this sliding problem. Therefore, special attention should be given to maintain and protect from further sliding problem.

ACKNOWLEDGEMENT

Above all, I would like to thank "Almighty God" who made it possible to begin and finish this work successfully. Next, it gives me a pleasure to thank all individuals and organizations who contributed to the success of this work.

First and foremost I am grateful to my advisors Dr.Tigistu Haile and Dr. Tilahun Mammo for their help during data processes, fatherly approaches, encouragements, constructive comments and suggestions throughout the research work. Thank you very much Dr.Tigistu for your unforgettable help you did during all the ups and downs of my field work.

My warmest gratitude goes to the Ethiopian Road Authority for allowing me car during my field work in the Debresina area and printing facilities as well. It was difficult to complete my field work without their help. I also thank for Ethiopian Institute of Geological Survey for the reference materials they gave me during my data collection and Ethiopian Meteorology Agency for their permission to use the rainfall data of the area.

Special appreciations go to Dr. Asmelash Abay, Prof. Gezahegn Yirgu, Dr.Tarun K.Raghuvanshi for their help in various geological and landslide explanations of the study area.

It gives me a special privilege to extend my deep thanks to my friends Hailemariam Siyum, Tesfay Kiros, Mohammed Yosuf, Alemayoh Ayele and others for their support and comments that they gave me during my research work.

Last but not least, I sincerely thank to all my beloved family for their love and encouragement. I do not have words to thank particularly my sister Helen for her treatments and bases for my success.

Table of contents

List of Figures

List of Tables

List of Annexes

Acronym

ACT	Action by Churches Together
2D	Two Dimensional
DEM	Digital Elevation Model
EIGS	Ethiopian Institute of Geological Survey
EMA	Ethiopian Meteorology Agency
ERA	Ethiopian Road Authority
ERT	Electrical Resistivity Tomography
GIS	Geographical Information System
GPS	Global Positioning System
Ha	Hectares
IGRF	International Geomagnetic Reference Field
MER	Main Ethiopian Rift
NE	Northeast
SW	Southwest
RMS	Root Mean Square Error
RTP	Reduction to the Pole
UTM	Universal Transversal Mercator
VES	Vertical Electrical Sounding

CHAPTER – ONE

1. INTRODUCTION

1.1 General

The Earth's surface is always in a dynamic change. These changes are more pronounced in mountainous terrains as a result of different mass wasting processes. One of these mass wasting processes is landslide. Landslide is a complex natural phenomenon that constitutes a serious natural hazard in many countries (Brabb and Harrod, 1989). A number of landslides areas are critical transportation passages (i.e., highways and railways), sites of service facilities (e.g., communication and power cables, hydrocarbon pipelines, etc.), and even residential quarters.

The term landslide is appropriate to describe a broad scope of mass movement (McCann and Forster, 1990) including abrupt or gradual rupture of rocks, debris, or Earth and their movement downslope due to the effect of gravity. A landslide could demonstrate varying movement type and extent of disruption in the course of a particular rupture. Furthermore, landslides could take place in areas where there are topographic inclines, e.g., mountain slopes, banks of rivers, and lakes or on landforms that have been stripped of their lateral constraining supports, e.g., river valleys. There are many factors that affect slope stability and hence the potential occurrences of landslides. According to Cruden and Varnes (1996) the factors are ranging from geologic causes (i.e., rock material strength, adverse orientation of structural discontinuities, fractures, etc.) to physical (e.g., high pore pressure from water saturation, earthquakes, volcanic eruptions, etc.) and even human activities (such as excavation, deforestation, mining, etc.).

Numerous catastrophic landslides that caused fatalities and property damage have been recorded in history. Moreover, the annual economic losses from slides can be very enormous, as established by the different landslides that have occurred in times past (Brabb and Harrod, 1989). The number of casualties and the degree of destructions depend on the size of the slide and the proximity to people and infrastructure. The possibility of an increase in potential risks is a consequence of rapid increase in urbanization and developments in landslide-prone areas. To avoid this loss of lives and the cost suffered from landslide incidences, it is useful to understand the causes and characteristics of the landslide processes, determine the extent of the slope instabilities, monitor slide-prone areas, and carry out appropriate mitigation measures.

1.2 Statement of the problem

Nowadays, Ethiopia has many existing and under construction main roads which are used to connect different parts of the country and the country to the neighboring countries. The five year goals of Growth and Transformation Plan (GTP) of Ethiopia include construction of roads even through different villages because these roads are believed to have a major contribution to the development of the country.

Problem of landslide has been the major threat to people, property and the natural or built environment such as roads, houses, farmlands, etc. Some of the roads of the country have been damaged by landslide problem and this may cause loss of lives, vehicles and inhibiting traffic between towns. Thus, road failure due to landslide problem can also cause severe hardship for those dependent on it for their livelihood by upsetting the regular transport condition of the main road.

Landslide is the main problem through the asphaltic road of Addis Ababa-Mekelle towns specifically because the road of the study area has been the main vein that connects Addis Ababa with many towns of northern Ethiopia. It is also located at an area highly susceptible to landslide and a large part of the main road is endangered with this problem (Figure 1.3). Therefore, this research was conducted to identify the major causes and to recommend possible remedial countermeasures of landslide around the Debre Sina–Armaniya asphalt road of Tarmaber Wereda.

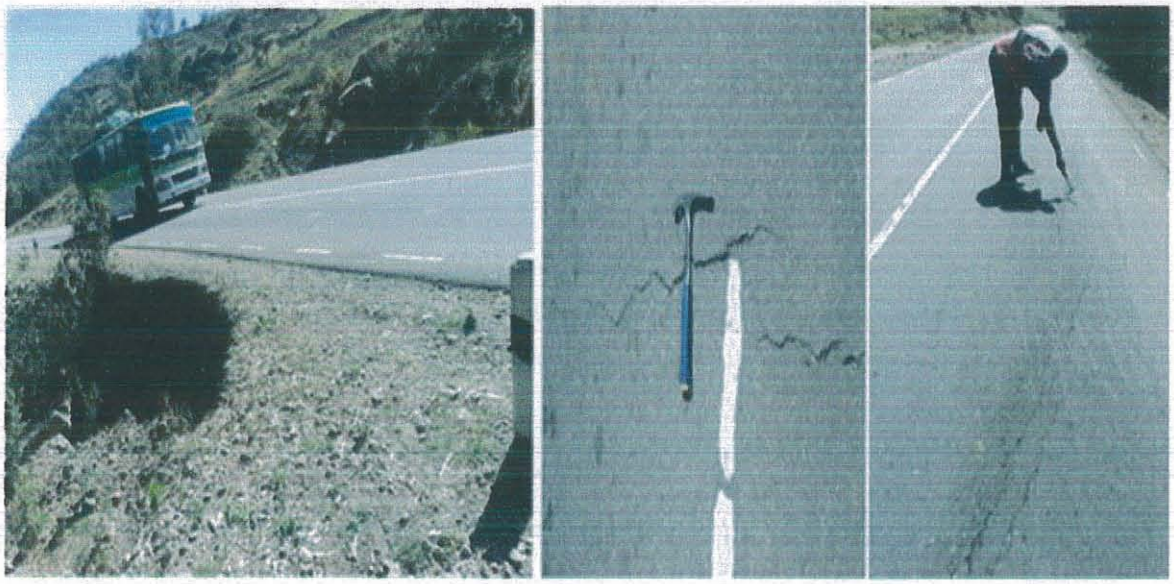

Figure 1.1 Slides showing views of landslide effects at the main asphalt road of the site.

1.3 Description of the Study Area

1.3.1 Location and accessibility

The study area is located between the towns of Debre Sina and Armania, Tarmaber Wereda, northern Shewa Zone of Amhara Regional State (Figure 1.2). It is at about 200 km NE of Addis Ababa. The study area is accessible through the Addis Ababa-Dessie asphaltic road. Planned geological traverses were accomplished by foot trails across the ups and downs of the rugged topography of the study area but the geophysical surveys are conducted on the sides of the main asphaltic road and areas adjoining it. The study area is bounded by geographic UTM coordinates of 586000-591000m E and 1088000-1093000m N. The total study area covers an area of 24.78 km^2.

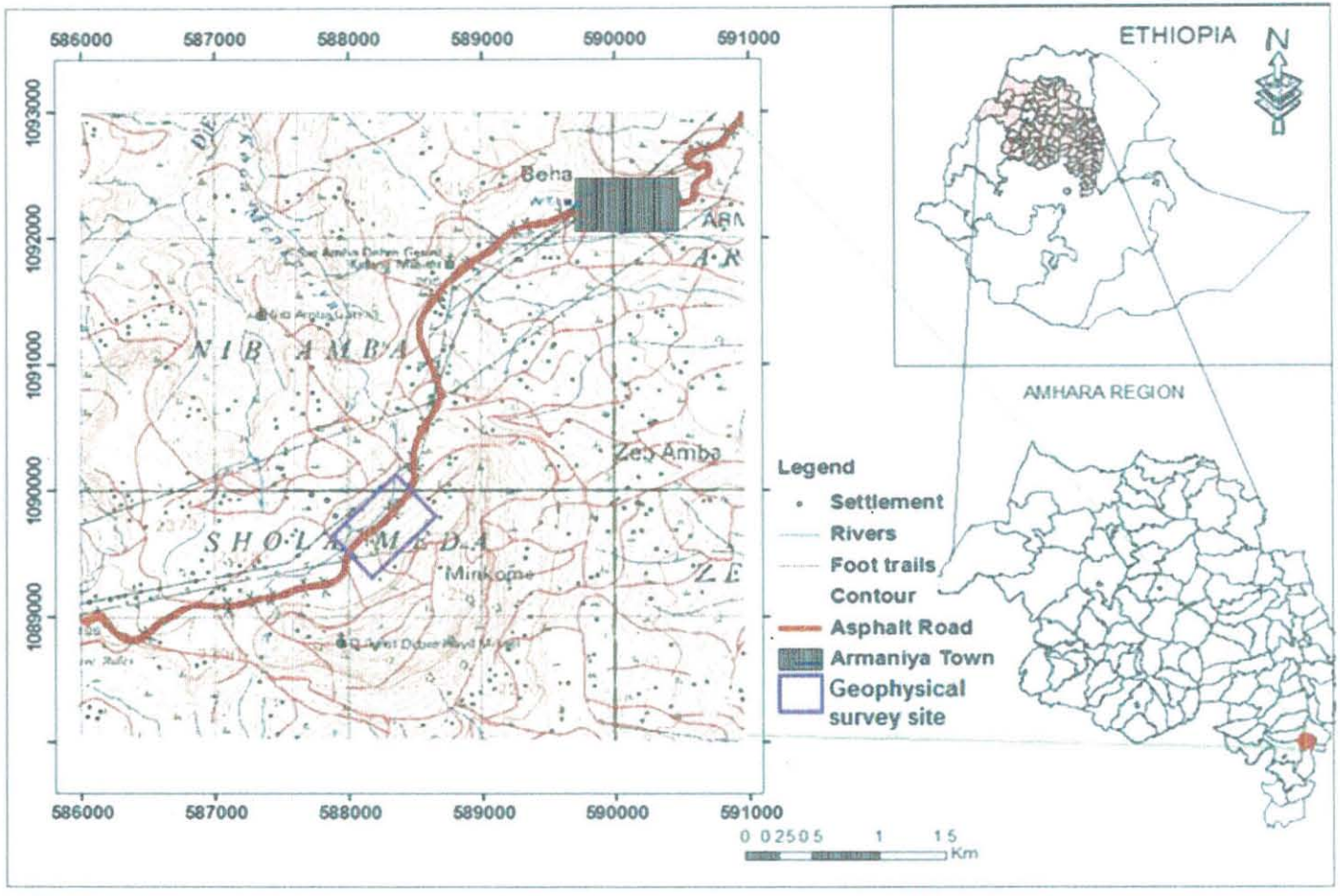

Figure 1.2 Location map of the study area.

1.3.2 Climate condition of the study area.

The climate of Ethiopia is generally characterized by different seasons. However, for the interpretation of the climatic condition in the study area, data from National Meteorological Service Agency of Ethiopia, at Debre Sina station, was referenced for thirty three years (1980-2012) and the study area is characterized by "Weyna dega" climatic zone

The study area is mainly known by wet and cold climate and rarely the temperature reaches below 00C. During winter it has cold and humid climate whereas relatively hot and dry climate in summer. Two main rainy seasons in the region are Belg (mid-February to mid-March) and Kiremte (mid-June to mid-Sept) with moderate and high precipitation, respectively. Monitoring the variability of climate that is responsible for the coming effect on an area needs the knowledge of the climatology of that area. This means knowing the long-term mean values of climatic parameters such as temperature, rainfall, etc. and their degree of variability or deviation from the mean is very important.

1.3.3 Physiography of the study area

The study area is part of the central Ethiopian plateau. It also occupies the southwestern margin of the Main Ethiopian Rift (MER) represented by very rugged topography as a result of rift forming tectonics. In the map of the area, there is a considerable difference in altitude ranging from 1800 m to 2600m above sea level. The topographic surface of the area is irregular, with many cliffs alternating with steep and gentle slopes, valleys and flat lying surface. The high altitude ridges and related steep escarpments physiographic region generally occupy the western and southern part, which consists of the highest elevation of the area. It is characterized by highly elevated and N-S trending ridges as well as mountain chains, which form steep escarpments. The main road passes through the mountainous topography which is bounded by cliff land on the eastern side and a relatively gentle slope on the western side.

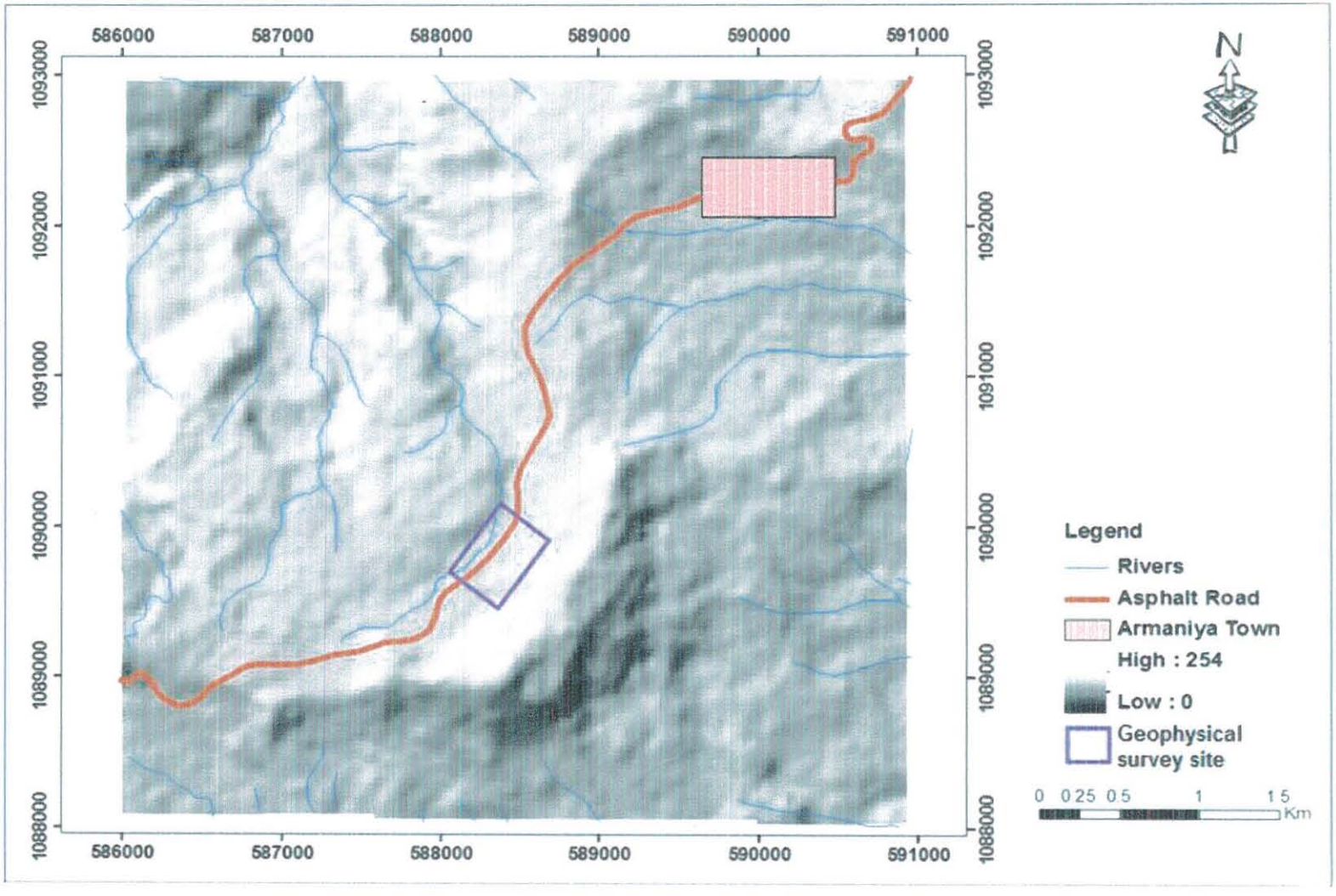

Figure 1.3 Digital Elevation Model (DEM) of the study area

1.3.4 Seismicity of the study area

The important steps in assessment of seismicity are identifying the seismic source zones, distance to the site and geology of the site. In this respect, the study area is located in the south western margin of Main Ethiopia Rift which is tectonically active. Based on the seismicity and the knowledge of the geology and tectonics, the region can be broadly divided into three seismic source zones Tilahun Mammo, 2005). These are the Afar Depression, the Escarpment and Ethiopian Rift System seismic source zones which are very near to the study area.

The earthquake epicenter map of the region in Figure 1.4 shows that small and intermediate earthquakes are dominant in areas close to the site. Moreover, the location of the earthquake is not uniformly distributed throughout the region, but it is clustered along the Main Ethiopian Rift system. The structural pattern of the region is characterized by a complex fault system with orientation almost NE–SW as shown in Figure 1.5.

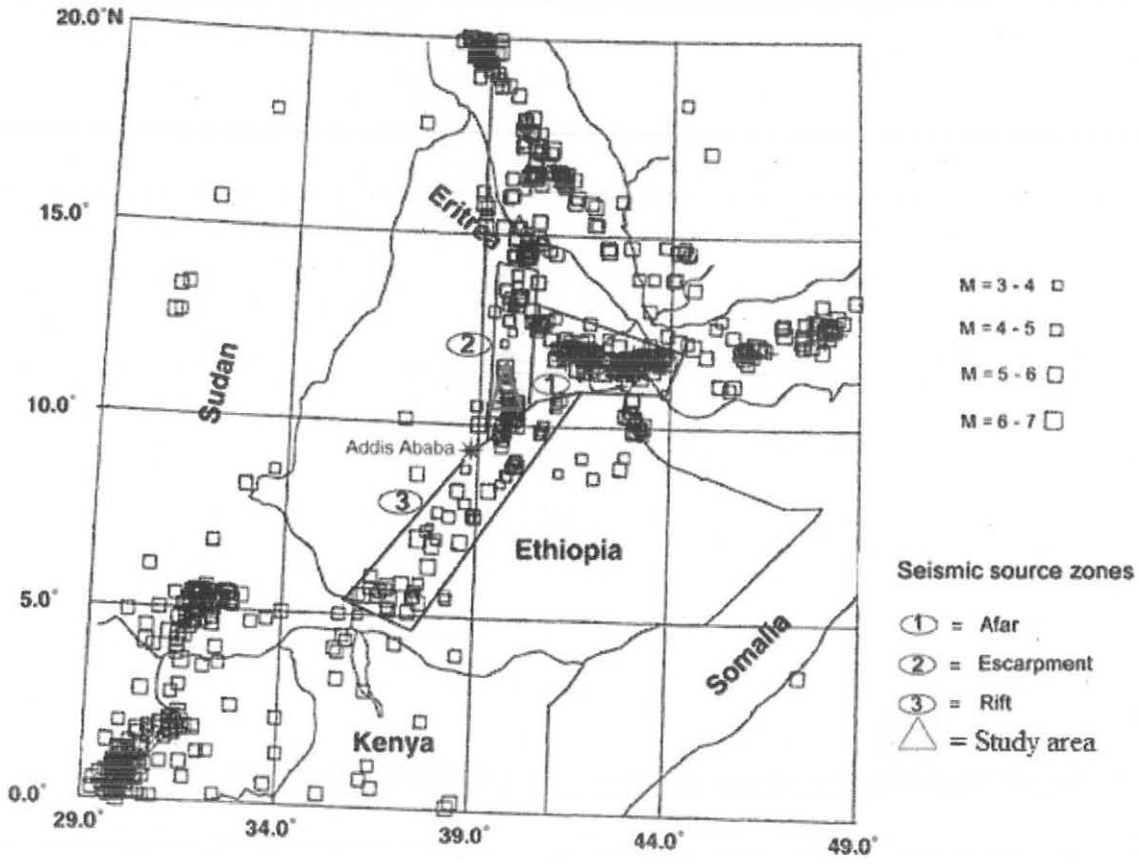

Figure 1.4 Seismicity of the region with the seismic source zones (Tilahun Mammo, 2005).

The geology of the project site is covered by recent loose sediments. The sediments and faults have an ability to amplify the amplitude of the seismic waves. Because of these reasons even small magnitude of earthquake might damage the building structures easily.

Plainly speaking, with the present static knowledge, earthquakes can never be predicted accurately and hence to develop a system of warning and eliminating the risk of loss to life is yet a distance dream (Singh, 1997). However, structures in many earthquake prone countries are now being designed more safely from information obtained from seismic zonation maps of this type.

According to the Ethiopia Building Code Standard (1995), the country is divided into five zones approximately equal seismic risks depending on the known distribution of earthquakes. These zones are no damaging zone (0 zones), less damaging zones (zones 1 and 2) and zones of major damaging (zones 3 and 4). From the seismic hazard map of Ethiopia, the project site is located at the boundary of zone four and very near to zone three as shown in figure 2.16. This map is based on the amplitudes of the ground acceleration to be expected during 100 years return period. According to the building code, the ground acceleration ratio (αo) depends on the seismic zones (Table 1.1).

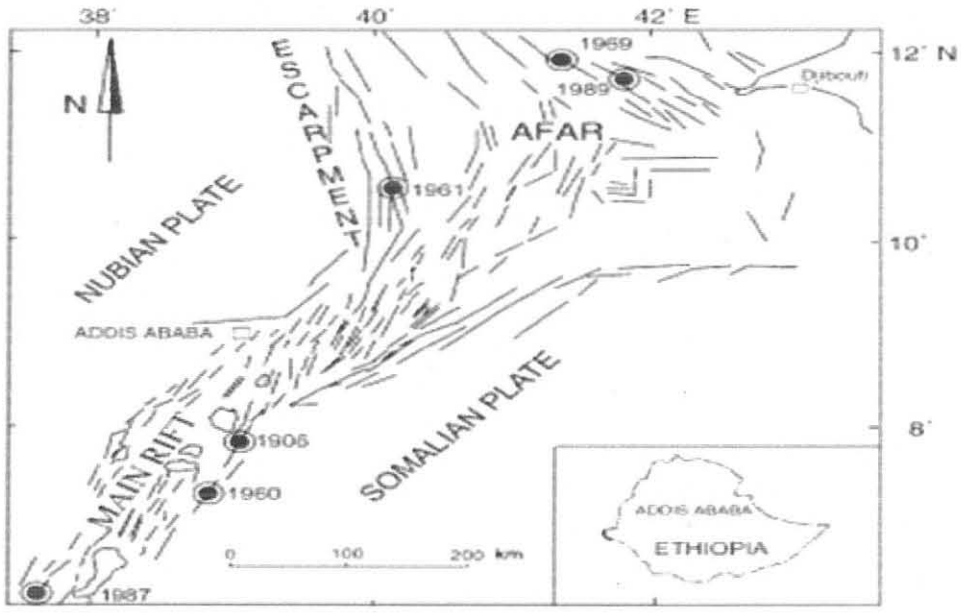

Figure 1.5 Structural pattern of the region and epicenters of major earthquakes of magnitude above 6.0 (Tilahun Mammo, 2005)

Table 1.1 Bedrock acceleration ratio

Zone	4	3	2	1
α^{o}	0.10	0.07	0.05	0.03

The ground acceleration value of the project site is 0.10g for 100 year return period. Therefore, design of any infrastructures at the study area should include all necessary seismic resistant design parameters.

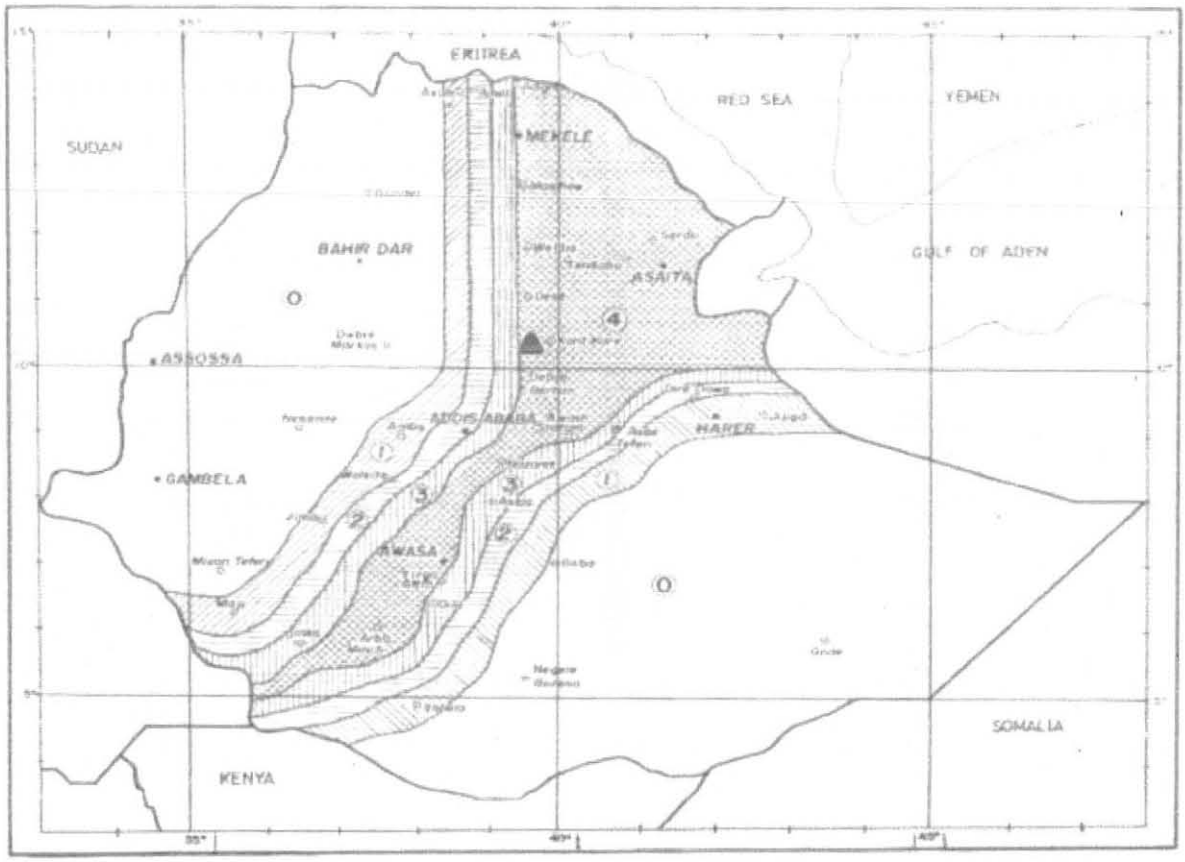

Figure 1.6 Seismic hazards zoning of Ethiopia (Ethiopian Building Code standards, 1995) and location of the study area (shaded triangle).

1.4 Objectives of the study

1.4.1 General objective

This research was conducted to study the subsurface conditions of the problematic section of the main asphalt road between Debre Sina and Armania with a view to; identifying the triggering mechanisms of the landslide problem, and recommend possible mitigation measures.

1.4.2 Specific objectives

The specific objectives of the research include:

- To produce geological map of the study area.
- To detect lateral and vertical variations and local anomalous geological conditions like lithological contacts and structures that contribute to the landslide occurrence over the area.
- To assess the possibility of future landslide occurrences in the section of the investigated area.
- To demonstrate the applicability and viability of geophysical methods for landslide problem study and their potential role in decision-making.
- To acquainted oneself with the field practices, data processing techniques and interpretation schemes of geophysical methods when used in landslide problem investigation.

1.5 Methodology

In order to achieve the objectives of the study formulated in section 1.4 various stages and techniques of data collection were employed. Literature on geophysical investigation techniques as applied to landslide studies were thoroughly reviewed. For this, different textbooks, journals, various official documents, published and unpublished papers from various professionals on geophysical investigations for landslide problem characterization were reviewed. But, primary data pertaining to the present research work of the study area were collected from the field activities during the reconnaissance and main field works. The relevant secondary data were also collected from respective offices like Ethiopian Road Authority (ERA), Ethiopian Institute of Geological Survey (EIGS), and Ethiopian Meteorology Agency (EMA). The major lithologies and geological structures were mapped following survey traverses.

The geophysical investigations were conducted using the techniques of Electrical Resistivity Tomography (ERT) and Magnetic Survey. Data were collected along selected profiles and over

random points (especially for magnetic method) well distributed to cover the investigation site. The spatial geophysical mapping, modeling and interpretation has been assisted using appropriate software such as the ElectreII, ProsysII, RES2DINV, Geosoft Oasis Montaj 6.4.2, Microsoft Excel and Surfer 9.11. The geological map and geological crossections were also developed using ArcGIS 9.3, Global Mapper 11, and 3DEM softwares.

Accordingly maps and models were produced and interpreted to obtain information required to meet the tasks set out in the research objectives. The generalized flow chart of methodological approach that was used for this investigation is given in Figure 1.7.

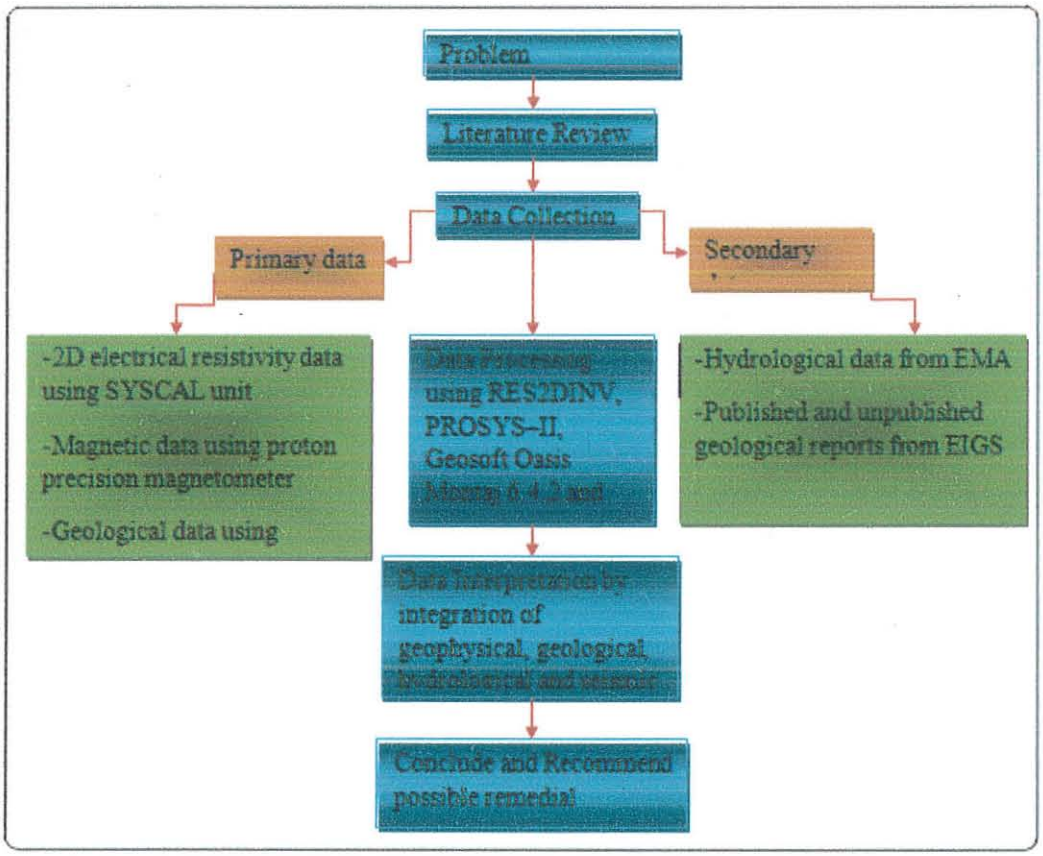

Figure 1.7 Flow chart of the methodologies applied for this research work investigation.

CHAPTER - TWO

LITERATURE REVIEW AND PREVIOUS WORKS

2.1 Literature review

A very basic but widely accepted and used definition for landslide was established by Cruden (1991) and Cruden and Varnes (1996) and defines a landslide as ''the movement of a mass of rock, debris or earth down a slope''. However, the term can be confusing if the parts of the word are considered. Cruden and Varnes (1996) note that it describes all kinds of mass movements and is not limited to granular soil (as land might suggest) or a sliding movement process. The term landslide is well established in the research community and will therefore also be used in this thesis as an overarching term referring to all movement types and material properties. Further on, the term mass movement is used interchangeably with landslide.

2.1.1 Types of landslide

The most widely used classification is the one developed by Varnes (1978) which takes into account both the type of material and the type of movement in combination for the classification of landslides into different types. This classification distinguishes five types of mass movement (fall, topples, slides, spreads, and flows) and combinations of these principal types along with different types of material (bedrock, coarse soils, and predominant fine soils).

There are various types of landslides depending on the type of material and motion involved in the process (Table 2.1). Hence, classification of landslides usually takes into account the type of material involved and the type of movement mechanism (Dai and Lee, 2002). Various systems of landslide classification have been proposed by various researchers (e.g. Varnes, 1978; Hutchinson, 1988; Cruden and Varnes, 1996; Hungr et al, 2001).

2.1.1.1 Falls

Falls are abrupt movements of masses of geologic materials that become detached from steep slopes or cliffs. Movement occurs by free-fall, bouncing, and rolling. Depending on the type of earth materials involved, the result is a rock fall, soil fall, debris fall, earth fall, boulder fall, and so on. All types of falls are promoted by undercutting, differential weathering, excavation, or stream erosion.

2.1.1.2 Topple

Topples is the forward rotation out of the slope of mass of soil or rock about a point or axis below center of gravity of the displaced mass. Toppling is sometimes driven by gravity exerted by material upslope of the displaced mass and sometimes by water or ice in cracks in the mass (Varnes, 1996).

2.1.1.3 Slides

Although many types of mass movement are included in the general term "landslide," the more restrictive use of the term refers to movements of soil or rock along a distinct surface of rupture which separates the slide material from more stable underlying material. The two major types of landslides are rotational slides and translational slides.

2.1.1.3.1 Rotational slide

Rotational slides are usually where sliding material moves along a curved surface and develop from tension scars in the upper part of a slope, the movement being more or less rotational about an axis located above the slope (Varnes, 1978).

2.1.1.3.2 Translational slide

Translational slides occur when the mass displaces along a planar or undulating surface of rupture, sliding out over the original ground surface (Varnes, 1996). The movement is frequently, structurally controlled by discontinuities and variations in shear strength between layers of bedded deposits, or by the contact between firm bedrock and overlying detritus. Translational slides tend to be more superficial than compound slides (Bell, 1999).

2.1.1.4 Lateral spreads

Spread is defined as an extension of a cohesive soil or rock mass combined with a general subsidence of the fractured mass of cohesive material into softer underlying material (Varnes, 1996). The dominant mode of movement is lateral accommodated by shear or tensile fractures (Varnes, 1978). Lateral spreads involve the horizontal displacement of the surface and are distinctive because they usually occur on very gentle slopes or flat terrain. They are more common in fine grained soils, such as clay, especially if the soil has been remodeled or disturbed by construction, or similar activities.

2.1.1.5 Flows

Flow and flow like landslide have various types of definitions and many classifications exist on literature. For example, according to Bell (1999) flows consist of slurry of loose rocks, soil, organic matter, air and water moving down-slope. They are distinguished from slides by having higher water content and are thoroughly deformed internally during movement (Hutchinson, 1995). A flow is a spatially continuous movement in which surfaces of shear are short-lived, closely spaced, and usually not preserved. The most referred and accepted of all definitions is that of Varnes (1978). Flows are rapid movements of material as a viscous mass where inter-granular movements predominate over shear surface movements and these can be debris flows, mudflows or rock avalanches, depending upon the nature of the material involved in the movement (Varnes, 1978).

Table 2.1 Abbreviated version of Varnes' classification of slope movements (Varnes, 1978).

Type of movement		Type of material		
		Bed rock	Engineering soils	
			Predominantly coarse	Predominantly fine
Topple		Rock topple	Debris topple	Earth topple
Fall		Rock fall	Debris fall	Earth fall
Slide	Translational	Rock slide	Debris slide	Earth slide
	Rotational			
Flow		Rock flow	Debris flow	Earth flow
Spread		Rock spread	Debris spread	Earth spread
Complex		e.g., rock avalanche	e.g., flow slide	e.g., slump-earthflow

2.1.2 Causes of slope instabilities

The equilibrium status of a natural slope can be affected by several direct or indirect factors. In every slope there are forces which tend to promote downslope movement and opposing forces which tend to resist movement. A change in any one or a combination of these factors can alter the equilibrium condition of slope, decreasing its stability and sometimes leading to the slope failure. This change may be caused by natural processes such as the faulting, rivers undercutting the toe of a slope or bank scouring by debris flows etc. and also anthropogenic activities such as excavation, cultivation or removal of material may also cause change in slopes. Varnes (1978) pointed out that there are a number of external or internal causes which may be operating either to reduce the shearing resistance or to increase the shearing stresses. Slope instability factors can be causative factor or triggering factor. Causes may be considered to be factors that make the slope vulnerable to failure, that predispose the slope becoming unstable while the trigger is the single event that finally initiates the landslide. Some of the major factors which influence the slope stability are described below.

2.1.2.1 Geological factors

Geology is vital component in landslide modelling, stability study and protection design of landslides. Thus, a critical understanding of the geological conditions of the area is crucial for any slope stability investigation.

The factors that control the mode of initial failure in rock slopes mainly include rock mass fabric, lithology contrasts, and geologic structure in the source slope (e.g. Hutchinson J.N, 1987; Cruden, et al., 1996; Guzzetti, et al., 1996; Chigira, 2000). The important geological factor that should be considered in landslide hazard investigation is summarized below as stated by numerous authors.

2.1.2.1.1 Types and properties of soil and rock materials

The mechanical properties of rocks may be influenced by particle size, properties of crystals and their preferred orientation (Chowdhury, 2010). Factors inherent in the nature of the materials which include the types and orientations of minerals and their degree of interlocking may have an influence on engineering characteristics of slopes, as it causes a marked anisotropy in the strength and deformation characteristics of soil/rock masses (Selby, 1993) as cited in Kifle Woldearegay (2005).

The type of material within a sloped terrain is also important factor. For example unconsolidated materials, such as soil and sediment, tend to be more prone to slope failure than rocks.

2.1.2.1.2 Discontinuities

Discontinuities represent a plane of weakness within a rock mass across which the rock material is structurally discontinuous and possess little or no tensile strength, varying in size from small fissures on the one hand to huge faults on the other (Bell, 2007). It is of paramount importance to study the properties of discontinuities because they influence the stability, the deformation and permeability of the slopes. The summarized notes are given from Hudson, et al, (1997), Bell (2007) and Price (2009).

2.1.2.1.3 Weathering of geologic materials

Weathering implies decay and change in state from an original condition to a new condition as a result of external processes and weakens rocks (Price, 2009).Two main types of weathering are recognized: physical weathering, in which the original rock disintegrates to smaller-sized material with no appreciable change in chemical or mineralogical composition, and chemical weathering, in which chemical and/or mineralogical composition of the original rock and minerals are changed (Clark and Samall, 1982).

The rate at which weathering proceeds depends not only on the impact of the weathering agents but also governed by the mineralogical composition, texture, porosity and strength of the rock on the one hand, and the incidence of discontinuities within the rock mass on the other hand (Bell,2007). Soil depth and type, which resulted from weathering, are affected by several factors including climate and parent rock mineralogy. Weathering depends on the original mineralogy, the nature of climate and biological environment (Crozier, 1986).

.2.1.2.2 Topographic factors

The two geomorphic factors which control slope instability are slope gradient and relative relief. According to Alexander (1999), mass movement will occur where ever a slope is steeped beyond its threshold angle of stability, which is the steepest angle at which it can maintain itself. The hill slope angle supplies the potential energy gradient on which a landslide moves (Cross, 1998). Therefore, at higher angles, the profile of the slope will alter itself to restore stability by undergoing slope failure. Relative relief which is the difference in height between the bottom and the top of the slope provides a further measure of gravitational force which exists within the slope (Cross, 1998). Therefore, the more steeper and the higher relative relief of the slope the more liable is to be unstable.

2.1.2.3 Hydrological conditions

Hydrology plays a crucial role in landslide initiation by destabilizing hill slopes. Identification of water source, water movement, amount of water and pressure are, as important as the identification of the material constituting the slopes. In an area with highly jointed rocks and the presence of thick overburden, the surface and ground water play a crucial role in the evolution of landslides.

2.1.2.3.1 Precipitation

The most common trigger of landslide is sufficient water input during precipitation events. Landslides triggered by rainfall occur in most mountainous area of the world. The mobilization of debris material during debris flow events is related either to the onset of sediment transport due to water runoff or to slope failures caused by an increase in pore-water pressures. Shallow debris-flows are often triggered by intense rainstorms of short duration whereas deep-seated landslides are triggered by antecedent rainfall (high cumulative rainfall) over days or weeks often combined with intense rainfall over a much shorter period (Chowdhury, 2010).

2.1.2.3.2 Groundwater

Groundwater is another factor that plays role in landslide initiation. Geology in turn influences the flow of groundwater, its direction, pressure and gradient at any point within a slope. Chowdhury (2010) states that water can influence the strength of the materials by: (1) chemical alteration and solution, (2) reduction of apparent cohesion due to capillary forces, which disappear on submergence or saturation, (3) increasing pore water pressures with consequent reduction of shear strength. The same author also mentioned that increase of pore water pressures due to the flow of groundwater is an important factor in the development of slope failures and the occurrence of landslides. In particular the presence of groundwater under pressure often facilitates severe slides of the flow type.

2.1.2.4 Seismicity

Earthquake is one of the principal triggering factors of landslides that cause great hazard to both of life and properties loss. The vibration released during earthquakes can cause failure of slopes which were previously stable. The possibility of an earthquake in triggering a landslide event depends on the shaking of the ground rather than on the actual magnitude of the earthquake

(Muthu and Petrou, 2007). The vibrations released during a quake can cause resettlement of the soil skeleton which in turn causes expulsion of water.

Rock falls and slides of rock fragments that form on steep slopes are common earthquake induced landslides although other type of landslide is also possible, including highly disaggregated and fast-moving falls, more coherent and slower-moving slumps block slides, and earth slides, and lateral spreads and flows that involve partly to completely liquefied material (Keefer, 2002).

Earthquakes reduce stability by imparting both a shearing stress and a reduction in resistance to slope material. Earthquake wave propagation has three principal effects (Crozier, 1986; Alexander, 1993) which includes (1) the direct mechanical effect of horizontal acceleration, which provides a temporary increment to shearing stress 2). The cyclic loading which weakens inter-particle bonding causes liquefaction and (3) the reduction in inter-granular bonding by sudden shock irrespective of the degree of saturation.

2.1.2.5 Manmade activities

Manmade activities affect the stability of the slopes both by increasing the shear stress and reducing the shear strength. Kumar (2009) explained that manmade activities will increase steepness and height of the slope, and mass of slope material due to extra load placed on it, and decrease in shear strength due to loss of vegetation and blasting etc, increased pore water pressure and drainage, increases infiltration etc, and withdrawal of lateral support by road cut.

The removal of lateral support by man's activities are important cause of slope failures in cuts for roads or house sites, excavations, quarries and open pit mines, canals and in the banks of reservoirs during drawdown. Likewise these actions alter stress conditions through the placing of fills, waste-piles, stock piles of ore rock, and structures where no surcharge existed before (Varnes, 1984).

According to Alexander (1999), ploughing or poorly organized drainage on slopes increases infiltration of water which leads to soil saturation and will increase pore water pressure which exerts a positive force that may cause the slope to fail.

2.1.3 Application of geophysical methods on landslide problem

In order to carry out a feasible and effective landslide mitigation procedure, knowledge of the subsurface structure and physical properties of the constituting materials are required. Surface examinations of landslide areas provide limited information in determining the causes of the

slides. For a deep-seated landslide, it may be impossible to define its rupture surface by surface inspection alone. Boreholes and geophysical methods, on the other hand, are useful in providing these much needed information for proper landslide investigation. Apart from the relative expensive costs of drilling boreholes in comparison to using geophysical methods to study landslides, the data acquired from a borehole is also single-point based.

In order to obtain adequate knowledge of the area, interpolations have to be made among numerous boreholes to fill in the spatial gaps. This makes geophysical techniques preferable, considering the lower cost, extensive lateral and depth coverage and reduced damage to formations. Geophysical techniques may provide valuable results on defining the geometry of landslides, describing their internal structures, revealing the effect of groundwater on them, the physical properties of the landslide materials, and the landslide mass movement (Göktürkler et al., 2008).

Resistivity methods have been widely used to study areas susceptible to landslides (e.g., Batayneh and Al-Diabat, 2002; Agnesi et al., 2005; Drahor et al., 2006; Lee et al., 2008). These measurements seek to distinguish different rock materials on the basis of their electrical resistivity properties. The resistivity values of the sliding masses are expected to be different from that of the undisturbed body because of the movement of materials and deformations by the slide (Jongmans et al., 2009).

Lapenna et al. (2005) encountered lower resistivity values in a landslide body, which was characterized by high content of clayey material and increase in water content; in comparison to the resistivity values of the unaffected rock. On the other hand, Meric et al. (2005) observed higher electrical resistivity values in a different landslide body, in contrast to the unaffected mass, due to a great level of fracturing related to air-filled spaces in the deformed mass. Thus, if there is substantial resistivity contrast between the different masses, the slip surface should be readily distinguishable. Electrical resistivity tomography (ERT) offers an electrical resistivity distribution (2D or 3D) of the subsurface and an even more highly resolved picture of the ground, to enable one to distinguish areas susceptible to landslides and the associated causative factors.

Typically, most of these geophysical methods are not utilized in isolation, on the contrary, they are used in conjunction with other techniques (as shown in Bogoslovsky and Ogilvy, 1977; Bichler et al., 2004; and Meric et al., 2005) to better understand the landslide geometry and the physical properties of the materials in the affected areas. Bearing in mind that different geophysical

methods are sensitive to varied physical properties, it is important to combine a variety of techniques during geohazard studies in order to obtain better insights into the landslides and their processes.

2.1.4 Landslide problem in Ethiopia

Landslides are one of the major destructive natural hazards in mountainous and rift margins of Ethiopia, resulting in loss of human life and property and severe damage to agricultural lands. Many researchers depicted/shown that landslides have affected human lives, infrastructures, agricultural lands and natural environment in the highlands and rift margins of Ethiopia (Lulseged Ayalew, 1999; Kifle Woldearegay, 2005). In the years 1990-1998 alone, landslides or landslide-generated hazards have claimed about 300 human lives, damaged over 100 km asphalt road, demolished more than 200 dwelling houses and devastated in excess of 500 hectares of land in different areas of the highlands of Ethiopia (Lulseged Ayalew, 1999) as cited in Asmelash Abay (2012).

According to the press reports of Walta information Centre of 2000, 2002, 2003a, 2003b, 2003c, 2003d as cited in (Kifle Woldearegay, 2005), 135 human lives have been lost, about 3500 people were displaced and an estimated 1.5 million US Dollar worth property has been damaged in the highlands of Ethiopia in the years 1998-2003 as cited in Asmelash Abay (2012). Few sites of landslide have been investigated in Ethiopia by Tenalem Ayenew (2005), EIGS (1998) and the likes. All of the landslide events have been observed to occur following a heavy rainfall along with a number of pre-conditioning attributes. These attributes include proximity to drainage, irrigation channel, infrastructure development (road), which usually have the effect of undercutting; the property of geologic formations, and soil condition.

2.1.5 Landslide history and impacts in the study area and its surroundings

Landslides in the study area started with various signs of slope failure some years back (Leta Alemayehu, 2007). Over the area, landslides that occurred as early as the Italian invasion times have been reported (eyewitnesses) in Tach Indode and Tid Amba localities. According to the eyewitnesses, the slide problem also happened in 1952 by developing fissures in the soils sediments of Shotel Amba and Gebreal localities. Again in 1985, fissures were observed at Disk Amba and Tid amba, specifically at Ketanit and Bado mesk (EIGS, 1980). Other landslides in the area predating the Italian invasion period have occurred in Majete, Yenat Metoria, and Work

Amba. G/silassie (2007) has further identified a number of landslides (specifically 11) from Action by Churches Together (ACT) (2006) and local authorities as cited in Asmelash Abay (2012). Table 2.2 summarizes the important landslide vents of the study area.

Table 2.2: Past landslide records of the area (G/silassie, 2007).

S.N	Locality name	Time of occurrence	Damage
1	Yizaba, Gishrit locality	1995	1575m^2 wood land was affected
2	Yizaba, Aynemariam locality	1995,1998 & 1999	Some residential units cracked and 3ha of bush land damaged
3	Shotel-Amba	1953 & 1998	Residential units, farmland and grazing areas were affected by both periods
4	Weibila	1995 & 1997	18 residential units and 30 hectare of farm land and grazing land was affected by the 1995 landslides
5	Sina/Aregai	October, 1971	35-40 hectare of forest land was destroyed
6	Armania	1953, 1979 & 1997	The asphalt road has been affected in all the three landslide events. Still active and a tensional cracks are observed at the roadside
7	Nib-Amba	1953, 1997 & 2000	>100ha of farm land, grazing area destroyed
8	Sholla-Meda	July, 2000	20ha of farm land, grazing area and settlement
9	Lay Indode	September, 2000	It destroyed 8 residential unit & 30ha of farm land and grazing land. It is still active and has been reactivated event rainy season
10	Tach Indode	1999 & September, 2000	It destroyed an estimated of 40ha of grazing land and farm land. It is still active and has been reactivated event rainy season
11	Yizaba, Shotel Amba, Armania,Ainemariam	September 2005	Over 900ha arable lands destroyed, more than 4049 peoples displaced, more than 1200 dwelling local houses destructed & over 75% crop harvesting failure specifically in the localities named Izaba and Shotel Amba

The Debresina area is one of the most landslide prone areas of Ethiopia and is located in the Afar Rift Margin. According to the publication of Asmelash Abay and Barbieri (2012); the sliding event that occurred in September 13-14, 2005 was one of the large scale and complex landslide of the area. They clearly stated the impact of this landslide event by referring to the aid reports of ACT (Action by Churches) released in 2006 and the information of local authorities. The event caused losses of over 900 hectares of arable land, displacement of more than 4,049 peoples, destruction of more than 1,200 dwelling local houses and over 75% crop harvesting failure specifically in the localities named Izaba and Shotel Amba. The prevalence of landslide

hazards in such terrains could certainly have major role in aggravating the food insecurity problem of the country as most people living here are farmers who are dependent on subsistent agriculture.

2.2 Previous studies in and around the study area

The following are some of the works in different landslide susceptible areas of Ethiopia:

Solomon Gerra (2010) has conducted integrated landslide investigations in Tarmaber and surroundings which is in the northwestern side of the study area. Based on this work, integrated geological, engineering geological, hydrogeological and geophysical investigations were carried out. Geophysical studies were also carrying out from April to May 2010 in the project area at five selected sites, namely, Kechine, Barmeda, Babota, Yebegoch-Gat and Yemariam-Wonz. Among the methods, Vertical Electrical Sounding (VES), magnetic and Seismic Refraction were implemented.

Engineering geophysical investigation along a proposed alternative route of Blue Nile Gorge has been conducted (EIGS, 1994). The survey methods used were refraction seismic, electrical resistivity (VES and profiling) and magnetic with the objectives of determining depth to the bed rock, locating possible structural features, and studying the nature of the overburden material.

The integrated engineering geological and geophysical investigations for landslide studies in Bonga town and its surroundings have been conducted (EIGS, 1999). The geophysical methods, which consisted of Refraction seismic, Vertical Electrical Sounding, Electrical resistivity profiling and magnetics, were conducted along 27 profiles covering a total length of 7.6 km.

Many researchers have visited the study area and it's surrounding for different purposes but there was no particular works along the main road by proposed geophysical investigation for the landslide problem mitigation of the study area. A number of works have been done by different scholars. Some of the relevant works are:

Asmelash Abay and Giulio Barbieri (2012) have conducted investigation landslide susceptibility and causative factors evaluation of the landslide area of Debresina, in the Southwestern Afar Escarpment, Ethiopia. Based on this work, the landslide susceptibility areas and different causative factors are outlined.

According to Mengesha et al., (1996), the olivine basalt of Debre Sina belongs to the Tertiary volcanism. This rock came out as lava flows through tectonic fractures and fault planes related to the great rift valley of East Africa.

Zanittine et al., 1974, noted that the ignimbrites of the Debre Berhan and Tarmaber area are covered by Tarmaber Basalt. In this work, K/Ar age determinations gave values of 15.4+/-0.3 Ma for the upper member of the ignimbrite sequence and 13+/-0.6 Ma for the overlaying basaltic flows.

Alula and Gashawbeza (1993) have conducted investigation for coal and oil shale on 145 sq km area located 30 km north of Debre Berhan. Accordingly, basalts, ignimbrites and inter-volcanic sediment, which contain carbonaceous shale and coal seams, are reported. Mengesha et al, (1996) in the 1:2, 000, 000 scale geological map of Ethiopia has described that the map area is covered by rhyolites, trachyte and transitional to sub-alkaline basalts of Alaji Formation as well as by transitional and alkaline basalts of Tarmaber-Megezez Formation.

Yonas and Matebie (2006) have mapped the entire project area and produced 1:50, 000 scale geological maps as well as accompanied report. Based on this work, the area is covered by various types of basalts, rhyolites, ignimbrites as well as by inter-volcanic sediments.

Leta Alemayehu (2007) has conducted landslide susceptibility modeling using logistic regression and artificial neural networks in GIS. Based on this work, the landslide zoning and slope instability problem of the selected area has been assessed using remote sensing technique and GIS.

CHAPTER – THREE

THEORETICAL BACKGROUND OF GEOPHYSICAL METHODS

3.1 2D-Electrical Imaging Survey

3.1.1 Introduction

Recently, a new concept of instrumentation and data acquisition has been introduced to make it possible the acquisition of many readings in a reduced amount of time specifically for environmental applications corresponding to shallow investigations depths, of the order of 10 to 80m. The technique is sometimes called Electrical Resistivity Tomography (ERT). The concept involves using multi-core cables which contain as many individual wires as number of electrodes, with one take-out every 5m, 10m … and 24, 48, 72, 96 … electrodes. The measuring unit includes relays which automatically carry out the sequences of readings introduced in its internal memory. The aim of this set-up is to take readings for many combinations of transmission and reception pairs, so as to achieve some kind of mixed wenner / schlumberger array. In such a way of proceeding, the total length of cable is the product of the electrode spacing by the number of electrodes.

The greatest limitation of the resistivity sounding method is that it does not take into account horizontal changes in the subsurface resistivity. A more accurate model of the subsurface is a two-dimensional (2-D) model where the resistivity changes in the vertical direction, as well as in the horizontal direction along the survey line. In this case, it is assumed that resistivity does not change in the direction that is perpendicular to the survey line. In theory, a 3-D resistivity survey and interpretation model should be even more accurate. However, at the present time, 2-D surveys are the most practical economic compromise between obtaining very accurate results and keeping the survey costs down (Loke, 1999).

3.1.2 Instrumentation and Field survey

One of the new developments in recent years is the use of 2-D electrical imaging/tomography surveys to map areas with moderately complex geology (Griffiths and Barker, 1993). Such surveys are usually carried out using a large number of electrodes, 25 or more, connected to a multi-core cable. At present, field techniques and equipment to carry out 2-D resistivity surveys are well developed.

Figure 3.1 shows the typical setup for a 2-D survey with a number of electrodes along a straight line attached to a multi-core cable. Normally, a constant spacing between adjacent electrodes is used. The multi-core cable is attached to an electronic switching unit which is connected to a laptop computer. The sequence of measurements to take, the type of array to use and other survey parameters (such the current to use) is normally entered into a text file which can be read by a computer program in a laptop computer. After reading the control file, the computer program then automatically selects the appropriate electrodes for each measurement. One technique used to extend horizontally length covered of the survey, particularly for a system with a limited number of electrodes, is the roll along method (Figure 3.1). After completing the main sequence of measurements, one of cable is moved to the end of the line.

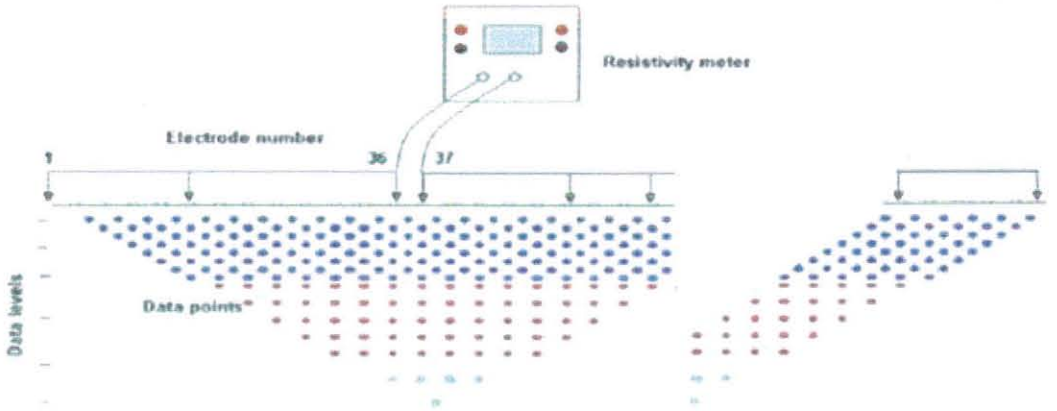

Figure 3.1 Generalized survey procedures with the main sequence in the left, roll along in the right and data points of 2-D resistivity imaging (Tigistu Haile, 2010).

3.1.3. Modeling of 2-D electrical resistivity imaging

Resistivity data is generally interpreted using the modeling process. A hypothetical model of the Earth and its geoelectrical section is generated. The theoretical electrical resistivity response over that model is then calculated. The theoretical response is then comparing with the observed field response and difference between the observed and calculated are noted. The hypothetical earth model is then adjusted to create a response which more fit to the observed data.

3.1.3.1 Forward Modeling

Forward modeling is a technique to model a subsurface by estimating the actual resistivity of the different geological structures. The estimation is made by calculating the apparent resistivity of the respective ground structure using the fundamental theoretical electrical equations.

The resistivity response for a 2-D model is calculated and displayed as a pseudo-section for comparison with the original field data. This approach is used to generate realistic subsurface geometries in definable model structures (Reynolds, 1997). Forward modeling operates through a process which divides the subsurface is into a large number of small rectangular cells (McDowell et al., 2002).

3.1.3.2 Basic Inverse Theory

Geophysical inversion is a method which finds a model that gives a response that is similar to the actual measured values. The model is an idealized mathematical representation of a section of the earth. The model has a set of model parameters of physical quantities which are required to be estimated from the observed data. The model response is the synthetic data that can be calculated from the mathematical relationships defining the model for a given set of model parameters. All inversion methods essentially try to determine a model for the subsurface whose response agrees with the measured data subject to certain restrictions.

In all optimization methods, an initial model is modified in an iterative manner so that the difference between the model response and the observed data values is reduced. The set of observed data can be written as a column vector **y** given by

$$y = col(y_1, y_2, \ldots . y_m) \tag{3.1}$$

where **m** is the number of measurements. The model response **f** can be written in a similar form

$$f = col(f_1, f_2, \ldots . f_m) \tag{3.2}$$

The difference between the observed data and the model response is given by discrepancy vector **g** that is defined by

$$g = y - f \tag{3.3}$$

In the least square optimization method, the initial model is modified such that the sum of squares error **e** of the difference between the model response and the observed data values is minimized and is given as (Loke, 1999).

$$e = \sum_{i=1}^{n} g^2 = g^T g \tag{3.4}$$

The above equation can be rewritten as

$$e = \sum_{i=1}^{n} \sqrt{(m_i - r_i)^2} \tag{3.5}$$

where, r_i is the i^{th} calculated reisitivity value, m_i is the i^{th} observed apparent resistivity and n is number of measured data. To get minimum **e** (root mear square error, RMS) the smoothness constrained least square method (deGroot-Hedlin and Constable, 1990) is used. It is given as

$$d\left(J^T J + U.F\right) = J^T g - UFr \tag{3.6}$$

where, $F = f_x f_x^T + f_z f_z^T$, f_x is vertical flatness filter, J is matrix of partial derivatives, U is damping factor, d is model perturbation factor, r is a vector containing the logarithm of the model resistivity value and g is discrepancy vector.

3.1.4 The relationship between geology and resistivity

Resistivity surveys give a picture of the subsurface resistivity distribution. To convert the resistivity picture to a geological picture, some knowledge of typical resistivity values for different types of subsurface materials and the geology of the area surveyed is important. Igneous and metamorphic rocks have high resistivity values, which greatly depend on degree of fracturing and the percentage of the fractures filled with water. Sedimentary rocks have lower resistivity value because is usually porous and have higher water content (Annex-III).

3.2 The Magnetic Method

3.2.1 Introduction

Magnetic prospecting, the oldest method of geophysical exploration, is used for mineral, groundwater, oil and gas, engineering (locating buried structures and weak zones) and environment applications. It is a very popular and inexpensive approach for near-surface metal detection. Engineering and environmental site characterization often begin with a magnetometer survey as a means of rapidly providing a layer of information on where utilities and other buried concerns are located. The principal operation of magnetic survey is quite simple. When a ferrous material is placed within the Earth's magnetic field, it develops an induced magnetic field. The induced field is superimposed on the Earth's field at that location creating a magnetic anomaly.

Detection depends on the amount of magnetic material present and its distance from the sensor (Rivas, 2009).

3.2.2 Basic Principles and Elementary Theory

The Earth's large scale magnetic field is superimposed by small scale magnetic anomalies related with magnetized rocks. Magnetization is the parameter corresponding to density in the gravity method. Magnetization is a vector quantity which is related with the concept of north and South Pole of a magnet (Kirsch, 2009).

Within the vicinity of a bar magnet a magnetic flux is developed which flows from one end of the magnet to the other (Figure 3.2). This flux can be mapped rom the directions assumed by a small compass needle suspended within it. The points within the magnet where the flux converges are known as the poles of the magnet. A freely suspended bar magnet similarly aligns in the flux of the Earth's magnetic field. The pole of the magnet which tends to point in the direction of the Earth's North Pole is called positive pole, and this is balanced by the south seeking or negative pole (Kearey et al., 2002).

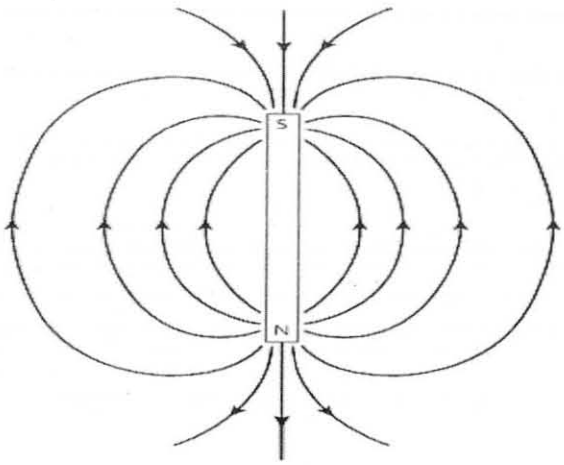

Figure 3.2 Magnetic flux surrounding a bar magnet (Kearey et al., 2002)

The force of **F** between two magnetic poles of strengths m_1 and m_2 separated by a distance r is given by

$$F = \frac{\mu_o m_1 m_2}{4\pi\mu_R r^2} \tag{3.7}$$

where μ_0 and μ_R are constants corresponding to the magnetic permeability of vacuum and the relative magnetic permeability of the medium separating the poles. The force is attractive if the poles are of different sign and repulsive if they are of like sign.

The magnetic field **B** due to a pole of strength m at a distance r from the pole is defined as the force exerted on unit positive pole at that point

$$B = \frac{\mu_o m}{4\pi\mu_R r^2} \tag{3.8}$$

Magnetic fields can be defined in terms of magnetic potentials. For a single pole of strength m, the potential **V** at a distance r from the pole is given by

$$V = \frac{\mu_o m}{4\pi\mu_R r} \tag{3.9}$$

The magnetic field component in any direction is then given by the partial derivative of the potential in that direction.

In the SI system of units, magnetic parameters are defined in terms of the flow of electric current. If a current is passed through a coil consisting of several turns of wire, magnetic flux flows through and around the coil annulus which arises from a magnetizing force **H**. The magnitude of **H is** proportional to the number of turns in the coil and the strength of the current, and inversely proportional to the length of the wire, so that **H** is expressed in Am^{-1}. The density of the magnetic flux, measured over an area perpendicular to the direction of flow, is known as the magnetic induction of magnetic field **B** of the coil. **B** is proportional to **H** and the constant of proportionality μ is known as the magnetic permeability (Reilly, 1972).

Common magnets exhibit a pair of poles and are therefore referred to as dipoles. The magnetic moment **M** of a dipole with poles of strength m a distance l apart is given by

$$M = ml \tag{3.10}$$

The magnetic moment of a current carrying coil is proportional to the number of turns in the coil, its cross-sectional area and the magnitude of the current.

When a material is placed in a magnetic field it may acquire a magnetization. This phenomenon is referred to as induced magnetization. The intensity of induced magnetization **J** of a material is defined as the dipole moment per unit volume of the material

$$J = \frac{M}{LA} \tag{3.11}$$

In other way the induced intensity of magnetization is proportional to the strength of the magnetizing force **H** of the inducing field.

$$J = \kappa H \tag{3.12}$$

where, **K** is the magnetic susceptibility of the material.

In a vacuum the magnetic field strength **B** and magnetizing force **H** are related by

$$B = \mu_o H \tag{3.13}$$

where, μ_0 is the permeability of vacuum (4π x $10^{-7}Hm^{-1}$). Air and water have similar permeability to μ_0 and so this relationship can be taken to represent the Earth's magnetic field when it is undisturbed by magnetic materials. When a magnetic material is placed in this field, the resulting magnetization gives rise to an additional magnetic field in the region occupied by the material, whose strength is given by $\mu_0 J$. Within the body the total magnetic field or magnetic induction, **B** is given by

$$B = \mu_o H + \mu_o J \tag{3.14}$$

Substituting equation (3.14)

$$B = \mu_o H + \mu_o \kappa H = (1+\kappa)\mu_o H = \mu_R \mu_o H$$

The magnetic permeability $\mu$is thus equal to the product of the relative permeability and the permeability of vacuum, and has the same dimensions asμ_0. For air and water μ_R is close to unity.

3.2.3 The Earth's Magnetic field

The geomagnetic field near the surface of the Earth originates largely from within and around the Earth's core. Ninety percent of the Earth's magnetic field looks like a magnetic field that would be generated from a dipolar magnetic source located at the center of the Earth and aligned with the

Earth's rotational axis. The remaining 10% of the magnetic field cannot be explained in terms of simple dipolar sources. Complex models of the Earth's magnetic field have been developed and are available. As observed on the surface of the Earth, the magnetic field can be broken into three separate components.

Main Field: This is the largest component of the magnetic field and is believed to be caused by electrical currents in the Earth's fluid outer core. It is produced in the core of the earth and accounts for the very large regional variations in the field intensity and direction. For exploration work, this field acts as the inducing magnetic field.

External Magnetic Field: This is a relatively small portion of the observed magnetic field that is generated from magnetic sources external to the earth. This field is believed to be produced by interactions of the Earth's ionosphere with the solar wind. Hence, temporal variations associated with the external magnetic field are correlated to solar activity.

Crustal Field (Anomalous Magnetic Field): This is the portion of the magnetic field associated with the magnetism of crustal rocks. This portion of the field contains both magnetism caused by the induction of Earth's main magnetic field and remnant magnetization (Thomas, 2003). Mathematically it can be expressed by:

$$B_T = B_{ext} + B_{\text{int}} = B_{ext} + B_D + B_{rm} \qquad (3.15)$$

where B_T is the total magnetic field, B_{ext} is external magnetic field, B_D is dipole field, which is mainly generated by the fluid outer core and Brm is the field of rock magnetism.

3.2.4 Temporal Variation of Earth's magnetic field

It was recognized that the earth's magnetic intensity changes its direction slowly and irregularly. Later measurements at magnetic observatories showed many changes in the magnetic field that have shorter periods than those originally observed. This temporal variation may be resolved into secular variation, diurnal variation and variations due to magnetic storms.

Secular variation: These are long-term (changes in the field that occur over years) variations in the main magnetic field that are presumably caused by fluid motion in the Earth's outer core. These variations occur slowly with respect to the time of completion of a typical exploration magnetic survey; as result .these variations will not complicate data reduction efforts.

Diurnal variation: These variations in the magnetic field that occur over the course of a day and related to variations in the Earth's external magnetic field. This variation can be 20 to 30nT per day and accounted for when conducting exploration magnetic surveys. Diurnal variations are believed to be caused by electric currents induced in the Earth from an external source.

Magnetic storms: Magnetic activity, occasionally in the ionosphere will abruptly increase, the occurrence of such storms correlates with enhanced sunspot activity. The magnetic field observed during these times is highly irregular and unpredictable, having amplitudes 1000nT. Magnetic surveying should be discontinued during such storms because of the impossibility of correcting the data collected for the rapid and high–amplitude changes in the magnetic field (Kearey, Brooks and Hill, 2002).

3.2.5 Magnetics Surveys Instrument

Magnetic field measurements are carried out with magnetometers. Magnetometers measure horizontal and/or vertical components of the magnetic field or the total field. There are two main types of resonance magnetometer: the proton free-precession magnetometer, which is the best known, and the alkali vapour magnetometer. Both types monitor the precession of atomic particles in an ambient magnetic field to provide an absolute measure of the total magnetic field (F). The proton magnetometer has a sensor which consists of a bottle containing a proton-rich liquid, usually water or kerosene, around which a coil is wrapped, connected to the measuring apparatus (Reynolds, 1997). Proton precession magnetometers measure the total intensity of the Earth's magnetic field vector at a resolution of 0.1–1nT (Kirsch, 2009).

3.2.6 Magnetic field survey procedure

The aim of magnetic survey is to investigate subsurface geology on the basis of anomalies in the Earth's magnetic field resulting from the magnetic properties of the underling rocks. A survey can be performed on land, at sea and in the air. Consequently, the technique is widely employed and the speed of operation makes the method very attractive (Kearey et al., 2002). Magnetic measurements are performed in grids or on profiles. Repeated magnetometer readings at base station have to be performed to record periodic and non periodic magnetic fluctuations related with ionospheric processes (Kirsch, 2009).

The method involves the measurement of variations in the total magnetic field of the earth, caused by local differences in the magnetization of the subsurface rocks and soils. The greatest

application in engineering studies is it locates boundaries between rocks, which display magnetic contrasts, such as faults or dykes. Significant progress has been made in the mathematical modeling of magnetic data, particularly of the variations in 1-D visualization. It is also possible to produce 2-D geological models from the magnetic data (McDowell et al., 2002).

In ground based surveys, it is important to establish a local base station in an area away from suspected magnetic targets or magnetic noise and where the locale field gradient is relatively flat. A base station should be quick and easy to relocate and reoccupy. The precise approach to the survey will depend on the type of equipments. If a manual push button proton magnetometer is deployed, the exact time of occupation of each station is needed and at least three reading of the total field strength should be recorded. Each of the three values should be within ± 1or 2nT and then an average of these three readings is calculated. As the survey progresses, the base station must be reoccupied every half an hour in order to compile a diurnal variation curve for later correction. Next to data entry, where required, there should be any comments about the terrain or other factors that may be considered to be important or relevant to subsequent data processing and interpretation (Reynolds, 1997).

3.2.7 Magnetic Data Reduction

The Earth's magnetic field changes over a daily period and these are what are called the diurnal variations. These are caused by changes in the strength and direction of currents in the ionosphere. On a magnetically quiet day, the changes are on average around 50nT but with maximum amplitudes up to 200nT at the geomagnetic equator (Reynolds, 1997). Therefore, one effect that must be compensated in magnetic survey is the variation in intensity of the geomagnetic field at the Earth's surface during the course of a day which is diurnal variation. It can be corrected by installing a constantly recording magnetometer at a fixed base station within the survey area by visiting a base station periodically (Lowrie, 2007).

The geomagnetic correction is a technique that removes the effect of geomagnetic references field from the survey data. The most rigorous method of geomagnetic correction is the use of the International Geomagnetic Reference Field (IGRF) (Kearey et al., 2002). For small sized area of investigation only diurnal corrections could be applied (Kirsch, 2009). The total field anomaly (ΔB) is calculated based on the following formula from the observed magnetic data (B_{obs}), the diurnal variation (δB) which, will be generated from the base station measurement and the dipole field (B_d) which will be determined from the international geomagnetic reference field.

$$\Delta B = B_{obs} \pm \delta B - B_d \tag{3.16}$$

3.2.8 Analytical Signal

Due to the dipolar nature of the geomagnetic field, magnetic anomalies observed anywhere other than the poles are asymmetric even when the causative body distribution is symmetric. This property complicates the interpretation of magnetic data. Reduction to the pole (RTP) is a technique that converts magnetic anomaly to symmetrical pattern which would have been observed with vertical magnetization. Analytical signal is a suitable quantity that can be calculated in frequency domain and its magnitude is independent of the magnetization direction thus; it can be used as RTP operator. Analytical signal is formed through the combination of the horizontal and vertical gradient of the magnetic anomaly. The analytical signal has a form over causative body that depends on the location of the body (horizontal coordinates and depth) but not on its magnetization direction (Roest et al., 1992).

In the reduction to the pole procedure, the measured total field anomaly is transformed into the vertical component of the field caused by the same source distribution magnetized in the vertical direction. The acquired anomaly is therefore the one that would be measured at the north magnetic pole, where induced magnetization and ambient field both are directed downwards (Blakely, 1995). The amplitude function of the analytical signal is defined as the square root of the squared sum of the vertical and two horizontal derivatives of the magnetic field anomaly:

$$|A(x,y)| = \sqrt{\left(\frac{\partial M}{\partial x}\right)^2 + \left(\frac{\partial M}{\partial y}\right)^2 + \left(\frac{\partial M}{\partial z}\right)^2}$$

where |A(x, y)| and M are the amplitudes of the analytic signal and the magnetic anomaly field intensity respectively. This signal exhibits maxima over magnetization contrasts, independent of the ambient magnetic field and source magnetization directions (Salem et al., 2002).

3.2.9 Magnetic properties of rocks and minerals

Magnetism of rocks is related with the magnetism of the rock forming minerals. Diamagnetic minerals like quartz and calcite have negative susceptibilities of the order of 10^{-5}. Minerals like feldspars and micas are paramagnetic and have higher (positive) susceptibilities ($10^{-4} - 10^{-2}$). The positive susceptibility of ferromagnetic minerals like magnetite ($k \sim 1 - 10$) is even larger by some orders of magnitude and in general most important for the magnetization of rocks (Kirsch, 2009).

Magnetic susceptibility is an extremely important property of rocks and to magnetic exploration method. The whole rock susceptibility can vary considerably owing to a number of factors in addition to mineralogical composition such as alignment and shape of the magnetic grains dispersed throughout the rock (Reynolds, 1997).

However the susceptibility of a rock mainly depends on its magnetite content. Sediments and acidic igneous rocks have small susceptibilities whereas basalts, dolerites, gabbros and serpentinites are usually strongly magnetic. Weathering generally reduces susceptibility because magnetite is oxidized to hematite. The susceptibilities, in rationalized SI units, of some common rocks and minerals are given in Annex- III (Milson, 2003).

CHAPTER - FOUR

GEOLOGICAL, HYDROGEOLOGICAL, LANDSLIDE AND GEOPHYSICAL INVESTIGATIONS OF THE STUDY AREA

4.1 Detailed geological investigations of the study area

4.1.1 Regional Geology

Several pulses of volcanic activity, which were related or preceded by major tectonic movements, were identified (Zanettin et al., 1974). Epierogenic uplift of the Afro-Arabian plate during Early Tertiary has given rise to the East African swell. The cause of this uplift is related to mantle plume, whose decompression resulted in temperature rise and melting. As a result, out pouring of enormous quantities of basaltic magma that gave rise to first eruption of the Ethiopian Flood Basalt Province has occurred (Mengesha et al., 1996).

However, currently available geochemical database strongly suggests that it was not until Late Eocene or Early Oligocene that wide spread volcanism, which formed the Trap Basalts of Ethiopia, was initiated. These early flood basalts now cover extensive regions of the NW and SE plateaus. The central Ethiopian plateau, within which the study area is located, is part of the NW Ethiopian plateau and the western margin of the Main Ethiopia Rift.

Tertiary volcanic rock of central Ethiopia plateau consists of Aiba basalt, Alagi rhyolites and basalts, Tarmaber basalt and Balchi rhyolites (Zanettine, 1974). The Alagi series contain interbeded layers of rhyolites and basalts with an age range of 32 to16 Ma. (Oligocene-Miocene) overlying the Aiba basalts (34-28 Ma; Middle -Upper Oligocene).

The Alagi rhyolites are first silicic rocks emitted in the central eastern Ethiopia plateau making up large ignimbrite unit lying directly on the Aiba basalts or inter-layered in varying quantities with the Alagi basalts (Zanettine et al., 1974). The Aiba basalt is a thick cover of flood basalts out poured on the Ashangi peneplain as a result of distensile crustal movement. The Tarmaber basalt that covers the Oligocene Alagi is termed as Tarmaber Meghezez basalt (Late Miocene). Except Tarmaber basalts, the Alagi volcanics and the Aiba basalts are formed by fissural type of volcanism.

According to Mengesha et al., (1996), the geology of the central Ethiopia plateau consists predominantly of alkali basalts with interbedded pyroclasts and rare rhyolites erupted from fissures. The upper part of these groups is more tuffaceous, containing lacustrine deposits and acidic volcanics.

4.1.1.1 Regional structures

The Southern Afar Rift is bounded by the Somalian Escarpment in the south, the Ali-Sabieh Block in the east, the Tendaho–Gobaad discontinuity in the north and the Main Ethiopian Rift to the west. This zone is a transition zone between the central Afar and the Main Ethiopian Rift and it is structurally characterized by: (1) North to Northeast trending dominant structures in the West, and East-West trending in the East (Beyene & Abdelsalam, 2005) (2) Northwest-trending transfer fault zones which can be traced to discontinuities in the western Ethiopian escarpment (Hayward & Ebinger, 1996). (3) The kinematically distinct Gulf of Aden normal faulting pattern (trending due to East-Southeast) found in the Southern part (Tesfaye, et al, 2003) as cited in Asmelash Abay (2012).

In general in this zone the three important structures, namely the NW-SE trending structures (parallel to the general trend of the Red sea); NE - SW trending structures (parallel to the main Ethiopian rift) and the E-W trending (parallel to the Gulf of Aden) are joined. The western bounding rift margins, where the study area is situated is characterized by this three important regional structures controlling the deep seated landslides along the rift margins, e.g. the Debresina landslide of September 2005 (Asmelash Abay, 2012).

The rift floor and its escarpments are highly faulted. The faults in the MER are parallel and sub-parallel to the NE–SW trending rift axis (Gidey Woldegebriel et al., 1990). The rift floor is affected by several faults that form smaller horst and graben structures. The NNE-SSW and N-S trending faults are the dominant faults.

4.1.2 Local Geology

4.1.2.1 Introduction

The project area has different tertiary volcanic rocks and quaternary superfacial deposits and these different units are briefly described below.

4.1.2.2 Aphanitic basalt

This rock unit crops out in the north western, western and eastern part of the project area. It also outcrops in the continuous cliff forming escarpments. It is characterized by moderately to steep cliff forming topography, which directly overlies the underlying pyroclastic rocks. Its thickness increases from central to western part and attains a maximum of 250 m.

The rock has pinkish gray in weather color, dark gray in fresh color, fine grained texture volcanic rock. It appears massive but it is highly weathering due to jointing and fracturing. It is characterized by different secondary structures like fractures, joints and shear zones (Figure 4.1). They are more intense as one goes from the central to the western part.

Figure 4.1 Fractured and weathered aphanitic basalt rock exposed at northeastern side of the area.

4.1.2.3 Vesicular basalt

It is exposed in the northern and western part of the study area. In the western side of the study area it is massive but in the northern part it is highly weathered and jointed rock unit. This weathering becomes very intense at the base where the rock is entirely changed to soil. The unit is columnarily jointed and rock falls are associated with these columnar joint. The rock has light gray weathered, dark gray fresh colored and fine to medium grained rock (Figure 4.2). It shows rounded to sub-rounded vesicles whose max size reaches up to 8 cm. Vesicles are filled-up by greenish and reddish brown secondary minerals, which could be zeolite and hematite, respectively.

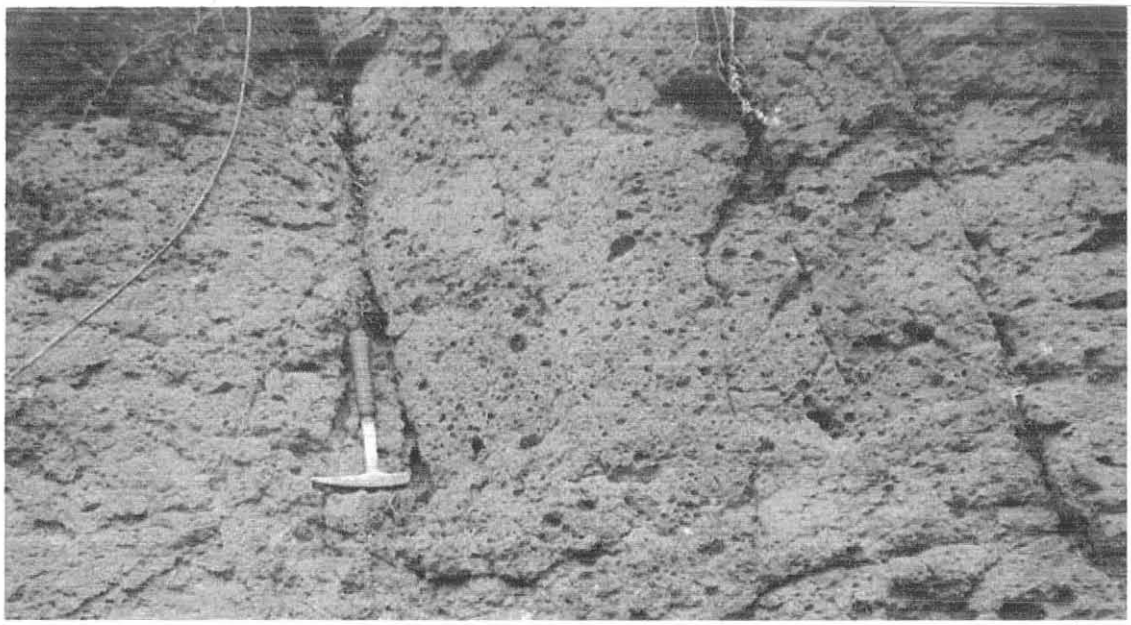

Figure 4.2 Jointed vesicular basalt rock at central part of the study area.

4.1.2.4 Ignimbrite

It is moderately to strongly stratified, often massive looking rock. Outcrops are always interlayered with the basalt and are exposed at various horizons. At different locations, this rock type has variable thicknesses. The lowest and highest thicknesses are observed in the western part, whereas in the central and southern part it is moderately thick. In the western part the thickness of this rock ranges up to 20 m, whereas in the southern part reaches up to 7m. It has yellowish gray weathered, light gray fresh colored and fine to medium grained rock unit (Figure 4.3). In western part of the study area it is strongly compacted but it highly jointed and weathered in the northern part. The fiamme and lithic fragments contained in this rock are highly aligned parallel to the plane of stratification.

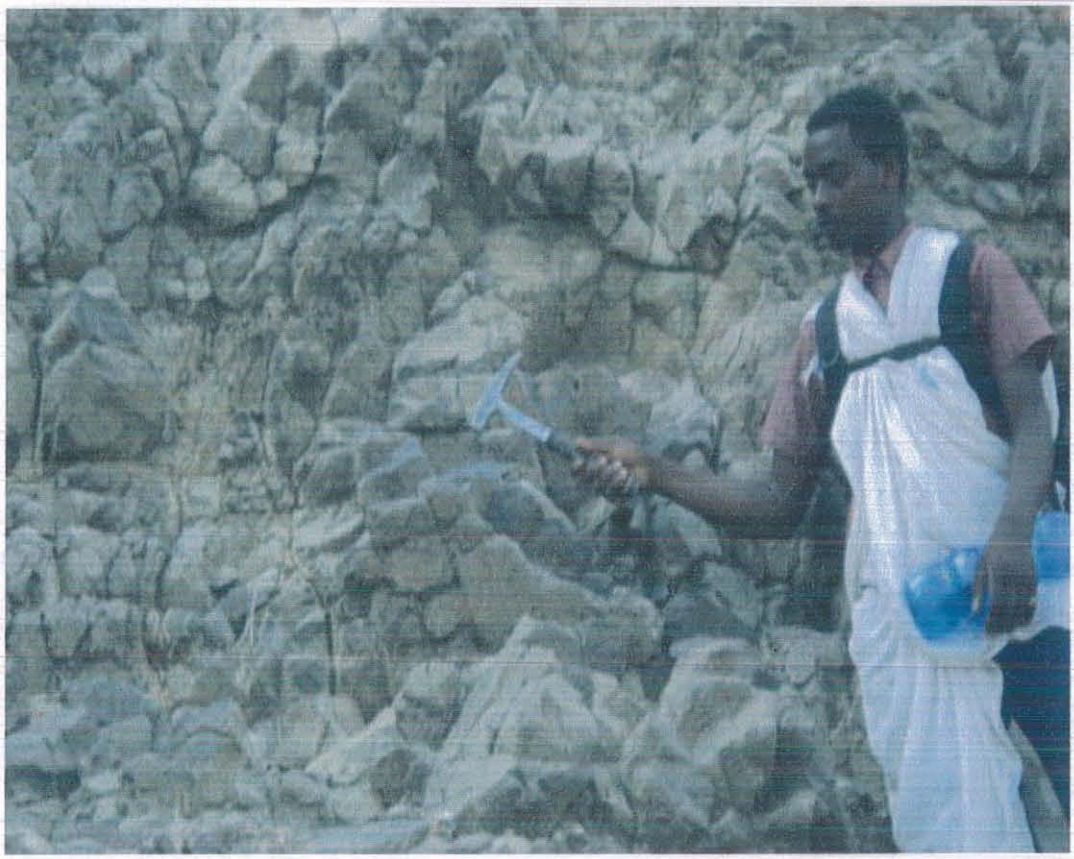

Figure 4.3 Fractured ignimbrite rocks located in between Sar Amba and Armania small towns.

4.1.2.5 Interlayered aphanitic basalt, rhyolite and ignimbrite rocks

This unit conformably overlies the underlying basaltic rock and crops out in the western part of the study area at UTM location of 587236E and 1091497N. The thickness of this rock unit approximately reaches up to 90m. The rhyolite and ignimbrite are closely interlayered each other whereas the basalt usually caped the two rocks. Detail description is presented below (Figure 4.4).

Rhyolite: it is layered and massive looking, brownish weathered and light gray fresh color and fine to medium grained rock. Joints as well as fractures are also present on this rock. Thickness of this rock was approximately reaches of 25m meters. This rock is inconsistently weathered and the weathered surface shows yellowish gray, brownish gray and dark gray color.

Ignimbrite: it is light gray to dark gray colored, fine to medium grained, highly compacted as well as well stratified rock. Often, it is subjected to two sets of joints; which are systematic and random type of joints. Its thickness approximately reaches up to 20m. The ignimbrite characteristically consists of fiamme, which is highly elliptical and aligned parallel to the stratification.

Aphanitic basalt: it is moderately to highly weathered stratifying rock. Layering is commonly sub-horizontal. The lowest and highest thicknesses are observed in the top and bottom part this lithological succession which is 15m and 30m thick respectively. Joints and fractures are observed in this type of rock. It has dark gray to bluish gray color, and fine grained texture.

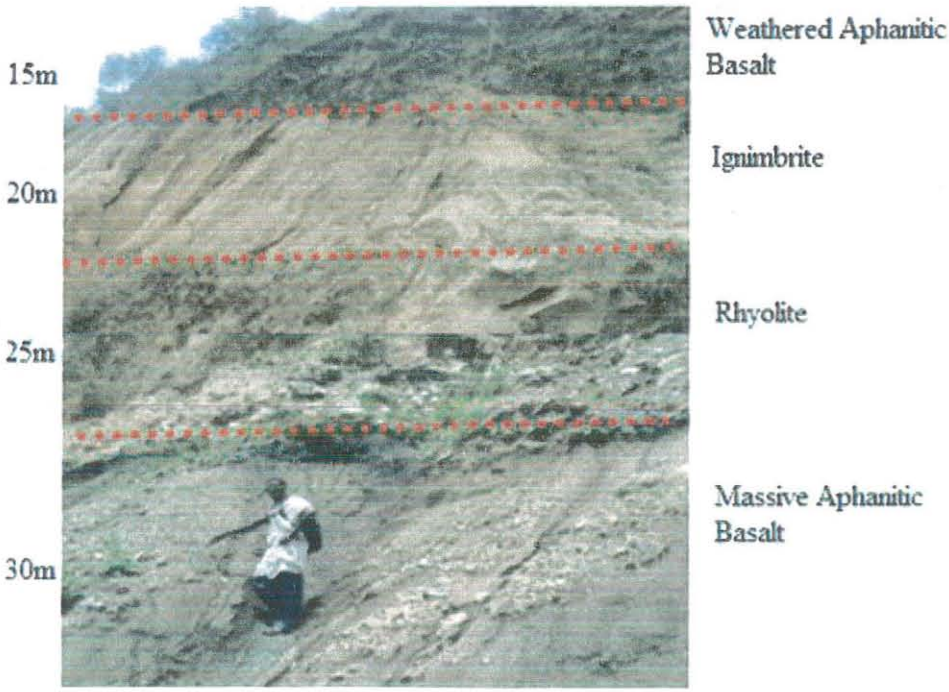

Figure 4.4 Lithological intercalations at western side of the study area (587236E, 1091497N).

4.1.2.6 Tuff

This pyroclastic unit is exposed at western and north western portion of the study area. It is characterized by whitish color and fine-grained texture (Figure 4.5). The tuff unit of the study area is relatively light in weight.

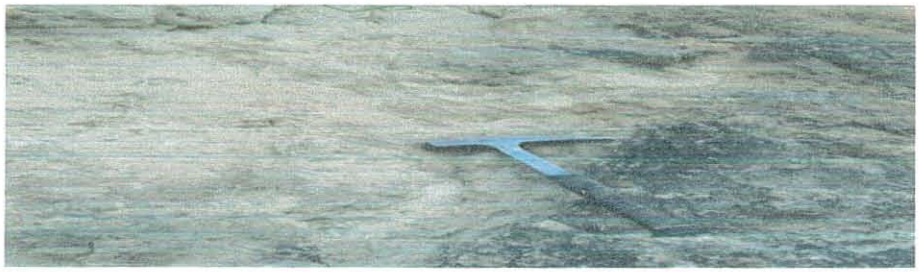

Figure 4.5 Tuff rock units at western side of the study area.

4.1.2.7 Quaternary sediments

These were exposed at the central, northwestern and northeastern part of the study area. These sediments were composed of cobbles, sands, silt and clay sized soil particles derived by weathering and erosion of different rocks. These deposits were mostly thick residual deposits and there were also some deposits of colluvium-eluvium and alluvial soil deposits in northwestern, eastern and northern part of the study area. The residual soils have formed from insitu weathering of parent materials. In western side of the study area colluvial soils are deposits that displaced from their original location of formation by gravity forces. It was easily observed from river and road cuts; the thickness of these deposits was ranged from 2m up to 20m throughout the study area.

Figure 4.6 Residual clay soils at Shola Wuha locality of the study area showing the deep near vertical fissures.

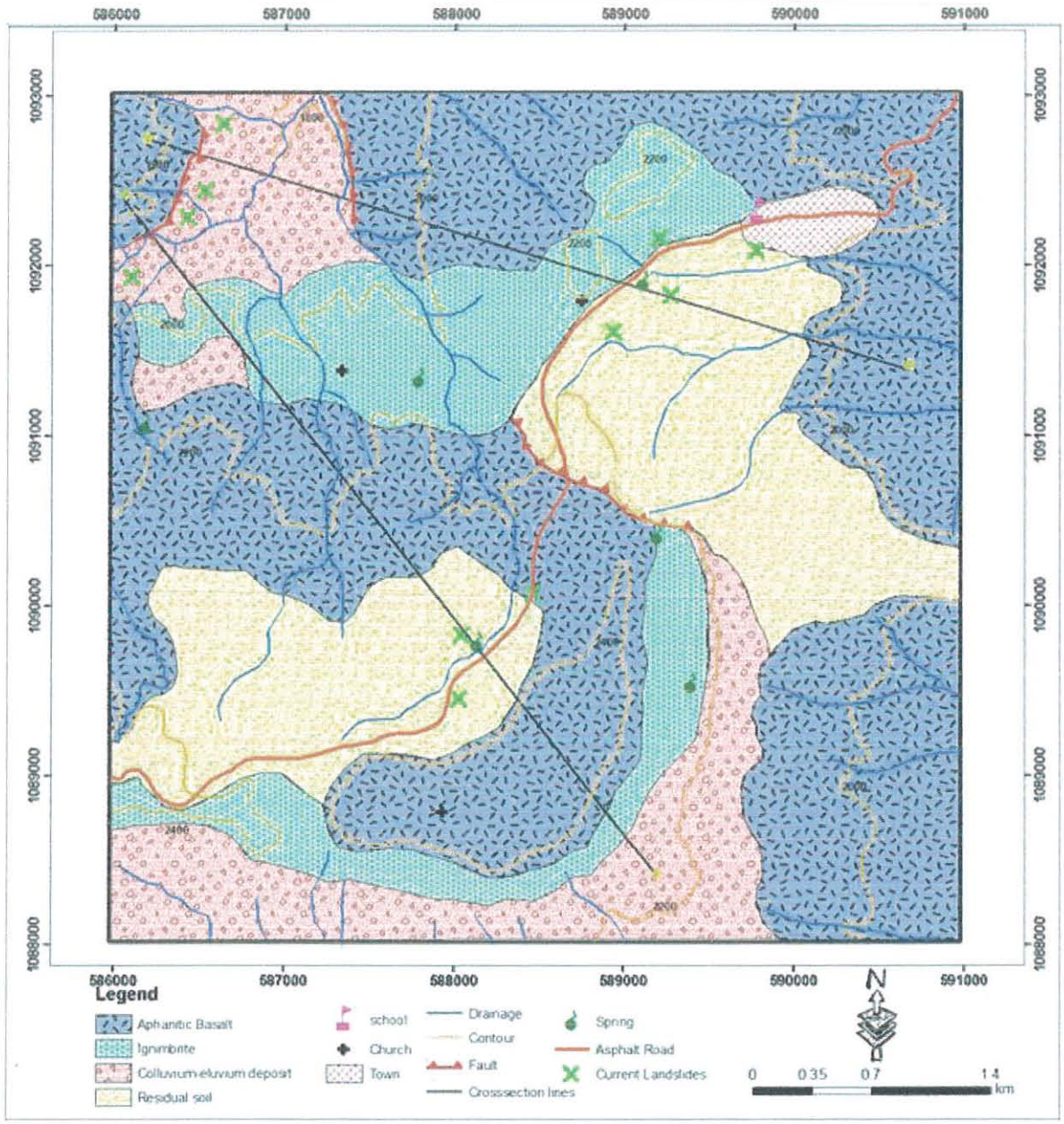

Figure 4.7 Geological map of the study area.

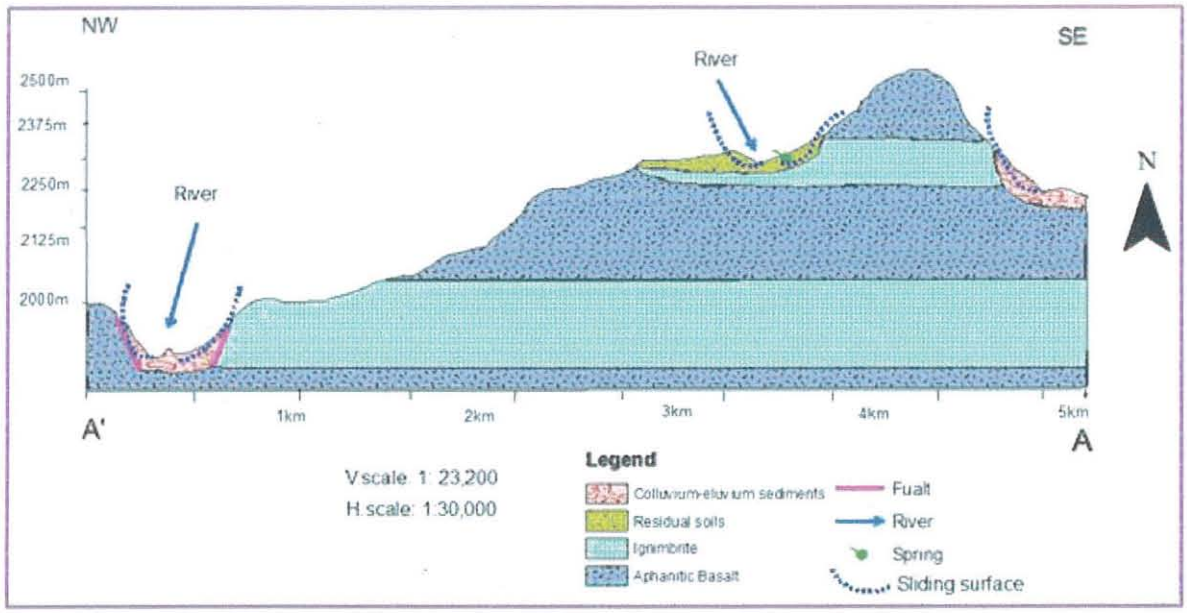

Figure 4.8 Geological cross-section along line A-A'

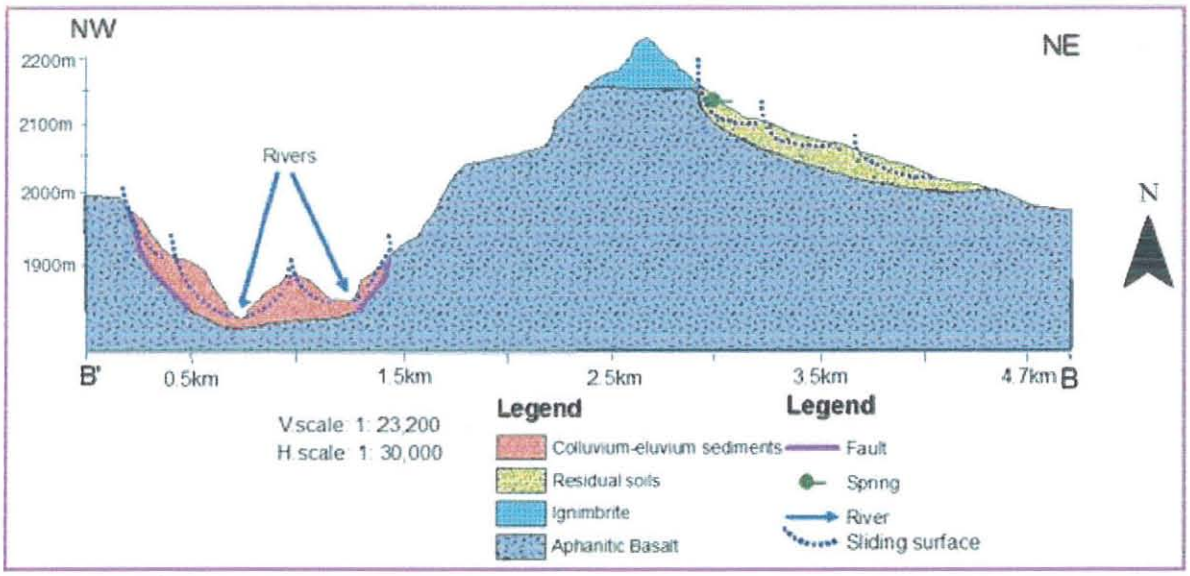

Figure 4.9 Geological cross-section along line B-B'

4.1.3 Local geological structures

In the project area, various structures such as joints, fractures, stratifications, lineaments as well as faults are observed.

4.1.3.1 Joints

The most commonly joint types observed in the study area are columnar joints (Figure 4.10) and normal systematic joints which were 30cm spaced and 20cm aperture. They can be one factor for the sliding problem of the study area.

Figure 4.10 Columnar joints observed in vesicular basalt at location of (588301E and 1091179N).

4.1.3.2 Faults

These structures are observed specially in the western part of the study area. The normal faults are megascopic structures, which have characteristically NNE-SSW and are parallel to the MER trend. They are discontinuous boundary faults that give rise to major fault-escarpments separating the rift depression from the Ethiopian plateau. These faults are normally long, widely spaced and are characterized by large vertical offsets (Figure 4.11).

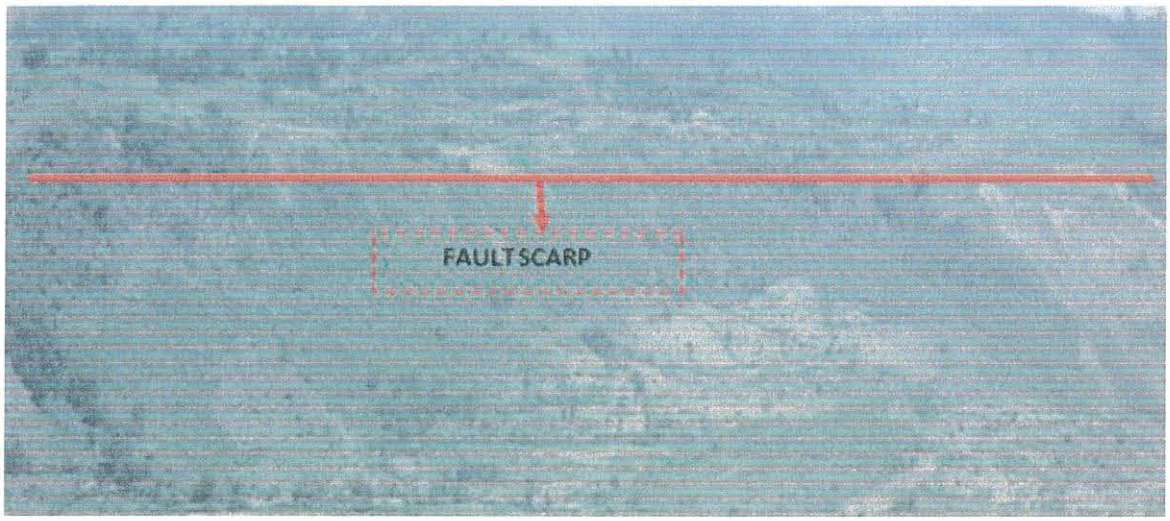

Figure 4.11 Fault escarpments at the western side of the study area.

4.1.3.3 Dykes

There are number of basaltic dikes with strike orientation of NW-SE exposed at southern side of the study area (Figure 4.12). These dikes have an average width of 1 to 2 meters. These are weak zones which were used as channel of basaltic lavas flows to the surface.

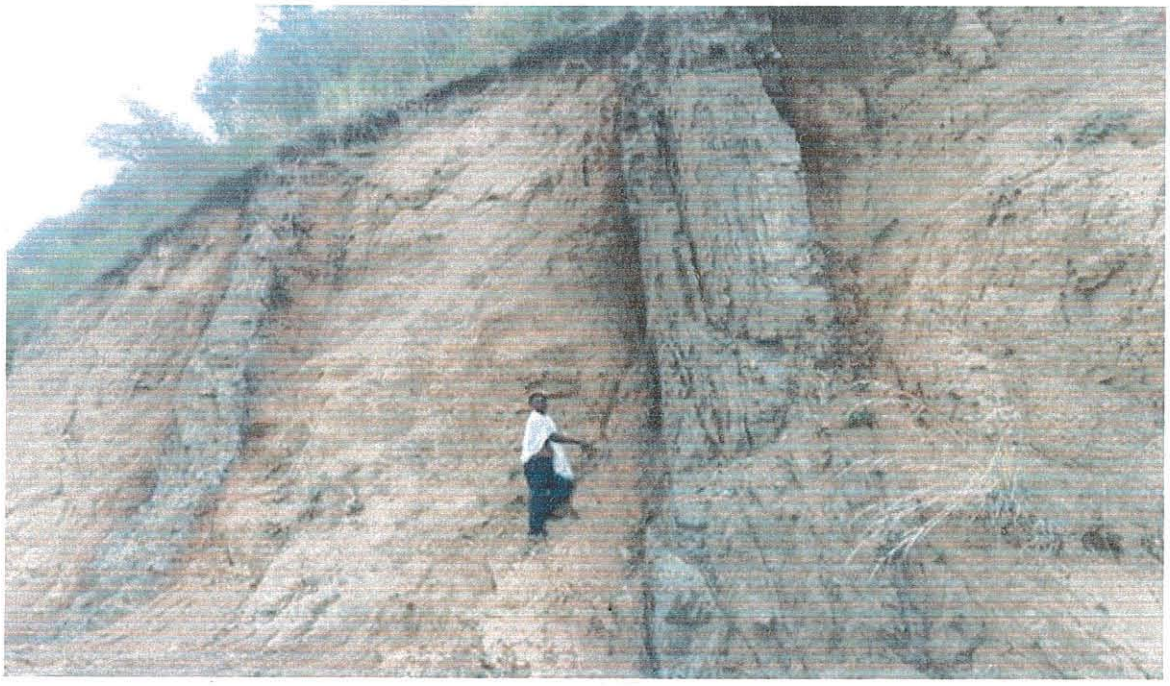

Figure 4.12 Dykes at the southern side of the study area (587578E, 1088507N).

4.2 Hydrogeological investigations of the study area

Hydrogeology plays a major role in controlling the occurrence of landslide in the study area. However, there are no boreholes data and other relevant studies that indicate the ground water level of the study area. Therefore, the hydrogeology was discussed based on the field observation of perennial streams and a number of springs of the study area.

4.2.1 Rainfall

Rainfall is one of the most important factors in triggering landslide conditions. The rainfall of the study area is characterized mostly by one long rainy season that last from June to September. The data measure at Debresina rain gauge station indicates the maximum annual rainfall was 727.2mm which was recorded in August, 1997; while the minimum was 0mm almost in most of the years starting from October up to February. The highest average monthly rainfall was also 432.65mm which was recorded in the month of August. The highest average annual rainfall was 201.8mm and recorded at the year of 1998 over the past 33 years recorded data at Debresina station (Annex-I). The sliding problem of the study area particularly at the main road was happened following intense rainy seasons.

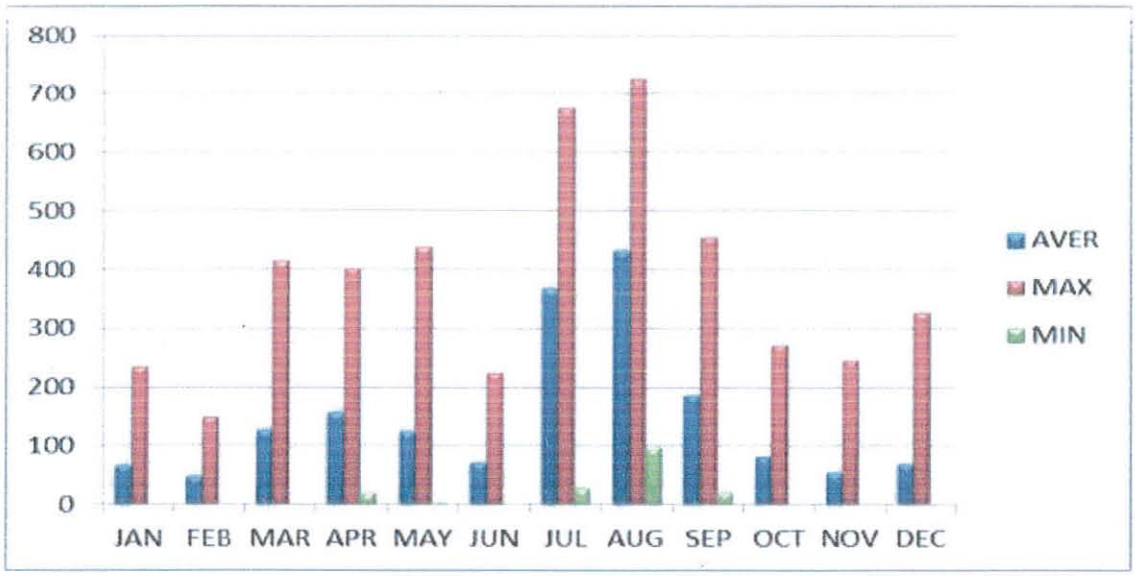

Figure 4.13 Bar graphs showing average, maximum and minimum monthly rainfall of the last 33 years at Debresina station (1980-2012).

4.2.2 Springs

The springs in study area have high discharge and many distributions. During the field work six springs were inventoried in the study area. The two springs are along the down road of the study area which have significant role in landslide of the main road. The observed springs were generally slope control and perennial; increase their yields drastically from dry to rainy season. They flow out in significant amount and can carry huge amount of debris. The springs are functionally helpful for water supply and other domestic purpose (Table 4.1).

Table 4.1Inventories of springs in the study area

Number of springs	UTM location		Elevation(m)	Mode of occurrence	Local place	Their important
	X	Y				
1	588199	1089672	2297	Slope control down the road	Shola Wuha	Free flow
2	589202	1090405	2216	structural control	Ayalfush	Water supply for Chira meda and Armaniya
3	586170	1091061	2074	Slope control	Alihudade	Water supply for local peoples
4	587790	1091340	2051	Slope control	Abil Amba	Water supply for local peoples
5	589120	1091906	2122	Slope control down the road	biera	Water supply for local peoples
6	589402	1089550	2224	Slope control	Zeb Amba	Free flow

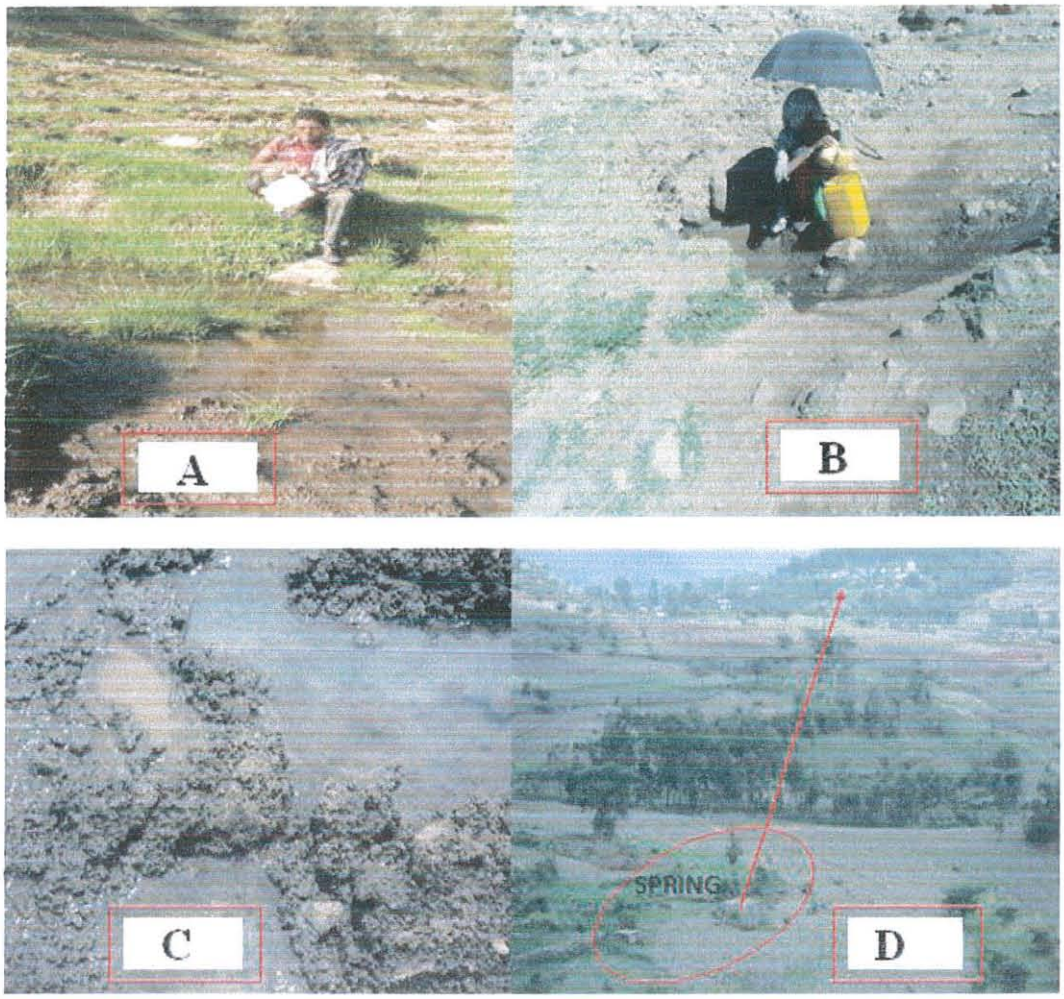

Figure 4.14 Photos showing some of the springs and seepage in the study area: (a) seepage from down the road of Dokakit kebele: (b) spring from down the road of Tikur Chicka locality: (c) seepage from the mountain of Zeb Amba at eastern side of the study area: (d) spring at Ayalfush locality that was used as water supply for Armaniya and Chira Meda towns.

4.2.3 Surface water of the area

There are a number of perennial streams flowing out from the study area. In the northeastern side of the study area which is around Armania town, all the streams are flowing into Meka main river. From field observation, these rivers have significant role in inducing landslide problem at the section of the main road and its localities.

The other rivers namely Koda Menkeriya, Nech Amba and Teter are found in northwest direction of the study area. They flow out from the area into Dem Aytemashy Main River. This locality also affected by sliding problem following the direction those streams.

All the streams found in southern side of the study area are also flowing out towards the Shenkorge main river. Generally, all these streams, springs and rainfalls have important role in inducing landslide problems.

4.3 Landslide investigations of the study area

The study area is characterized by different types of landslides but the abundant occurrences are rotational types. These rotational landslides are located especially at southern, western and northeastern direction of the study area.

4.3.1 Types of landslide in the study area

4.3.1.1 Rock slide

These are occurred mostly at the road cut of northeast of the study area. They are observed on slopes where competent and relatively less competent rocks are in contact (Figure 4.15). They vary in size from very small to large blocks of rocks.

Figure 4.15 Rock slides at main road of study area

4.3.1.2 Rock falling

The study area consists of individual rock blocks that detached from a steep slope and descending by falling or rolling and coming to rest on gentler slopes in the area. Where these occur frequently, the bedrock is usually moderately to highly fracture with parallel and intersecting discontinuities with slopes. The falling of rocks varies in size mostly as a single rock, single block, mass of blocks and often occurs rapidly without warning. The whole main asphalt road of the study area has rock falling problem and the drainage system is disturbed by this kind of problem (Figure 4.16).

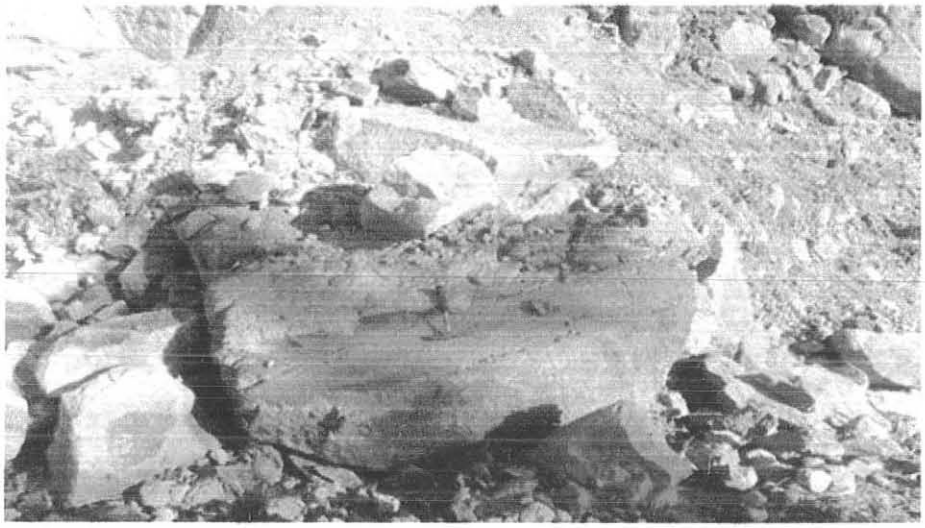

Figure 4.16 Rock falls at main road of study area

4.3.1.3 Rotational slides

These slides in the area are common at steep slopes especially during the periods of intense rainfall. They tend to be deep failures and occur along planes of weakness between overlying colluvial soils and highly weathered rocks. Recently, these have started at gentle slopes of the main road. Rotational slides are usually where sliding material moves along a curved surface and develop from tension scars in the upper part of a slope (Figure 4.17).

Figure 4.17 Tensional cracks down the road at Shola Wuha locality

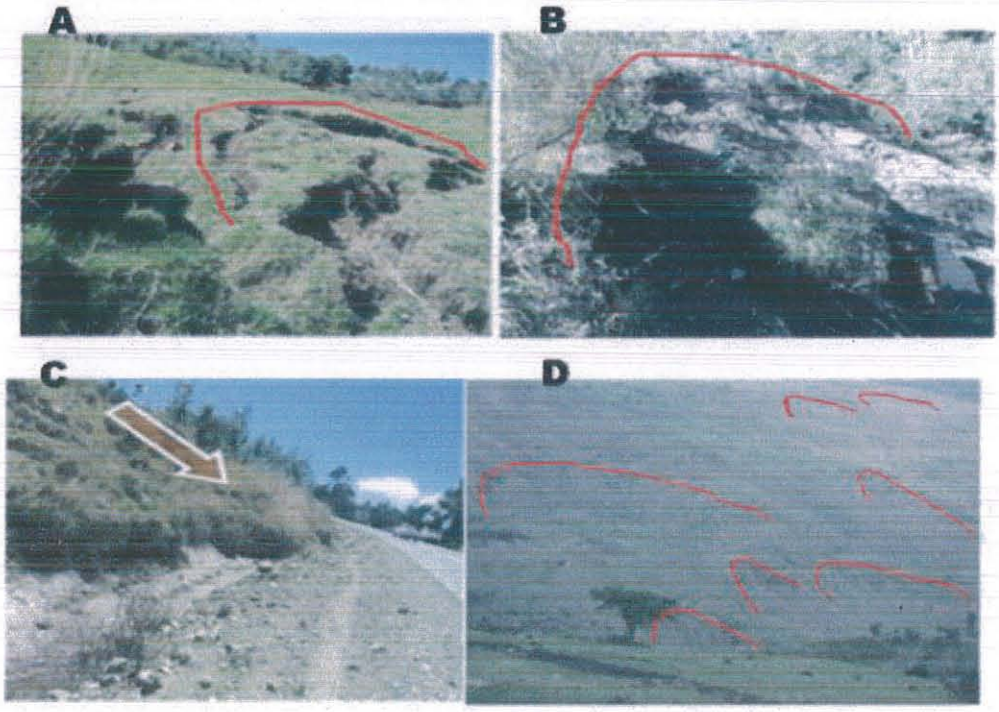

Figure 4.18 Different types of rotational landslide: A&B are slides down the road at Shola Wuha locality; C) slide occurred above the main road at Shola Wuha locality and D) many rotational slides at northwestern near Shotel Amba locality.

4.3.2 The causes of landslide in the study area

From the field observations, the sliding problem in the area is due to the highly weathered geological lithologies, topography, hydrology and human activities which are some of the most

important factors that have caused landslides in the study area. Deforestation for housing, agricultural activities, search for building material and road construction have generally assumed to be the preconditioning agents of slope failure in the area. Based on the all rounded information and interpretations the major factors which influence the slope stability are described below.

4.3.2.1 Geological causes

The geological rocks in the study area were highly affected by intense and deep weathering conditions and this considered as one of the main cause for landslide problem. Thus, the lithological map of the study area has been prepared from the intensive field surveys. The main lithological units of the study area are aphanetic and vesicular basalts, ignimbrite, tuffs, and quaternary sediments (alluvial, colluvial and residual soils). The ignimbrites and tuffs are highly altered and weathered and when they get water, they lose their shear strength and serve as lubricant for other overlaying lithology. Therefore, the degree and depth of weathering of each lithology have significant role for landslide initiations in the target area.

4.3.2.1.1 Geological structures

These structures were interpreted and compiled from satellite images geophysical and geological field work surveys. Since the study area is found at the Afar Rift Margin which is worldwide known for its extensional tectonic movement and normal faults, then, faults are very important factor for the landslide problem of the study area. The western side of the study area is affected by active landslide problem because of the N-S directional fault. This part of the study area has a steep slope mountain by the action of fault and drainage system below it.

4.3.2.2 Topographical causes

4.3.2.2.1 Slope steepness

This is an important factor to cause landslide problem. In most landslides of the study area, steeper slopes have a greater chance of sliding problem but landslides are also common in the gentler slopes. The slope map of the area is derived from the 30m DEM using the slope function of the spatial analyst of ArcGIS 9.3. A map of slope classes is generated by grouping the slope angles into three major classes (figure 4.19). The landslide in the area has occurred in all classes of slopes but dominant at the higher slope of the area.

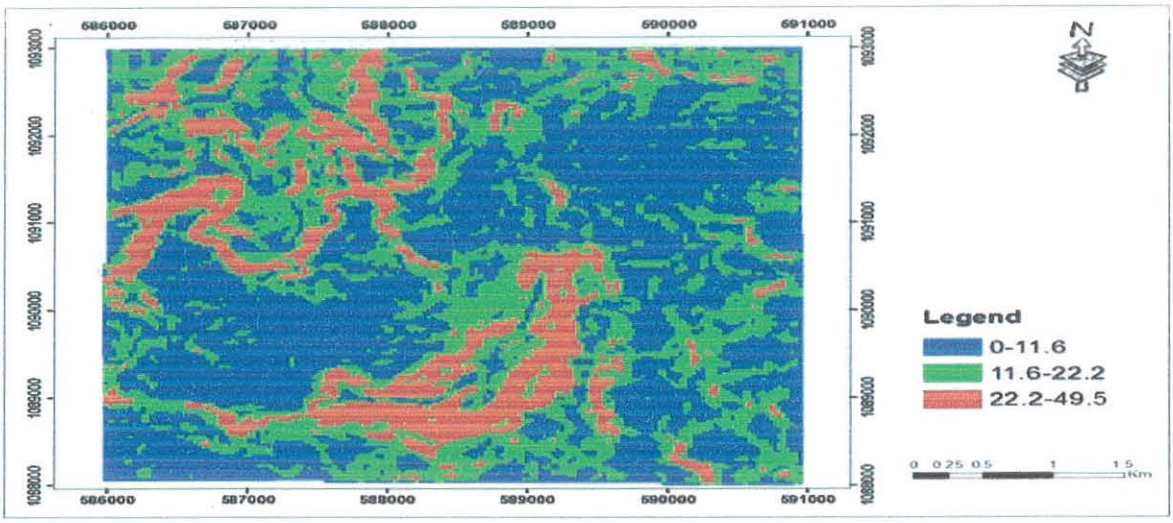

Figure 4.19 Slope map of the study area.

4.3.2.3 Hydro-meteorological causes

This plays a crucial role in landslide initiation. Some of the major significant hydrologic processes are discussed as follows:

4.3.2.3.1 Drainage systems of the study area

The drainage systems in study area outflow in all directions. Most drainage systems of the area have been created following the geological structures. The tectonic morphology of the study area is greatly modified by stream cuts, which finally could influence slope stability by over steepening the lower sections of the slopes and removal of materials that provided support at the toe. For this reason the drainage was considered as one causative factor in the landslide problem study.

4.3.2.3.2 Springs

Generally, the mountains of the study area are the sources of different springs. The main road of the interest area has also many seasonally and perennial springs which are emanates under the road. From the field observations, the main asphalt road is already failed to direction of the place where the springs are located. The study area has a higher potential of springs and groundwater and these are used as a lubricant and also can produce water pressures that cause landslides.

4.3.2.3.3 Rain fall

The slopes in the study area were mostly influenced by intermittent springs, rivers and high precipitation during rainy season. The most common trigger of landslide is sufficient water input

during precipitation events. The mobilization of debris material during debris flow events is related either to the onset of sediment transport due to water runoff or to slope failures caused by an increase in pore-water pressures. Both runoff formation and slope instabilities are a function of rainfall intensity and cumulative precipitation or water input in another way.

4.3.2.4 Seismically causes

Earthquake is one of the principal triggering factors of landslides that cause great hazard to both of life and properties loss. The geological structures like dykes and faults of the study area are important situation for earthquake happening. Interviews with local people also confirmed that earthquake shake was felt around the study area. Thus, the most probable triggering factor for the landslide is the earthquake. Earthquakes reduce stability by imparting both a shearing stress and a reduction in resistance to slope material. The earthquake shocks may be responsible for triggering new landslides and reactivating old landslides.

4.3.2.5 Impact of landslide on the study area

The landslide problems caused by several factors have also several impacts on the property and main road of the locality of the study area. The principal impact of was cracking and subsidence of the main road starting from Shola Meda up to Armaniya town which is around 3km coverage of the main road of the study area. Particularly at Shola Wuha locality (588353E, 1089748N), the landslide is active and the landslide scarps remains 90cm to reach the main asphalt road as shown in the first photographs of Annex-V. The remaining main road of the study area was also cracked and subsided in many parts of the localities (Annex-V).

The other impact of landslide in surrounding of the main road in the study area was also cracking of the foundation of national electric poles and many local houses of the study area (Annex-V). Most of the local houses have cracking of wall and floor and many of the residents change their houses to other palace. The national electric poles of the study area have also highly damaged particularly the poles at Shola Wuha and Tikure Chika localities which have cracked and subsiding foundations and have the tendency to fall down.

4.4 Geophysical investigations of the study area

4.4.1 Electrical Resistivity Tomography (ERT)

4.4.1.1 ERT Data Acquisition and Instrumentation

Three profiles were surveyed to collect ERT data parallel to the main road of study area. Profile-1 covers 360m horizontal distance and the other two profiles also cover 450m each. The ERT survey was conducted to study the subsurface condition of the road in order to delineate the sliding surface and also provide information about the associated processes on the basis of the contrasts in the subsurface resistivities.

The electrical resistivity data was collected using the IRIS instruments SYSCAL R1 plus Switch 72 resistivity meter that utilizes 72 electrodes, through interconnectable four reel cables accommodating 18 electrodes each, 72 short connector wires and two reversible connector boxes (Figure 4.20). The cables used in the particular instrumentation have pick up/connection points spaced at 5m. The instrument records automatically with a present format uploaded into the unit and the system takes measurements almost independently once the arrays are laid along the profile.

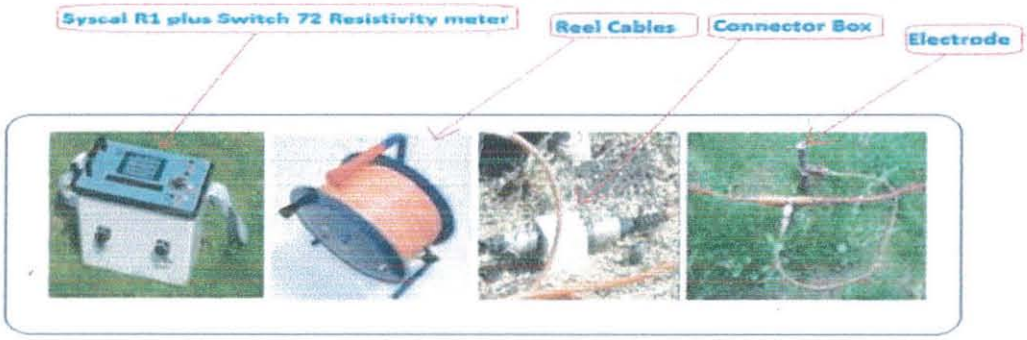

Figure 4.20 Instrumentation of 2D electrical imaging.

Reel cables are connected each other with connector boxes and each cable outlet is connected to electrode by the connector wires. A twelve volt external battery was used for this survey. In the survey, the instrument is normally put at the center, where the deepest depth is recorded, and the four cables reels spread on both side of the resistivity meter. The two cables are in one side of the resistivity meter while the other two are spread on the other side of the resistivity meter (Figure 4.21).

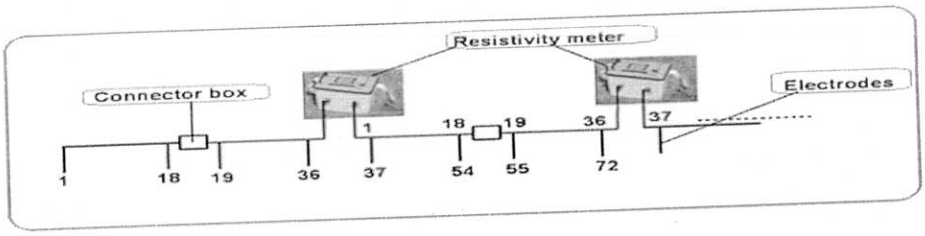

Figure 4.21 General Field layout of 2D electrical imaging, the bottom electrodes for the main sequence where as the top electrodes for the roll along.

The three parallel profiles are about 50m apart. The first profile (P_1) is 100m distant above the road and it is surveyed by one main sequence which covers a horizontal distance of 360m. The other two profiles P_2 and P_3, which are parallel to P_1, are positioned above the road and down the road respectively. These two profiles P_2 and P_3 are surveyed by one main and one roll along sequences which covers a horizontal distance of 450m and contains 945 data points each. The main sequence contains 648 data points covering 360m horizontal distance while each of the roll along sequences contain 297 data points covering a horizontal distance of 90m.

Table 4.2 Acquisition parameters for the ERT survey.

Parameter	ERT Profile 1	ERT Profile 2	ERT Profile 3
Electrode spacing (m)	5	5	5
Length of profile (m)	360	450	450
Depth of investigation (m)	65	65	65
Number of electrodes	72	90	90
Number of data points	648	945	945
Array type		Schlumberger Wenner	
Equipments		SYSCAL R1 Plus Switch 72	
Sequence type	Main	Main and Roll Along	Main and Roll Along

4.4.1.2 Data Processing and Presentation

The data generated at field from each main and roll along sequences are downloaded to a computer using the Prosys-II software. Then the data from each roll along sequence is added to the main sequence before the processing stage with the help of this software. After the summation, the summed data is filtered, by automatic filtering, and the noisy data is rejected. Finally the filtered data is saved in the Prosys-II software in ".dat" form and exported to RES2DINV software for processing. An automatic iteration process that fits the modeled data with the calculated one proceeds to analyze the data. The final output of RES2DINV software, the inverted 2D model resistivity section, is the processing product of 2D survey (Figure 4.22). Finally such figures are used for interpretation purpose and to correlate the results of 2D imaging analysis with results of other methods.

The data obtained in the prosys–II software is started from 90m for each roll along. Because of this, the roll along sequences were adjusted with proper distance before add to the main sequence. In the case of roll along one the data started from 90m, so no distance adjustment is needed. The second roll along sequence data sheet was recorded after 90 meter of the first roll along data; it was shifted by 90 meter after getting in the Prosys-II software. This step was continued for the rest roll along data by increasing total roll along distance by 90 meter that means 180m to the 3rd roll along, 270m to the 4th roll along and 360m to the 5th roll along. After adjusting the distance, the rolls along sequences were added to the main sequence. Topography was incorporated to the 2D electrical resistivity section because the project site is on undulating terrain.

Figure 4.22 shows, for example, the resistivity cross-sections prepared for Profiles-2 using the RES2DINV software. Good quality of data was used with RMS error of less than 8.2%. Finally the results obtained from the RES2DINV were correlated with the geological information's and magnetic profiles using the surfer 9 software.

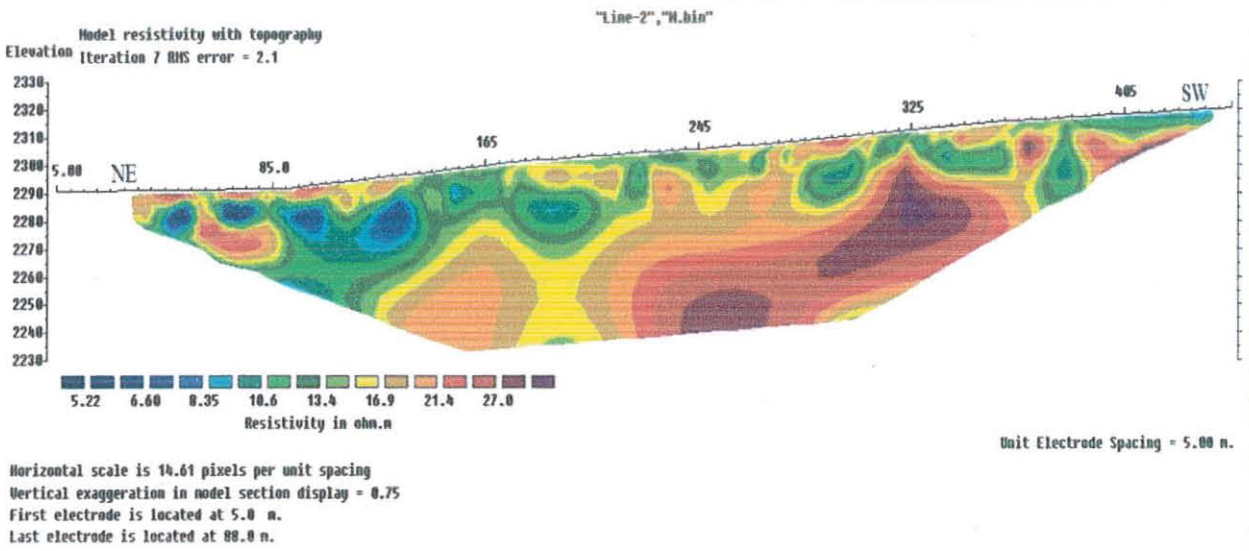

Figure 4.22 Resistivity model with topography of profile-2 resulting from a 2D inversion of data

4.4.2 Magnetic method

4.4.2.1 Data acquisition and Instrumentation

Magnetic data were collected using Proton Precision Magnetometer instrument. The surveying was stated by establishment of a base station within the study area at a place which is easily accessible and as far as possible from magnetic noise. In addition to the magnetic readings the geographic coordinates of the point at which the readings are taken and the time of reading was recorded using Global Positioning System (GPS). Similar to that of the electrical resistivity data, magnetic data were also collected along the predefined profile lines, which were used to conduct electrical resistivity surveys. In addition, magnetic data are also collected randomly within and at the boundary of the study area. Magnetic data were collected from 158 data points with average spacing of 15m along the selected profile lines and at random points. At the field survey three magnetic readings were taken for a specific point and then average of this readings were used for the processing and interpretation purpose (Figure 4.23).

4.4.2.2 Magnetic data processing and presentation

The diurnal variation was removed from the observed magnetic field data using the Microsoft excel 2010. The main magnetic field at the base station is obtained from the International Geomagnetic Reference Field (IGRF). The IGRF value of the area was 35907.61. The IGRF value at the base station is subtracted from the diurnal corrected total magnetic field of each station.

Finally, the corrected magnetic anomaly was obtained by subtracting the diurnal variation and IGRF values from the survey data. This was used for processing to produce anomaly map, profile plots, analytical, and horizontal gradient maps and finally magnetic modeling maps.

Magnetic profile data were picked up from the magnetic anomaly map corresponding to the profiles of the 2D electrical resistivity imaging lines. This helps to counter check and integrating the results from the two methods for detail interpretations.

Since the study area is found within the low latitude magnetic equator and the survey covers very small area, then the variation of magnetic field with latitude and longitude is insignificant and hence normal corrections were not done. In addition to this, in magnetic equatorial regions where inclination is less than 15 degrees, reduction to the pole is generally unstable and cannot be derived (Getech, 2007). Due to this reason reduction to the pole was not also done. Rather than reduction to the pole and normal corrections, other data enhancement technique was applied to produce magnetic map, which may help to highlight particular characteristics or features to aid qualitative interpretation. Analytic signal was done by using Geosoft software package program called MAGMAP.

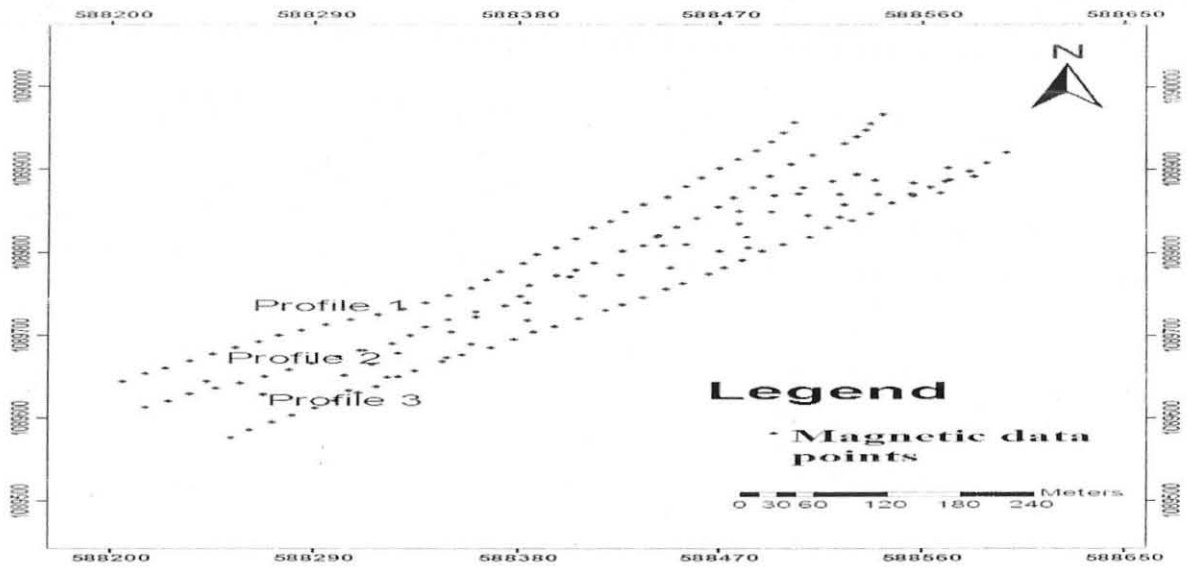

Figure 4.23 Magnetic data distribution.

CHAPTER - FIVE

RESULTS AND JOINT INTERPRETATIONS

5.1 Electrical Resistivity Tomography and Magnetic Profiles

5.1.1 Introduction

Geophysical investigations were surveyed at the above and down of the affected road, and have important information about the sliding surface of study area and geological weak zones. These results illustrate the benefits of electrical resistivity imaging techniques for characterizing the landslide problem. Since the layers in the inverse model of imaging have highly disturbed and fragmented subsurfaces, then it was difficult to correlate with the vertical lithological stratification of the study area and with magnetic profiles models. Moreover, the depth of the lithological succession was around 90m; whereas the depths of the geoelectrical tomography sections are about 65m, i.e. the depth of the geoelectrical sections is relatively smaller as compared to the depth of the geological stratifications. Because of this depth difference and deep landslide disturbance problem, the correlations of geoelectrical sections with the vertical geological layers and magnetic models were not done but the individual magnetic profiles have good correlation with electrical imaging models in indicating weak zones of the surveyed area.

5.1.1.1 Profile-1

The inversion of profile one by including topography was done after filtering and removing of the noisy data from 648 data points of the 2D electrical resistivity of profile-1, 600 data points were used for the inversion of this profile. The profile was only main sequence and with total length of the profile extended to 360m, and its inversion result is given in the Figure 5.1. The program produced a good inverse model after six iterations and 3% RMS errors. The resistivity inverse model of profile-1 has a lot of disturbed zones which have high susceptibility to slide and different geological structures that are suitable conditions for landslide happening.

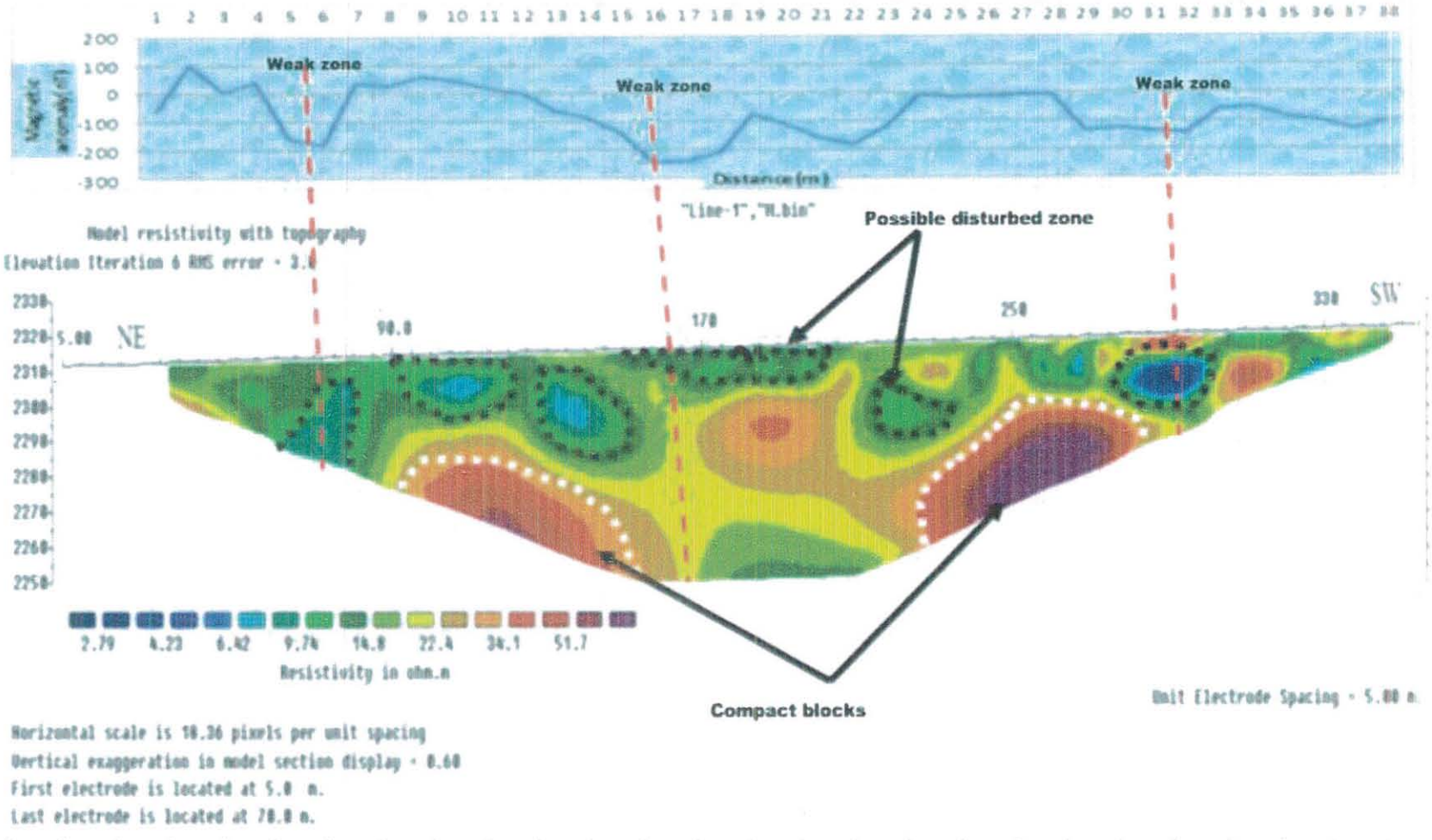

Figure 5.1 Interpretation of profile-1 a) magnetic profile, b) 2D electrical resistivity section.

The resistivity value of the possible disturbed subsurfaces and geological weak zones is very low and varies from 2.79 to 14.8 Ωm. This low resistivity in some of the areas within the profile line is possibly due to intensive degree of weathering and water percolation from the surface along the fractures. In addition to this, these resistivity ranges are the response of fragmenting and sliding surface, which is composed of expansive dark clay and highly to completely weathered basalt rock. The thickness of this disturbed and susceptible to slide surface increases from southwestern to northeastern directions.-.

The second ranges of resistivity is from 14.8 – 34.1 Ωm and this may be the response of the highly to completely weathered and fractured ignimbrite rock. This range of resistivity value has indicated subsurface geology that are easily weathered and disintegrated into fragments of blocks and the presence of weak zones. The thickness of this range of resistivity is deeper in the center of the profile and in locations where weak zones are found.

The third range of resistivity is greater than 34.1 Ωm which is the response of the compacted blocks. These massive blocks which are maybe bed rocks have dislocated at the center of the profile by the intrusion of geological structures may be faults. Depth to the compact rock is varying due to the presence of deep geological structures. It is shallower in the southwestern side as compared with the northeastern side of the 2D electrical profile.

The magnetic profile along the 2D electrical imaging of profile-1 was plotted as shown in the Figure 5.1a. This profile shows considerable amplitude variation in the magnetic anomaly signatures. The minimum negative peak value is -240.3nT at a distance of about 170m and the maximum positive peak value is 103.02nT at a distance of about 30m from the northeastern end of the line. There is a positive correlation between the magnetic anomaly plot and the 2D electrical profile in detecting the weak zones. The magnetic anomaly plot shows a presence of fractured zone at 70m, 170m and 300m of the profile which are also interpreted same from the 2D electrical imaging plot.

5.1.1.2 Profile-2

The inverted model resistivity with topography was done after filtering out the noisy data from the 945 resistivity raw data points, a total of 908 data points were used for the inversion. Integrating the main and one roll along sequences and covers 450m length of the profile to produce the inversion section plot shown in Figure 5.2. The software has applied inverse model by iterating

just seven times to yield a quality data with RMS error of 2.1 %. This profile could be classified into three ranges of resistivity value by carefully examine the entire depth resistivity informations.

The first range shows a very low resistivity anomaly that varies from 5.22 to 13.4 Ωm. This range of resistivity is almost similar to the first profile-1 which has a fragmented and sliding surface of expansive clay and highly weathered basalt rock. Like profile-1, the thickness of this resistivity range increases from southwest to northeast direction of profilr-2. The greater thickness of disturbed and sliding surface is located at northeast direction and this could be due to the high degree of weathering and weak zones along this direction.

The second range of resistivity is from 13.4 to 21.4 Ωm which may possibly the response of moderately to highly weathered ignimbrite rock. This range of resistivity is localized in between 165 and 245m horizontal distances and some extent towards SW direction. The thickness has increased at the center and decreased to SW direction. This range value has no extent towards NE direction and this may be due to sliding problem and accumulation of clay soils and slide deposits at this location. The thickness where this range of resistivity is located at this profile become greater in comparison to other profiles due to the presence of weak zones which are attributed to the intensively weathered and fractured earth materials resulting a fragments of rocks.

The third range of resistivity is greater than 21.4 Ωm which may possibly the response of massive basalt rock. This massive block of basalt rock is characterized by large depth at northeastern direction but shallower in the southwestern of the 2D electrical resistivity profile as shown in Figure 5.2. This compact rock is again broken equivalently to the massive rock mapped in profile-1. The two small blocks on the two end of the profile are dissected by weak zone and similarly, one block from the compact rock at the center of the profile is also displaced by localized structures. Therefore, the weak zone and slope factor may possibly interpret as deriving force for sliding problem at this profile and in other profile as well. The locations of these weak zones are intense at NE direction of this profile.

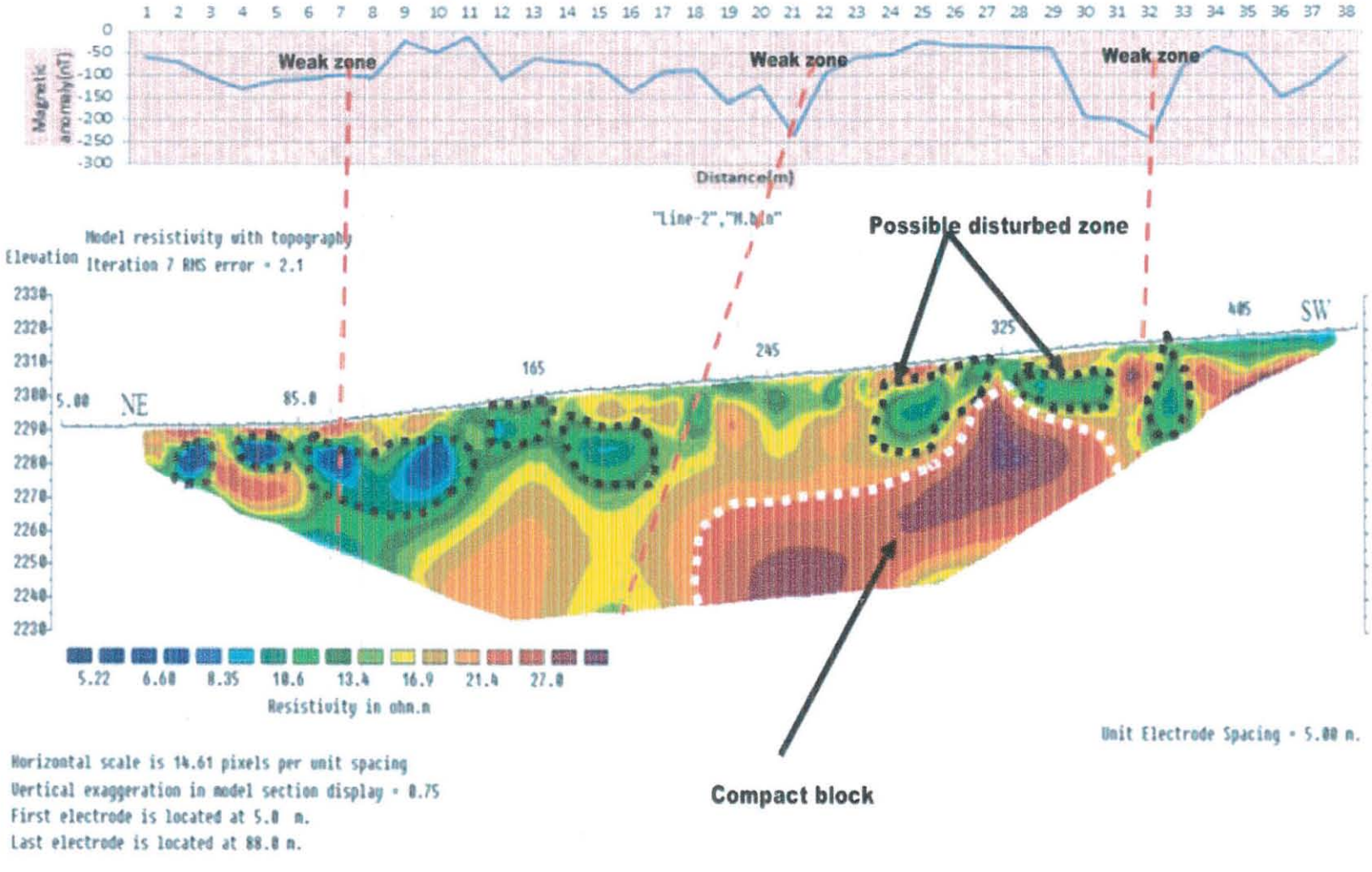

Figure 5.2 Interpretation of profile-2 a) magnetic profile, b) 2D electrical resistivity section.

The magnetic profile along the 2D electrical imaging profile-2 is also plotted as shown in the top section of the 2D image in Figure 6.2a. The extreme values whose minimum negative peak value of -235.5nT at a distance of about 185m and the maximum positive peak value of -11.15nT at a distance of about 110m from northeastern end point of the profile. The magnetic field profile almost coincides with the 2D electrical resistivity imaging model in identifying the weak zones. The magnetic profile plot shows the presence of weak zones in almost at three parts of the profile survey and these are confirmed by electrical imaging model profile.

5.1.1.3 Profile-3

An important feature of this image is the vertical decrease in resistivity with depth, where low resistivity range values are reached beyond the depth investigation of the instrument. This result suggests that the presence of massive rock at deeper depth than the other profiles. The inverted model resistivity with topography was done after filtering out the noisy data from the 945 resistivity raw data points, a total of 891 data points were used for the inversion model. The length of this profile is again 450m resulting from a combination of a main and one roll along sequences. The inversion result is shown in Figure 5.3. The software produced good inverse model after iteration of about seven times and showing a good data quality with RMS error of 2.8%. This profile could be again classified into three resistivity value ranges in agreement with the other two profiles but with great variations in depth of the resistivity range values.

The obtained inversion model with topography from this line is characterized by a high degree of disturbances and huge thickness of alluvial, colluvial and residual soil deposits. Along the profile, the low range resistivity value is varies from 4.32 to 20 Ωm and these resistivity responses are that of the dark expansive clay soil and due to intensive degree of weathering and water percolation from the surface along the fractures . As compared with the low resistivity range value in the other two profiles, this value of range is relatively thicker and localized at NE of the profile and also deposited under the fragmented boulders of basalt rock towards the southwest direction. This low resistivity soils are deposited at the whole profile especially at the lower depth and are almost absent at the shallow depth of NE direction of the profile starting from 245m and above horizontal distance. From center of the profile to the direction of NW, the disturbed and fragmented blocks are suspended and sliding following the sloped surface above this low range resistivity values.

The second resistivity range varies from 20 – 43Ωm which may be the response of the slightly to highly weathered and fractured ignimbrite rock. Generally, the thickness of this value in NE

direction is disappeared and there is an indication of this resistivity value in the SW direction of this profile.

The third resistivity value is found only at shallower depth of SW direction of the profile with highly fractured, fragmented and weathered blocks that shows a significant resistivity variation within it. The suspended blocks that have this resistivity range value have the tendency to slide down the slope especially in NE direction of the profile.

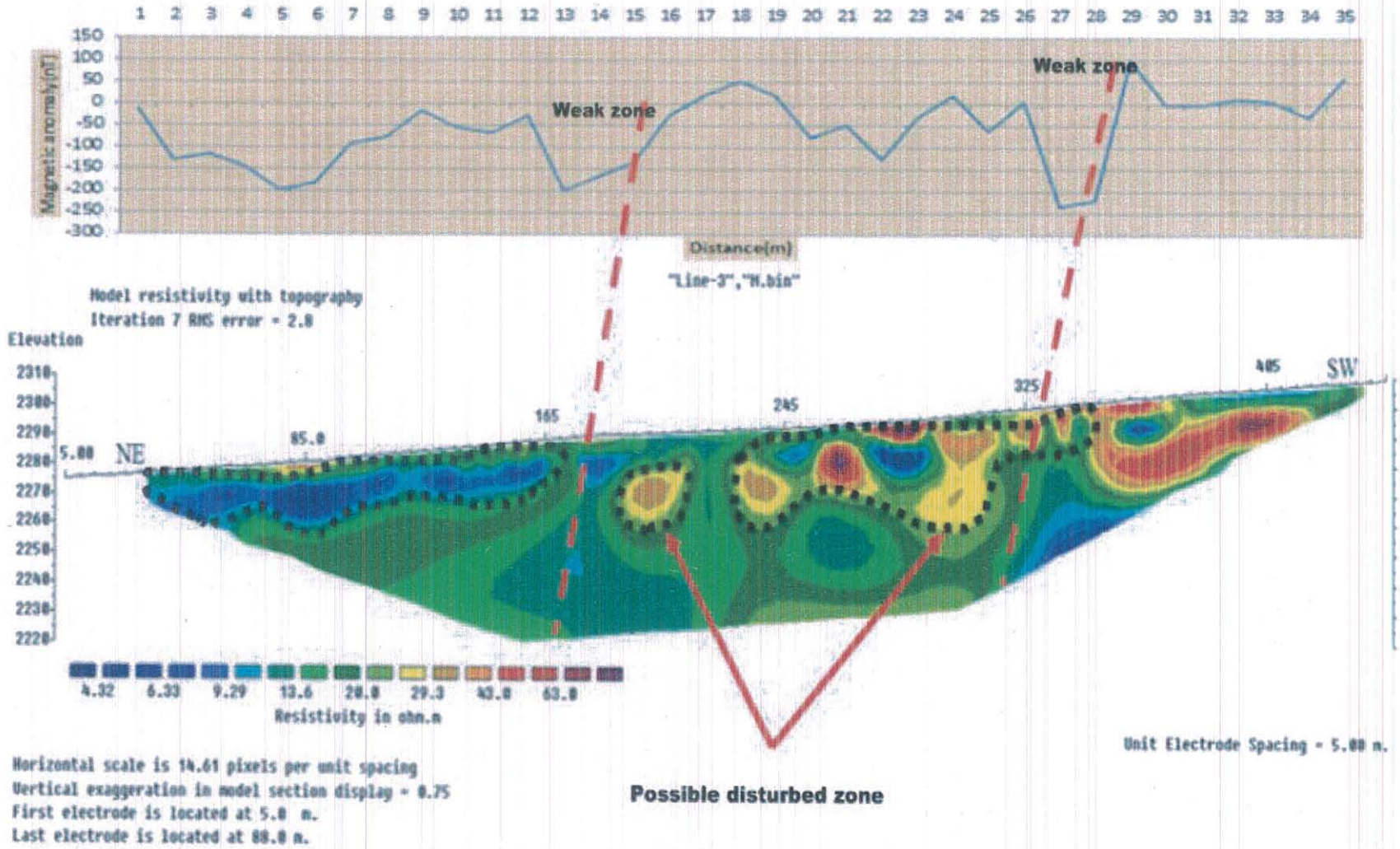

Figure 5.3 Interpretation of profile-3 a) magnetic profile, b) 2D electrical resistivity section.

There is also very low resistivity zone at the bottom of the third resistivity range value of SW direction of the profile. Generally, the low resistivity range is dominantly cover almost the whole profile horizontally and vertically extents which may possibly due to high degree of weathering and water percolation from the surface along the fractures.

Magnetic profile along the same line on which 2D electrical imaging of profile-3 was plotted as shown on the top of the inverted resistivity model (Figure 5.3a). The minimum negative peak value is -233.5nT at a distance of about 325m and the maximum positive peak value is 96.3nT at a distance of about 360m from the initial station position on the northeastern side of the line. The magnetic field profile roughly coincides with the 2D electrical resistivity profile plot to identify the weak zones. The magnetic profile clearly shows the presence of two fractured zones which could also be interpreted same to other two 2D electrical resistivity sections.

5.1.1.4 Combination of the 2D electrical resistivity profiles

Figure 5.4 illustrates how the three 2D electrical resistivity sections of profile-1, profile-2 and profile-3 can be arranged horizontally to give a full of representation of the area. This way of representation is important to understand the continuity of the sliding surface and weak zones within the survey area. The plot clearly depicts that there is continuous fractured zone within the three profiles shown in Figure 5.4. There are also possibly rotational sliding shallow subsurfaces in all the three profiles. The there is an occurrence of landslide especially in northeast direction of profile three which clearly correlate with failure section of the road.

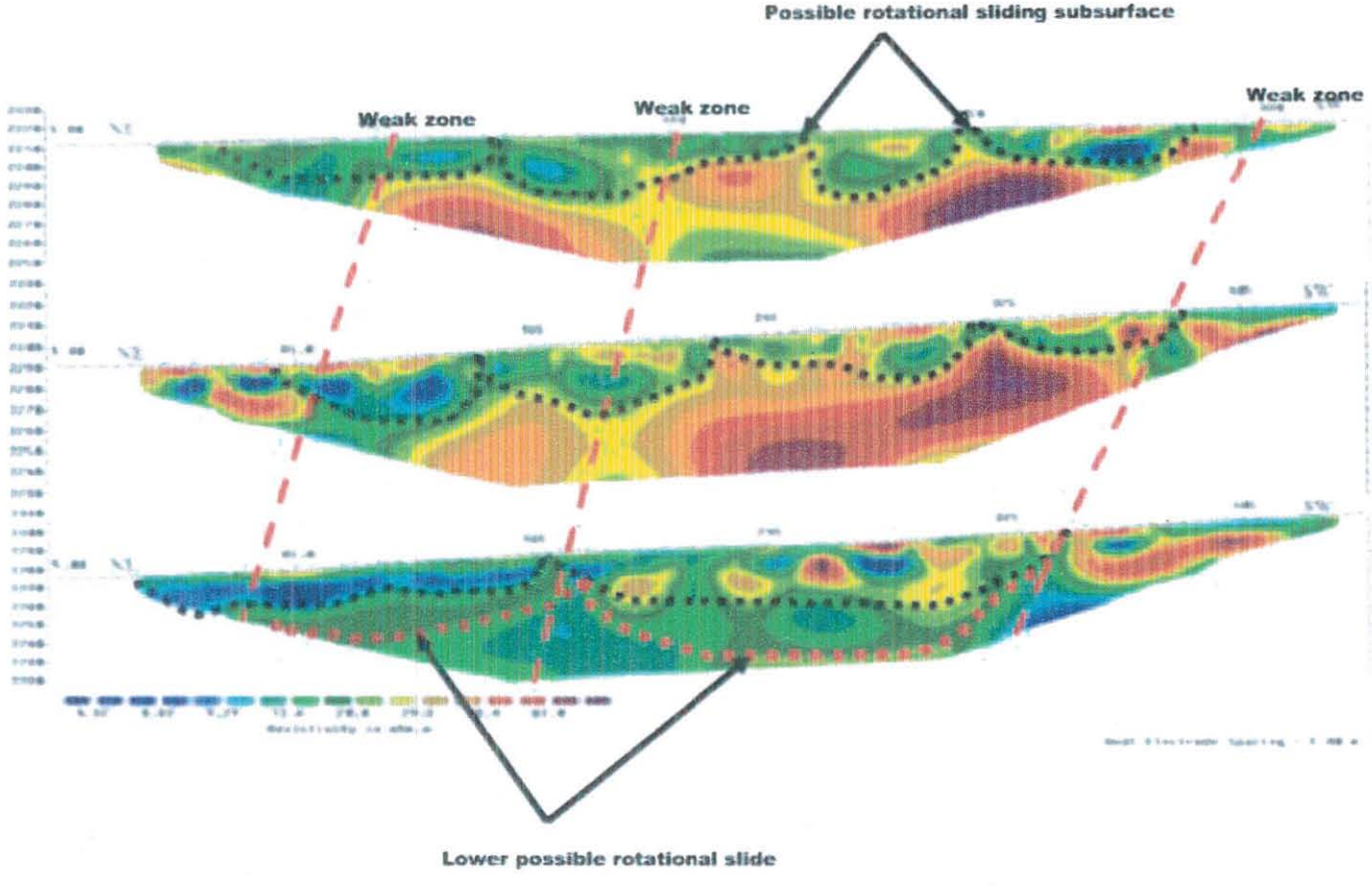

Figure 5.4 the net representation of Profile-1, Profile-2 and Profile-3 together with their sliding subsurface.

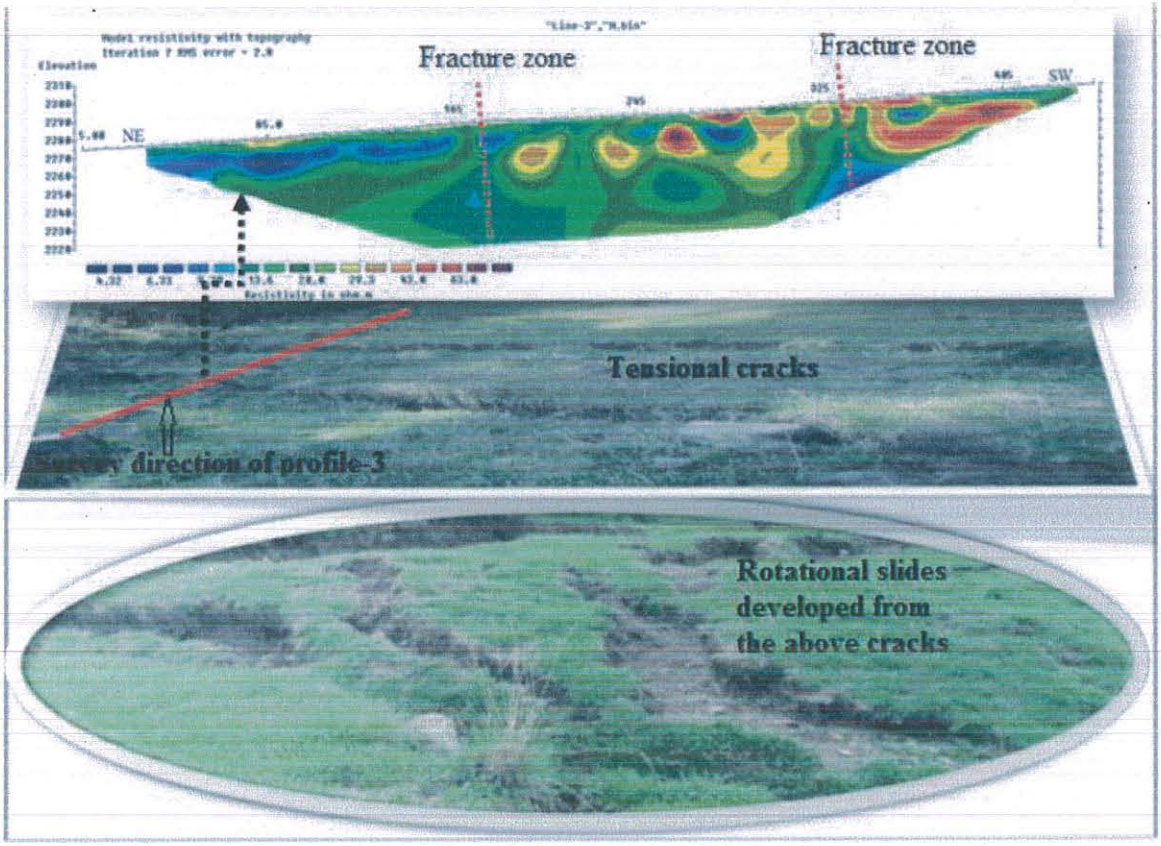

Figure 5.5 correlating of model resistivity of profile-3 with the surface sliding problem of the main road

5.2 Magnetic Data Interpretation

Magnetic survey is very helpful in identifying geological structures and contact zones of different lithologies. Therefore, the corrected data is then processed using different software and different maps and models were produced like magnetic anomaly maps, analytical signal map, tilt derivative and 2D magnetic models. Finally, these maps and models are interpreted as follows;

5.2.1 Total Magnetic Intensity map

The raw magnetic data were corrected for diurnal variation and removal of anomalous instrumental readings through close examination of the data. IGRF determined values were then used to reduce the resulting data to the magnetic anomalies. The data that is produced from the corrected magnetic data is given with the magnetic anomaly map of the survey area as shown in Figure 6.6. From the magnetic anomaly map, the subsurface condition shows that high and low magnetic response corresponding to the presence of high and low magnetic materials. The high magnetic anomaly response is probably due to the result of massif basalt rock and covers more in the southwestern and some in central part of the study area.

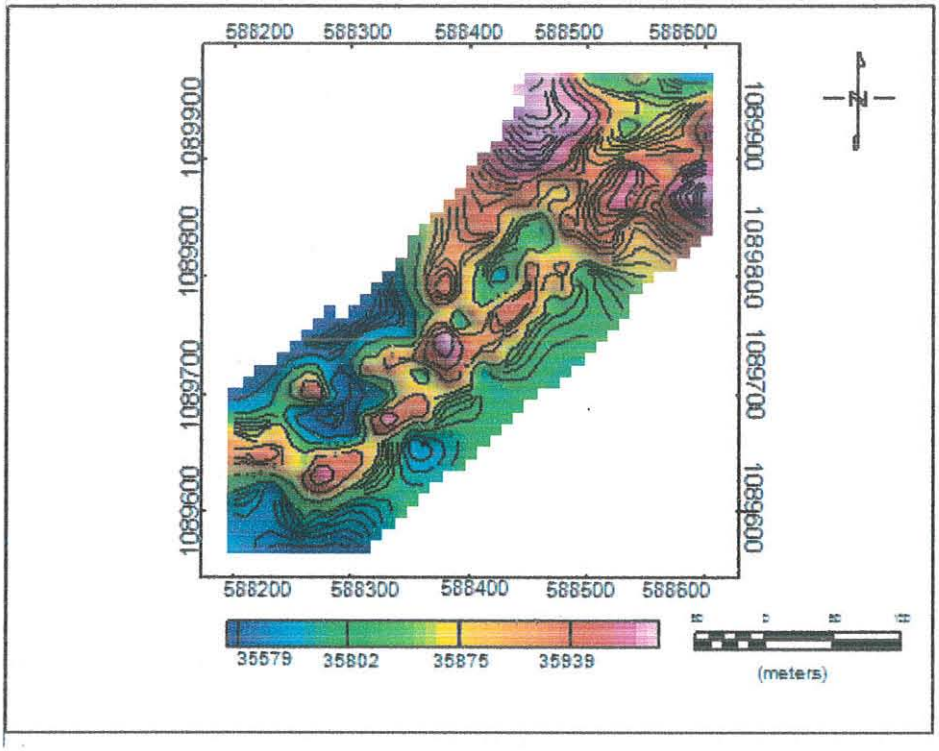

Figure 5.6 Total Magnetic Intensity map of the study area.

The intermediate and low magnetic anomalies zones may be the response of jointed, fractured and weathered basalt and ignimbrite rocks and the overlain colluvial deposits as well. It covers almost the northeastern and central parts of the survey area.

5.2.2 Analytical signal map

From the magnetic data it was possible to construct an analytical signal map shown in Figure 5.7. The map shows the responses of anomalous bodies just from the upper part of their sources. The analytic signal map is well resolved for shallow anomaly sources but may not be as such well resolved for deep sources and is good at locating the edges of shallow bodies. The amplitude of the simple analytical signal peaks (maxima) over magnetic contacts does not depend on the directions (inclinations) of magnetization. In addition to these, the map shows zones within the survey area associated with geological contacts.

This analytical map shows that the anomalous bodies are in northeastern part of the survey area. From this map one can indicate the failure surface and possible sliding surface of the study area.

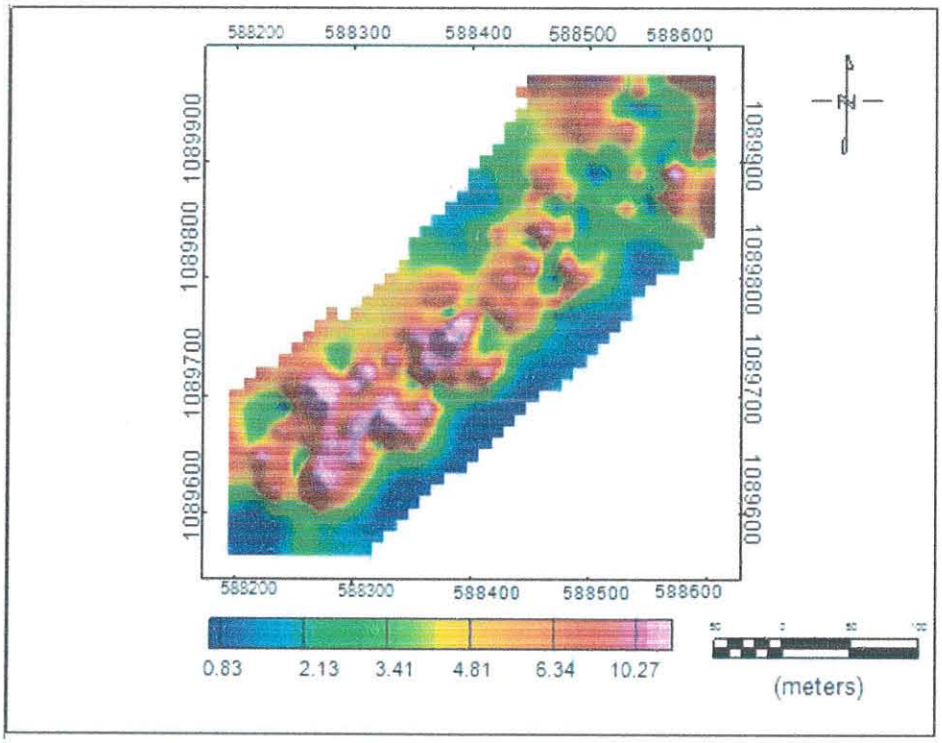

Figure 5.7 Analytical signal map of the study area.

5.2.3 Horizontal gradient map

This map is important for edges detection of magnetic causative bodies. It is also important to enhance lithological changes, structural regimes, deformation styles and trends. The horizontal gradient map of the study area was developed by 45° gradient direction which is counter clockwise from +X axis. The map shows that two linear features in center and southwestern part of the survey area that are may be fractures or faults.

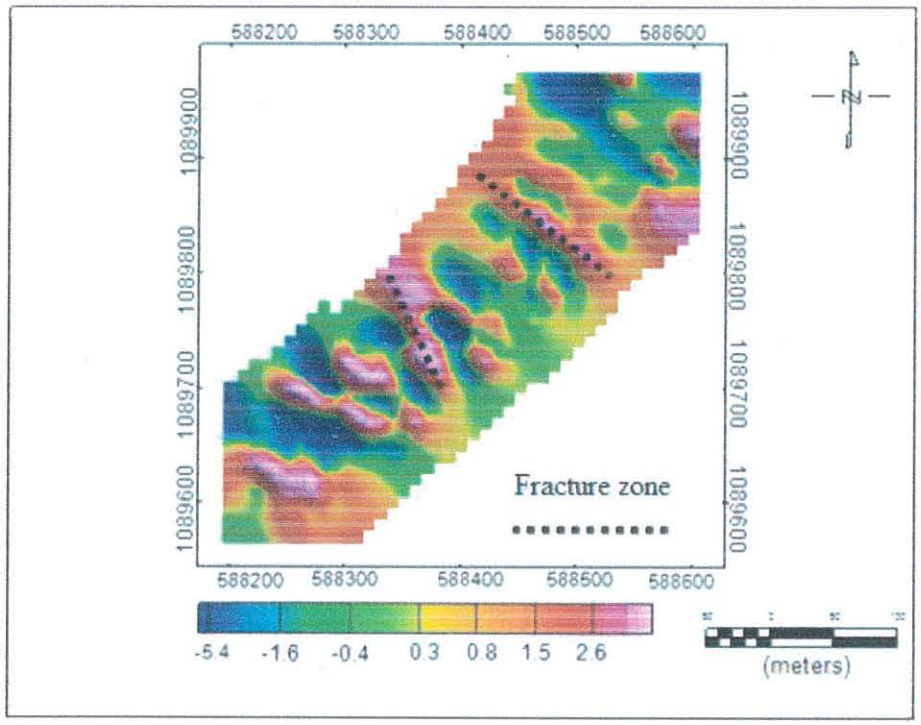

Figure 5.8 Horizontal gradient map

5.2.4 Magnetic 2D-Models

The 2D-magnetic model of the profiles was developed from the observed layer parameters of geological lithologics. To see the subsurface variations of lithologics, geological contacts and structures, the models were done along the three profiles by picking magnetic data from the residual magnetic map.

5.2.4.1 Magnetic model of Profile- 1

The magnetic model of profile-1 shows the variations of magnetic susceptibility starting from center to northeastern direction of the profile. The first layer of basalt rock is thinned out at 157m horizontal distance of the profile. This may be due to the occurrence of fault zones and the effect of weathering at the specified locations of the profile. The correlation of ERT and magnetic models interms of depth is difficult because the depth of ERT is shallower than the magnetic models and also the image of electrical resistivity shows that very disturbed and fragmented subsurface condition. But both models indicate the location of fracture zone at this profile.

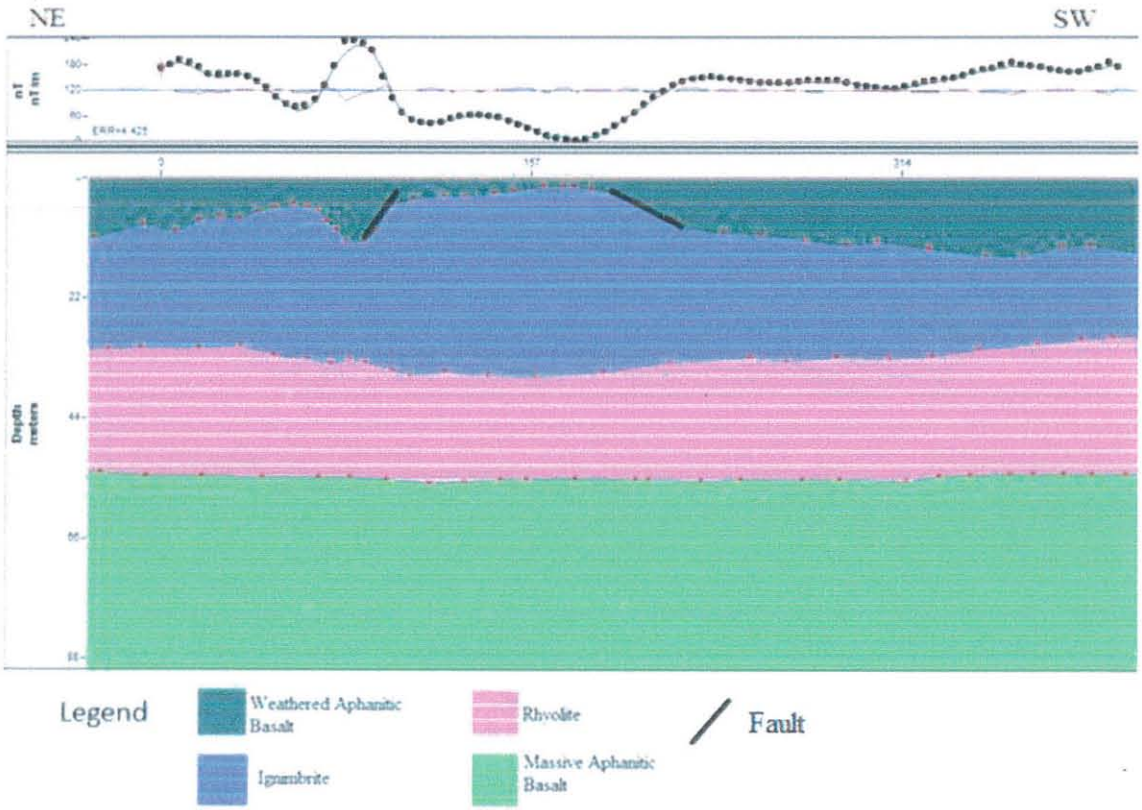

Figure 5.9 Magnetic model of profile-1

5.2.4.2 Magnetic model of Profile- 2

In this model, the variations of magnetic susceptibility also start from center of the profile towards NE direction. This variation indicates the series of fault zones at northeast direction of the profile. The layer of geological rocks is disturbed at this particular failure zone. The ERT and magnetic models of profile-2 show that the fractured and disturbed zones of the geological layers.

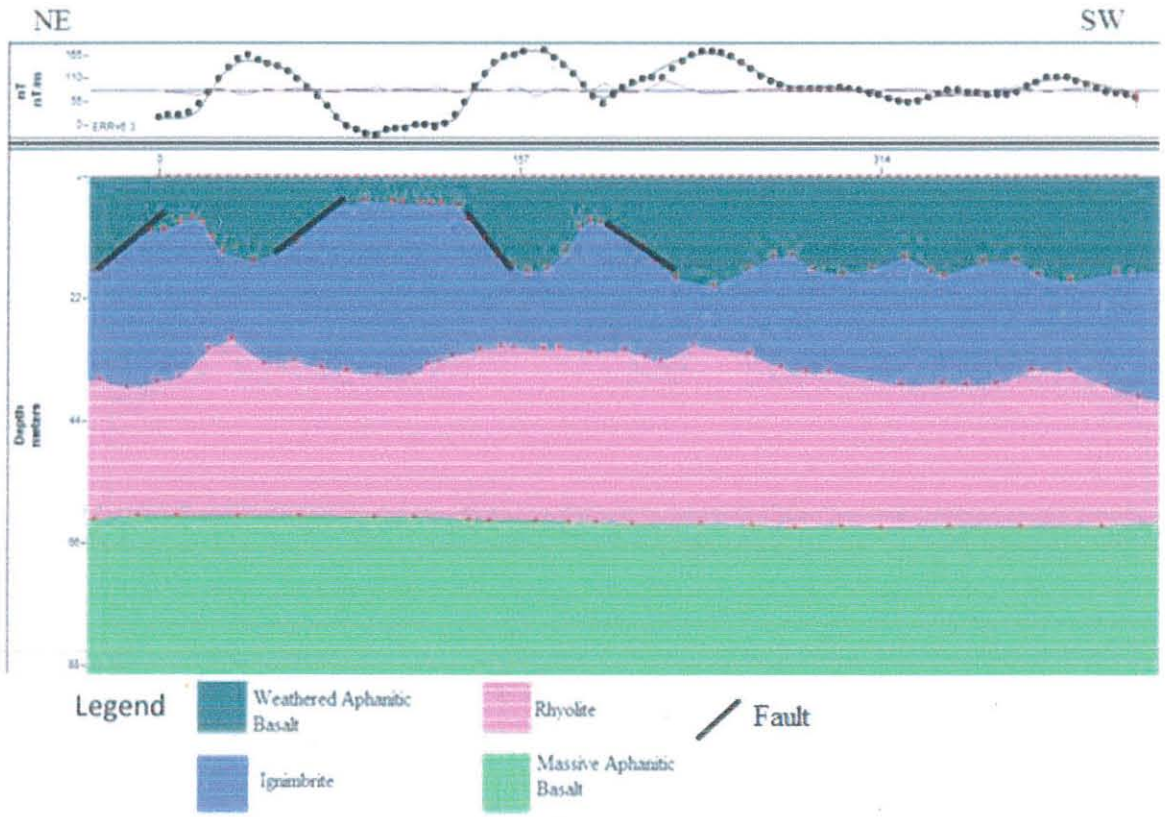

Figure 5.10 Magnetic model of profile-2

5.2.4.3 Magnetic model of Profile- 3

Similarly, magnetic model of profile-3 shows that the occurrence of disturbed and fractured zone at the same horizontal distance with the other two profiles. But the first layer of basalt rock is thick at this specific distance than the other profiles.

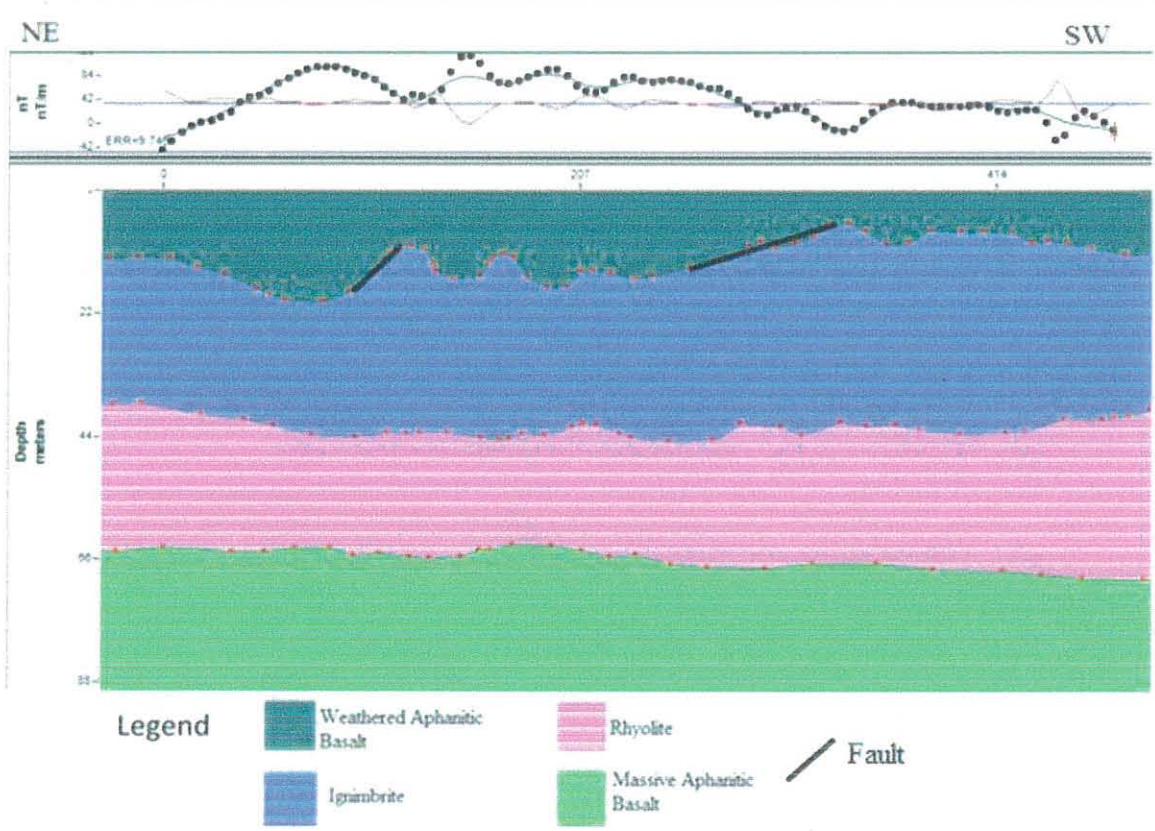

Figure 5.11 Magnetic model of profile 3

5.2.4.4 Combination of the 2D Magnetic models

In all the three profiles, the modeled layers reveal sharp contacts and disturbed locations of the geophysical surveyed site particularly from the center to NE of the profiles. This is due to the occurrence of geological structures as it was already checked from the result of the 2D electrical resistivity model and magnetic maps and profiles. In the three models, thickness of the top weathered basalt rock is increase from profile 1(above the main road) to profile 3(down the main road) (Figure 5.12). This is clearly indicate that the thickness of the highly weathered basalt rock is high just down the road and this is also significant input for sliding problem of the main asphalt road at the center and northeast direction of the profiles. Therefore, these models are clearly outlining the current failure and future possible subsurface of the main road.

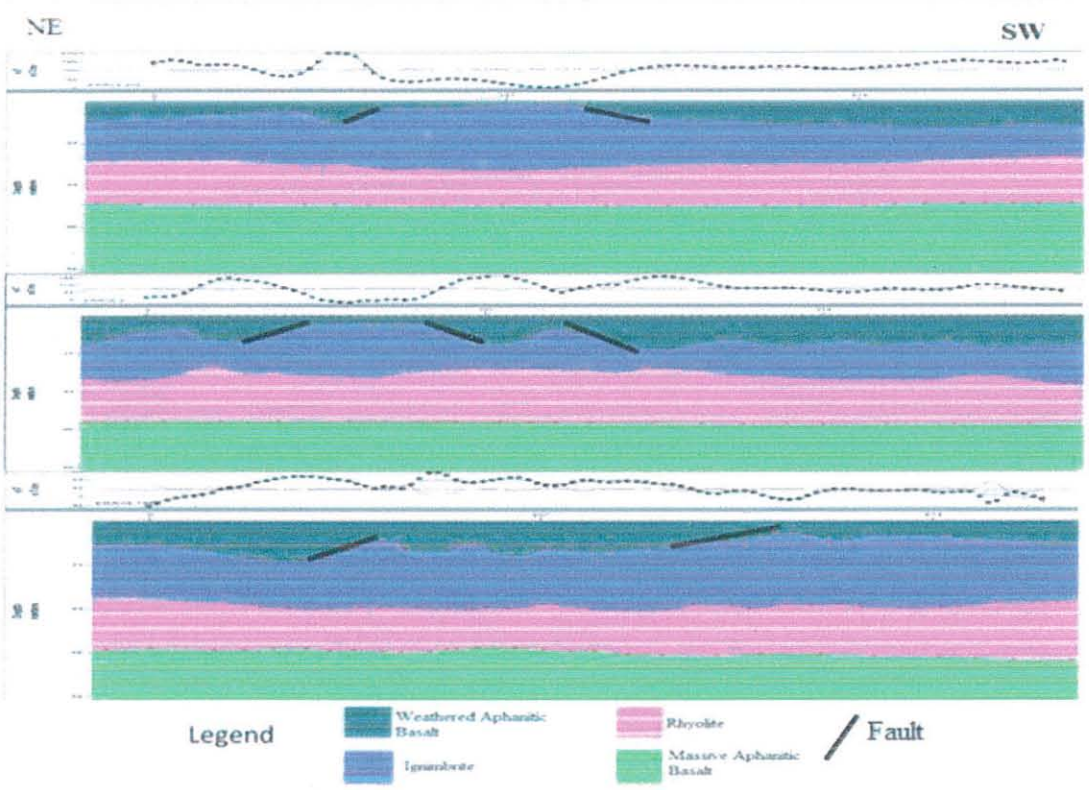

Figure 5.12 Net representations of 2D-Magnetic models along profile-1, 2 & 3 of study area.

CHAPTER - SIX

CONCLUSION AND RECOMMENDATION

6.1 Conclusions

Geophysical and geological investigations have been conducted for landslide problem characterization of the existing main road of the study area. The purpose of this research was to provide an understanding of the subsurface processes and extents of landslide on a major asphalt road of the study area by means of geophysical techniques with the target of reducing landslide risk to lives and infrastructures. Due to the significant contrasts between the physical properties of the disturbed and undisturbed mass, the results from the geophysical techniques have clearly outlined valuable information's about the subsurface conditions and possible processes of the landslide affected road section.

Electrical resistivity tomography (ERT) and magnetic methods in combination with geological information's were employed in carrying out the study of landslide. Some additional investigations were also made on the geology, seismicity, ground water conditions of the area and its possible consequence on the local landslide problem of the site. The research involved the acquisition, processing, and interpretation of the 2D-electrical resistivity and magnetic data. Hence different maps and models including inverted 2D model section maps, magnetic anomaly map, analytical signal map, tilt derivative map, Euler depth solution map, 2D-magnetic modeling and magnetic anomaly profile plots were developed using different mapping and interpretation software's. The interpretation of subsurface geology from 2D models was done using supporting information's obtained from lithological stratifications of field observations.

ERT data modelling was also performed with the topography information of the study area to indicate the undulated and sloped nature of the area. The image indicates that the cause of sliding problem in the area was due to its uneven topography and the associated weak zones. The interpretation of ERT data shows that there is a possible occurrence of landslide at all northeast direction of the survey profiles of the area.

Based on the combined interpretations, the subsurface condition of the main asphalt road is in highly disturbed and fragmented zones. Moreover, the clay soil is dominant at northeast direction of the area in the whole three profiles. Particularly, profile three indicates huge subsurface depth

of the road is covered totally by fragmented and residual sediments which are suitable for sliding happenings in the area particularly northeast of the survey area.

Therefore, northeastern side of the main asphalt road of the survey area needs special care and speedy remedial measures because all the result of the study indicate the possible sliding surface is in the northeastern side of the surveyed area and this is also confirmed through field observations.

The magnetic profiles remarkably coincide with the 2D electrical resistivity profiles in mapping the weak zones. The high magnetic anomaly response is probably due to the result of highly magnetized volcanic rocks that could be found in the area. The higher the magnetic response the shallower the fresh volcanic rocks are believed to be the bedrocks in the area. The intermediate and low magnetic anomalies are the responses of different degree of fracturing of the volcanic rocks and regions around the weak zones.

The occurrences of springs and seepages have significant influence on the initiations of landslide problem. Finally, the main triggering factors for landslide problem in the area have clearly outlined. These are intense weathered condition of the geological lithologies and geological structures, sloped morphology, high rainfall conditions and seismicity of the area.

6.2 Recommendations

Based on the outcomes of this research, the following recommendations are made in relation to the land sliding problem in the main asphalt road of the area:

- The geophysical investigations have revealed that sub-surface conditions of the road are highly susceptible to active landslide which may have adverse effect on the existing road. Therefore, it is strongly recommended that concerned organizations will take appropriate remedial measures on the slope and drainage system of asphalt road.
- The slide problem at particularly place of Shola Wuha (Figure1.3) which is 90cm remaining to reach the asphalt road. The sliding surface has a length of 24m and depth of 3m; moreover, there is also renewed culvert which is again cracked perpendicularly to the road and following this cracked culvert, there is another crack for about 293m length on the road towards south east direction. So, it is strongly recommended taking immediate remedial measure like; maintaining the cracked culvert and building retaining wall or gabion structures down the failed road side.

- The main road is highly affected by landslide problem, especially from Shola Meda up to Armaniya town; moreover, the geophysical results indicate that the subsurface condition of the main road has significant thickness of clay soils, fracturing basalt rocks and weak zones to the direction of northeast of study area. Therefore, it needs special remedial measures and prevention techniques form future sliding problems.
- From field observations, occurrence of groundwater, springs and seepages have important role for sliding problem of the road and the whole study area, especially in the rainy season they increase in number and discharge rate in all sloped area of study. Therefore, proper control of external and internal drainage system of the road is required. Because the existing drainage system is filled by secondary materials and some section of the road has no proper drainage system.
- Introducing of early warning system technology and periodic monitoring, if not initiate farmers to be involved in landslide hazard management and develop an early warning system as a cheaper means of reducing and avoiding the risk and loss from landslides in Debresina localities.
- Stabilization of slopes, avoid loading, and settling of local peoples in areas of high risk will reduce the risk of landslide to human beings, bridges and roads.
- The current study covered only one section of the main road but the problem is in the whole Addis Ababa- Dessie- Mekelle main road. So, to prevent all types of economic losses and inhibiting traffics from this landslide problem, additional detailed and comprehensive investigation will be required for the whole main asphalt road.
- Because of the financial problem and shortage of time the current study was limited to 2D-Electrical Imaging, Magnetic and Geological investigations part only. So, it will be good for future researchers to include Seismic refraction and geotechnical investigations.

REFERENCES

Agnesi, V., M. Camarda, C. Conoscenti, C. Di Maggio, I. S. Diliberto, P. Madonia, and E. Rotigliano, 2005. A multidisciplinary approach to the evaluation of the mechanism that triggered the Cerda landslide (Sicily, Italy): Geomorphology, 65, 101–116.

Alexander D. E., (1993).Natural Disasters. UCL Press and Chapman & Hall, New York, 632pp.

Alexander, D. E., 1999. Landslide; Natural disasters. Pp 242-266. Kluwer academic publishers, The Netherlands.

Alula, H. and Gashawbeza, M., 1993. Report on coal occurrence of Mush Valley. EIGS, Addis Ababa.

Asmelash A., (2012). Remote Sensing & GIS-based Mapping on Landslide Phenomena & Landslide Susceptibility Evaluation of Debresina area, Ethiopia: PhD Thesis. Università degli Studi di Cagliari.

Asmelash A., Giulio B., (2012). Investigation of landslide susceptibility and causative factors evaluation of the landslide area of Debresina, in the Southwestern Afar Escarpment, Ethiopia: Journal of Earth Science and Engineering 2, 133-144.

Ayalew L., (1999).The effect of seasonal rainfall on landslides in the highlands of Ethiopia, Bull Eng Geol Env. 58: 9-19, Q Springer-Verlag.

Ayenew T., Barbieri G., (2005).Inventory of landslides and susceptibility mapping in the Dessie area. Northern Ethiopia, Eng. Geology 77:1-15.

Batayneh, A. T., and A. A. Al-Diabat, 2002, Application of a two-dimensional electrical tomography technique for investigating landslides along the Amman–Dead Sea highway, Jordan: Environmental Geology, 42, 399–403.

Bell F.G., (1999). Geological hazards: their assessment, avoidance, and mitigation. E & FN Spon, Routledge, London, 648pp.

Bell F.G., (2007).Engineering Geology, 2nd Edit, Butterworth-Heinemann, UK: 593pp

Beyene A., Abdelsalam M. G., (2005).Tectonics of the Afar Depression: A review and synthesis. Jour. of African Earth Sciences 41, 41-59.

Bichler, A., P. Bobrowsky, M. Best, M. Douma, J. Hunter, T. Calvert, and R. Burns, 2004, Three-dimensional mapping of a landslide using a multi-geophysical approach: the Quesnel Forks landslide: Landslides, 1, 29–40.

Blakely R.J. (1995), Potential theory in Gravity and Magnetic applications. Cambridge University Press, Australia. pp 461.

Bogoslovsky, V.A. and A.A. Ogilvy, 1977, Geophysical Methods for the Investigation of Landslides, Geophysics, V0l.42, N0.3, pp, 562-571.

Brabb, E. E., and B. L. Harrod, eds., 1989, Landslides: extent and economic significance: Proceedings of the 28th International Geological Congress Symposium, Washington D.C., A. A. Balkema Publisher.

Chigira M., (2000).Geological structures of large landslides in Japan, Jo. Nepal Geol. Soc.22: 497-504.

Chowdhury R., et al., (2010).Geotechnical Slope Analysis. Taylor & Francis Group, London, UK, 751PP

Clark M.J. and Samall R.J., (1982).Slopes and Weathering. London, Cambridge University Press, 112pp.

Cross, M., 1998. Landslide Susceptibility mapping using the matrix assessment approaches: a Derbyshire case study. In: Maund, J. G. & Eddleston, M. (EDS) Geohazards in Engineering geology. Geological society, London, Engineering geology special publications 15. Pp 247-261.

Crozier M.J., (1986).Landslides: causes, consequences and environment. Croom Helm, London, 252pp.

Cruden D.M., (1991). A simple definition of a landslide. Bull. of the Int. Asso. Eng. Geology, 43:27-29.

Cruden D.M. and Varnes D.J., (1996). "Landslide types and processes". In: Turner, A.K. and Shuster, R.L. (eds) (1996). Landslides investigation and mitigation. Special report 247:36-75. Transportation Research Board, Washington, D.C., US National Research Council.

Dai F.C., and Lee C.F., (2002). Landslide characteristics and slope instability modeling using .GIS, Lantau Island, Hong Kong. Geom, 42, 213-228.

DeGroot-Hedlin, C. and Constable, S. (1990). Occam's inversion to generate smooth, two dimensional models form magneto telluric data. Geophysics, v 55, 1613-1624.

Drahor, M. G., G. Göktürkler, M. A. Berge, and T. O. Kurtulmuş, 2006, Application of electrical resistivity tomography technique for investigation of landslides: a case from Turkey: Environmental Geology, 50, 147–155.

EIGS, 1980. A report on the survey of landslides in Mafud Woreda, Yifat and Timuga Awraja Shewa Administrative Region. Disaster preparedness planning program relief and rehabilitation commission. 26 pp.

EIGS, 1994. Engineering geophysical investigation along proposed alternative route, Blue Nile Gorge. EIGS. Ethiopia. Unpublished report.

EIGS, 1998. Investigation of slope instability problem in the Blue Nile gorge. EIGS. Ethiopia.

EIGS, 1999. Integrated engineering geological and geophysical investigation for Landslides study in Bonga town and its surrounding. EIGS. Ethiopia. Unpublished report.

Ethiopian Building Code Standard (1995). Code of Standards for Seismic Loads. Ministry of Works and Urban Development, Addis Ababa, Ethiopia.

Gebreselassie A., (2007).The Social, economic and environmental impacts of landslides in the high lands of Ethiopia. MSc Thesis, Faculty of Dry Land Agriculture and natural resources, Mekelle Univ.

Getech (2007). Advanced Processing and Interpretation of Gravity and Magnetic Data (available at http: //www.getech.com).

Gidey Woldegabriel (1990). Geology, Geochronology and Rift, Addis Ababa, Ethiopia.

Göktürkler, G., Ç. Balkaya, and Z. Erhan, 2008, Geophysical investigation of a landslide: The Altındağ landslide site, İzmir (western Turkey): Journal of Applied Geophysics, 65, 84–96.

Griffiths, D.H. and Barker, R.D. (1993). Two-dimensional resistivity imaging and modelling in areas of complex geology, Applied Geophysics, v 29, 211-226.

Guzzetti F., Cardinali M., and Reichenbach P., (1996).The influence of structural setting and lithology on landslide type and pattern, Env. Eng. Geosci. 2:531-555.

Hayward N., and Ebinger C.J., (1996).Variations in the along-axis segmentation of the Afar Rift System: Tectonics, v.15:244-257.

Hudson J.A., and. Harrison J.P., (1997).Engineering rock mechanics, an introduction to the principles. Elsevier Sci. Ltd, UK: 458pp

Hungr O., Evans S.G., Bovis M., & Hutchinson J.N., (2001). "Review of the Classification of landslides of the flow type''. Environ. and Eng. Geosci., VII: 221-238.

Hutchinson J.N., (1987).Mechanisms producing large displacements in landslides on pre-existing shears, Mem. Geol. Soc. of China, 9:175-200

Hutchinson J.N., (1988).Morphological and geotechnical parameters of landslides in relation to geology and hydrology. In: Landslides, Bonnard C(ed.). Proc. 5th Inter. Symp. on Landslides 1988, Lausanne, Balkema, Rotterdam, 1:3-35.

Hutchinson J.N., (1995). Keynote paper: Landslide hazard assessment. In L.slides, Proc.of VI. Inter. Symp. on Landslides, Feb., Christchurch, New-Zealand A. A. Balkema, Rotterdam, The Netherlands, 3:1805-1841.

Jongmans, D., G. Bièvre, F. Renalier, S. Schwartz, N. Beaurez, and Y. Orengo, 2009, Geophysical investigation of a large landslide in glaciolacustrine clays in the Trièves area (French Alps): Engineering Geology, 109, 45–56.

Kearey. P. Brooks. M. and Hill. I., (2002). An Introduction to Geophysical Exploration, 3rd ed., Blackwell Science Ltd., pp 160.

Keefer D.K., (2002).Investigating landslides caused by earthquakes-a historical review. Surveys in Geophy.23:473-510.

Kirsch, R. (2009). Groundwater Geophysics. 2nd Edition. Hamburger Chaussee, Germany, p 275-286.

Lapenna, V., P. Lorenzo., A. Perrone, S. Piscitelli, E. Rizzo, and F. Sdao, 2005, 2D electrical resistivity imaging of some complex landslides in the Lucanian Apennine chain, southern Italy: Geophysics, 70, no. 3, B11–B18.

Lee, C. -C., C. -H. Yang, H. -C. Liu, K. -L. Wen, Z. -B. Wang, and Y. -J. Chen, 2008, A Study of the hydrogeological environment of the Lishan landslide area using resistivity image Profiling and borehole data: Engineering Geology, 98,115–125.

Leta A., (2007). Landslide Susceptibility Modeling Using Logistic Regression and Artificial Neural networks in GIS: a case study in Northern Showa area, Ethiopia. MSc Thesis, Addis Ababa university earth science department: 75pp.

Loke, M.H. (1999). Electrical imaging surveys for environmental and engineering studies. A Practical guide to 2-D and 3-D surveys, Penang, Malaysia, pp 67.

Lowrie, W. (2007). Fundamentals of Geophysics. 2nd Edition. Cambridge University, p 326.

McCann, D. M., and A. Forster, 1990, Reconnaissance geophysical methods in landslide

Investigations: Engineering Geology, 29, 59-78.

McDowell, P .W, Dr Barker, R. D, Butcher, A.P, Dr Jackson P.D, Pro. McCann, D.M and Dr Sdipp, B.O (2002). Geophysics in Engineering Investigation. 6 Storey's Gate, Westminster, London, pp 249.

Mengesha T., Tadiwos C. & Workineh H., (1996). Explanation of the Geological Map of Ethiopia, Scale 1:2,000,000, 2nd edition. Addis Ababa: The Federal Democratic Republic of Ethiopia.

Meric, O., S. Garambois, D. Jongmans, M. Wathelet, J. L Chatelain, and J. M. Vengeon, 2005, Application of geophysical methods for the investigation of the large gravitational mass movement of Séchilienne, France: Canadian Geotechnical Journal, 42, 1105–1115.

Milson, J. (2003). Field Geophysics. 3rd Edition. University College London, pp 249.

Muthu K., Petrou M., (2007).Landslide-Hazard Mapping Using an Expert System and a GIS.IEEE Transactions on Geosci. & Remote sensing, 45(2):522-531

Reid, A. B., Allsop, J. M., Granser, H., Millet, A. J., and Somerton, I. W. (1990). Magnetic interpretation in 3D using Euler deconvolution. Geophysics, 55; 80-91.

Price D.G., (2009).Engineering geology, Principles and Practice. Springer-Verlag Berlin Heidelberg: 460pp

Reilly (1972). Use of International System of Units in Geophysical Publications. N. Z. J. Geol. Geophysics, 15, 148-58.

Reynolds, J.M. (1997). An Introduction to Applied and Environmental Geophysics. John Wiley and Sons limited, England, UK. p 116-209, 415-522.

Rivas, J.E. (2009). Geothermal training programme: gravity and magnetic methods Ahuachapán and Santa Tecla, El Salvador, United Nations University, pp 13.

Roest, W.R., Verhof, J. Pilkington, M. (1992). Magnetic interpretation using 3D analytic signal. Geophysics, 57, 116-125.

Salem, A., Ravat, D., Gamey, T. J. and Ushijuma, K. (2002). Analytic signal approach and its applicability in environmental magnetic investigation. Journal of Appl. Geophysics, 49; 231-244.

Selby M.J., (1993).Hill slope Materials and Processes, 2nd ed. Oxford University Press: New York, 451pp.

Solomon G. (2010). Integrated landslide investigations in Tarmaber and surroundings, north Shewa zone, Amhara regional state. EGS, Ethiopia. Unpublished report.

Tesfaye S., Harding D.J., Kusky T.M., (2003). Early continental breakup boundary and migration of the Afar triple junction, Ethiopia. Geol. Society of America Bull.115:1053-1067.

Thomas, M.B. (2003). Introduction to geophysical exploration: magnetic notes on main magnetic field (available at galitzin.mines.edu/…/notes).

Thompson, D.T. (1982). EULDPH, A new technique for making computer-assisted depth estimates from magnetic data, Verduzco B., Fairhead J.D., Green C. Geophysic., v 47, 31-37.

Tigistu Haile (2010). Applications of electrical resistivity tomography (at www.mawari.net.). pp 6.

Tilahun Mammo (2005). Site-specific ground motion simulation and seismic response analysis at the proposed bridge sites within the city of Addis Ababa, Ethiopia. Engineering Geology, v 79, 127 - 150.

Varnes D.J., (1978).Slope movement types and processes. In: Schuster RL, Krizek RJ (eds.), Landslides: Analysis & Control. Natio. Aca. of Sci, Transport. Resear. Board, W.DC, Special Rept.176:11-35.

Varnes D.J., (1996).Landslide Types and Processes. In: Turner, A.K., and R.L. Schuster (eds), Landslides: Investigation and Mitigation, Transportation Research Board Special Report 247, National Research Council, Washington, D.C. N. Academy Press.

Woldearegay K., (2005). Rainfall-triggered landslides in the northern highlands of Ethiopia: Characterization, GIS-based Prediction and Mitigation. PhD Thesis. Facul. of Civil Eng. Graz Univ. of Techno. 176pp.

Yonas H. and Matebie M., 2006. Geology of Sela Dingay(C) and Debre Berhan (J) sub sheets of Debre Berhan map sheet. GSE, Addis Ababa, Ethiopia.

Zanettin, B. & Justin Visentin, E., (1974).The volcanic succession in central Ethiopia, 2: The volcanics of the western Afar and Ethiopia rift margins.Memorie degli Istituti di Geologia e Mineralogia dell"Universita di Padova 31: 1-19.

Annex-I: Average, maximum and minimum monthly rainfalls of Debresina Metrological station for last 33 years (1980-2012).

MONTH	AVER	MAX	MIN
JAN	67.35152	235.4	0
FEB	47.58485	149.8	0
MAR	127.6182	415.2	0.5
APR	157.1212	401.1	20.8
MAY	124.6152	437.6	4
JUN	71.48485	225.5	0
JUL	368.6273	675.3	27.7
AUG	432.6455	727.2	97
SEP	185.5424	454.6	21.1
OCT	81.29643	271.7	0
NOV	54.84349	245.9	0
DEC	69.18485	327.4	0

Annex-II: Resistivity of some common rocks is given in (Loke, 1999).

Material	**Resistivity (Ωm)**	**Conductivity (Siemen/m)**
Igneous and Metamorphic Rocks		
Granit	$5 \times 10^{3} - 10^{6}$	$10^{-6} - 2 \times 10^{-4}$
Basalt	$10^{3} - 10^{6}$	$10^{-6} - 10^{-3}$
Slate	$610^{2} - 4 \times 10^{7}$	$2.5 \times 10^{-8} - 1.7 \times 10^{-3}$
Marble	$10^{2} - 2.5 \times 10^{8}$	$4 \times 10^{-9} - 10^{-2}$
Quartzite	$10^{2} - 2 \times 10^{8}$	$5 \times 10^{-9} - 10^{-2}$
Sedimentary Rocks		
Sandstone	$8 - 4 \times 10^{3}$	$2.5 \times 10^{-4} - 0.125$
Shale	$20 - 2 \times 10^{3}$	$5 \times 10^{-4} - 0.05$
Limestone	$50 - 4 \times 10^{2}$	$2.5 \times 10^{-3} - 0.02$

Annex-III: Magnetic susceptibilities and resistivities of some common rocks, soils water and minerals (Milson, 2003)

Mineral or rock types	Susceptibility (k) (rationalized SI units)	Mineral or rock types	Resistivity (ohm- m)
Dolomite (pure)	-12.5 to 44	Igneous and Metamorphic Rocks	
Dolomite (impure)	20,000	Granite	$5x10^3$-10^6
Limestone	10 to 25,000	Basalt	10^3-10^6
Sandstone	0 to 21,000	Slate	$6x10^2$-$4x10^7$
Shale	60 to 18,600	Marble	10^2-$2.5x10^8$
Schist	315 to 3000	Quartzite	10^2-$2x10^8$
Slate	0 to 38,000	Sedimentary Rocks	
Gneiss	125 to 25,000	Sandstone	8-$4x10^3$
Serpentenite	3,100 to 75,000	Shale	20-$2x10^3$
Granite	20 to 50,000	Limestone	50-$4x10^2$
Rhyolites	250 to 37,7000	Soils and waters	
Pegmatite	3,000 to 75,000	Clay	1-1000
Gabbro	800 to 76,000	Alluvium	10-800
Basalts	5000 to 182,000	Groundwater (fresh)	10-100
Oceanic Basalts	300 to 3,6000	Sea water	0.2
Perdotite	95,000 to 196,000		

Annex-IV: Photographs showing landslide effects on the main road, electrical tower and local house of study area.

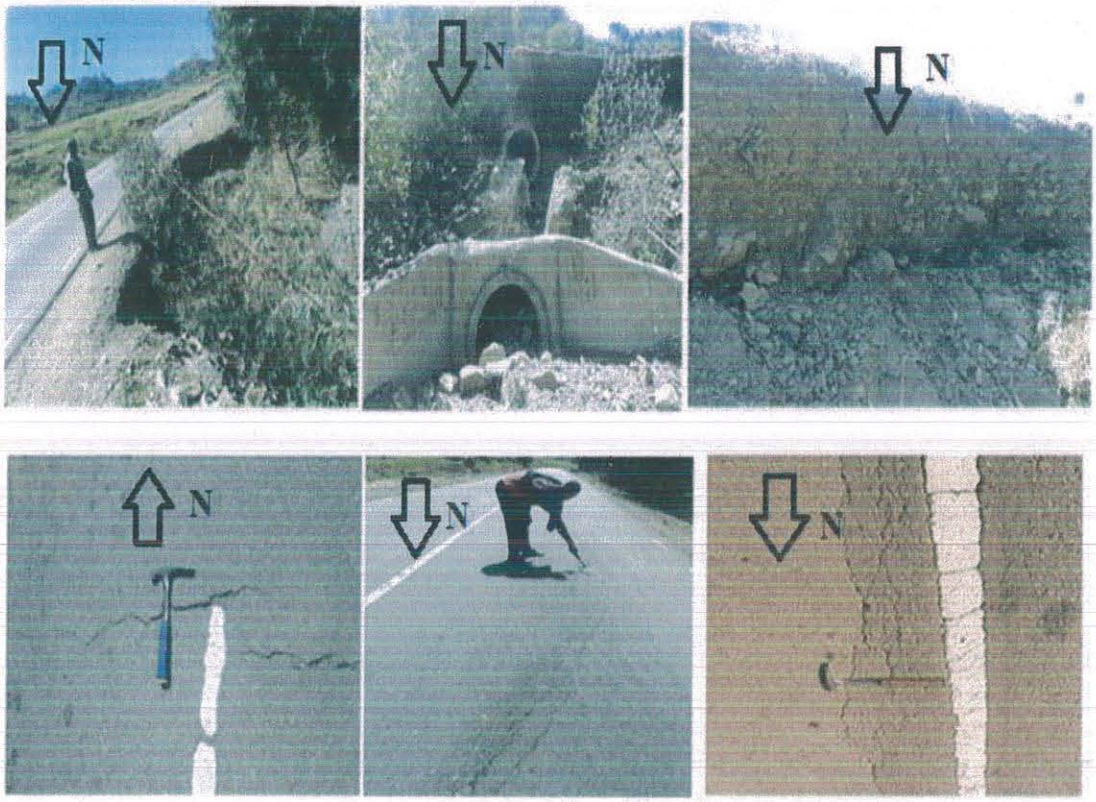

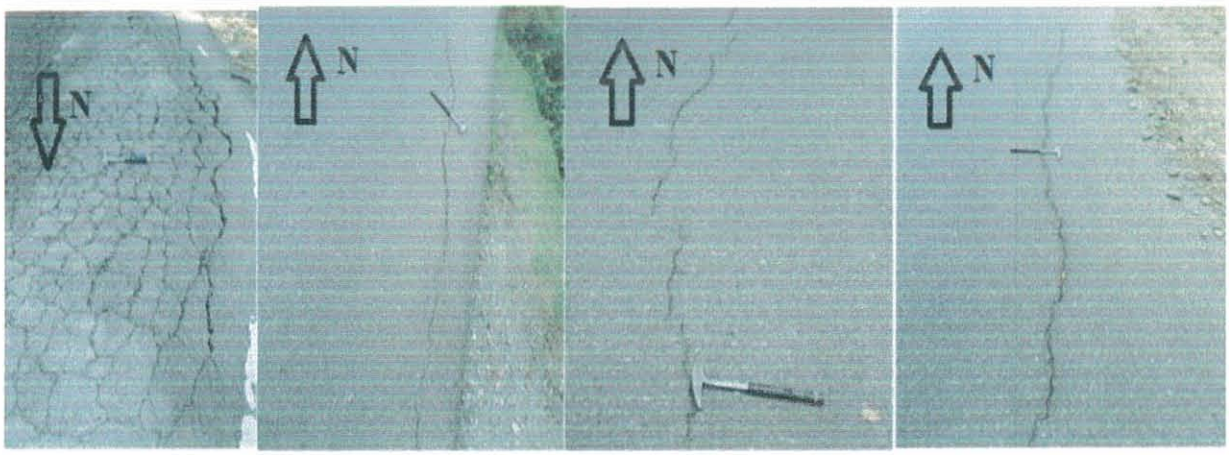
N
N
N
N


N
N